ESR STUDIES OF REACTIONS INVOLVING METAL IONS AND FREE RADICALS

ELECTRON SPIN RESONANCE STUDIES

OF

REACTIONS INVOLVING METAL IONS AND FREE RADICALS

By

CONSTANTINE T. CAZIANIS, B.Sc., M.Sc.

A Thesis

Submitted to the School of Graduate Studies

in Partial Fulfilment of the Requirements

for the Degree

Doctor of Philosophy

McMaster University

August 1973

DOCTOR OF PHILOSOPHY (1973) McMASTER UNIVERSITY
(Chemistry) Hamilton, Ontario.

TITLE: Electron Spin Resonance Studies of Reactions Involving Metal Ions and Free Radicals

AUTHOR: Constantine T. Cazianis, B.Sc. (Univ. of Athens)
M.Sc. (St. Louis Univ.)

SUPERVISOR: Professor D. R. Eaton

NUMBER OF PAGES: xii, 153

SCOPE AND CONTENTS:

This thesis is concerned with the application of Electron Spin Resonance to several problems of primarily inorganic interest. In each case the system examined contains both free radicals and metal ions or complexes and ESR has been used to probe the chemistry involved.

An introductory chapter reviews the literature which is pertinent to the research. This is followed by a discussion of those parts of ESR theory which are required to evaluate the results and by a description of the experimental aspects of the work.

Chapter IV presents the results of a study of the synthesis and reactions of some "spin-labelled ligands". Such compounds are defined as molecules with two functional groups, one of which provides a Lewis base site suitable for complexing to a metal and the other comprises a group bearing

an unpaired electron. The ESR spectra obtained when these ligands are complexed to metal ions have been shown to provide information on the relative electron accepting power of the metal ions and, in some cases, on the rates of very rapid ligand exchange reactions.

It was found that when some of these spin-labelled ligands interact with very strong Lewis acids, such as BF_3 and $AlCl_3$, new ESR spectra appeared. These spectra have been assigned to products arising from rearrangements of alkyl groups on the spin-labelled ligand. The chemistry of these processes is discussed in Chapter V.

Chapter VI is concerned with the photochemistry of metal acetates. The electron accepting or donating abilities of metal ions in electronically excited states will be different from those of corresponding ions in their ground states. In some cases, electron transfer to or from associated ligands can lead to the formation of free radicals. Such processes have been investigated for a wide variety of metal acetates. The radicals produced have been identified by means of the ESR spectra observed in frozen solutions.

Finally, Chapter VII reports an investigation of certain satellite lines observed in association with methyl radical ESR spectra obtained by irradiating metal acetates. These satellites have been assigned to double quantum transitions arising from the simultaneous flip of the electron spin and the nuclear spin of a proton on a neighbouring sol-

vent molecule. Measurement of the relative intensities of the satellites and the main lines provides information on the environment of methyl radicals in an ice matrix. Data on the variation with temperature of the average methyl radical-solvent molecule distance of separation is presented.

ACKNOWLEDGEMENT

I wish to express my sincere appreciation and thanks to Dr. D. R. Eaton for his help and encouragement throughout the research and preparation of this thesis.

I would further like to thank Dr. J. J. McCullough for the preparation of the di-t-butyl nitroxide, Dr. J. Warkentin for helpful discussions of rearrangement reactions and Mr. B. Campbell for the preparation of some zinc complexes used in this work.

I am indebted to Dr. C. Charalambous for his help in calculations of ESR spectra.

Finally, I express my thanks to the National Research Council of Canada for the financial support of this research.

TABLE OF CONTENTS

LIST OF TABLES

LIST OF FIGURES

CHAPTER I

INTRODUCTION

The technique of electron spin resonance (ESR) spectroscopy is of central importance to the study of free radicals. The paramagnetism of these molecules provides a very sensitive probe into their detailed electronic structure.

The ESR method, being applicable only to molecules with unpaired electrons, suffers some disadvantage since the large majority of the molecules in which the bonding is of interest are diamagnetic.

Among the several techniques which have been introduced in attempts to extend the range of molecules amenable to study by ESR, is the spin-labelling concept which has been utilized in the present work in a study of metal-ligand bonding and charge distribution of metal compounds in solution. Also, the photochemical action of ultraviolet light on metal acetates and related organometallic compounds has been applied to a study of the chemistry of excited states of these molecules in frozen acidified aqueous solutions.

In general, the method of spin labelling could include all ESR studies in which small paramagnetic probes are used to obtain information on the surrounding environment (in contrast to studies aimed at determining the structure of the paramagnetic species). It has been introduced into biological chemistry(1), where a number of enzymes and other

biologically active molecules have been chemically modified by the introduction of the spin label in the vicinity of the active site. A wide variety of nitroxide free radicals(2-6) have been used as spin labels. The relatively unreactive N-O group contains the unpaired electron necessary to produce an ESR signal, and the reactive functional group at the other end of the molecule is allowed to interact with the macromolecule of interest. This topic could also include ESR studies of copper and manganese ions bound to biomolecules and some studies of organic free radicals produced by irradiating biomolecules(7,8).

In inorganic chemistry, many physical techniques have been used to study the kinetics of the complexing of metal ions in solution, but the applications of electron spin resonance to this field have been rather sparse. The large majority of the paramagnetic metal ions have ESR characteristics which are not favourable for solution studies. However, there are a few exceptions to this general behaviour which have been exploited in a number of studies of variations in line width with temperature, concentration, solvent viscosity etc. Five-coordinate vanadyl acetylacetonate, for instance, is known to add a sixth ligand in coordinating solvents such as pyridine or piperidine. When this happens the ^{51}V hyperfine coupling constant decreases and there are concomitant changes in g-factor and correlation time which, coupled with measurements of line widths, provide a basis for

estimates of the rate of exchange of solvent with the complex (9). Corden and Rieger(10) have studied the ESR spectra of Cu(II) bis (di-n-Butyldithiocarbamate) as a function of temperature and solvent composition in mixtures of methyl-cyclohexane with several nitrogen bases. They presented evidence for the formation of a short-lived 1:1 adduct and obtained the equilibrium constants for the adduct formation as well as the adduct lifetimes. Also, Farmer, Herring and Tapping(11) have reported a similar study of the fast Lewis acid-base reaction between copper(II) bis-(diethyl dithiocarbamate) and pyridine.

The possibility of complexing metal ions with spin-labelled ligands provides an alternative way to study metal-ligand bonding by ESR. It is necessary that the ligands used are only slightly perturbed from those commonly occuring in metal complexes so that the conclusions derived in such studies can be extended to the corresponding unlabelled ligands. This approach has a number of practical advantages in the form of sharper lines, the absence of quadrupolar broadening and g-factor anisotropy.

The precedent for such a possibility was perhaps provided by the occurence of neutral complexes of 2,2' - dipyridyl which in many cases are stable compounds(12,13). Also Weissman and Brown(14) studied a series of even-electron paramagnetic chelates of the type $M^{2+}(R^{-})_2$, where M = Be,Mg,Sr,Zn and R = derivatives of 2,2' -dipyridine and 1',10 phenanthro-

line. Solutions of most of these compounds in rigid 2-methyl-tetrahydrofuran exhibited ESR spectra characteristic of triplet molecules in which the spins reside singly on each ligand and are separated by M^{2+}. However, the interactions of the unpaired electrons with the metal ion are sufficiently strong to lead to complete delocalization and it becomes debatable whether it is more correct to describe the compound as a complex of a radical with a metal in a high oxidation state or a complex of a non-radical ligand with a metal in a lower oxidation state.

In other cases, e.g. the ESR study on complexing of the o-semiquinone radical with diamagnetic metal ions(15), modification of the spin density distribution within the ligand due to the effect of complexing of the metal was observed. The redistribution of the spin density reflects change in the effective Coulomb integral of the semiquinone oxygen atom(16,17) and hence the relative strength of the metal-oxygen bond in these complexes. Also, ESR studies involving such radical ligands as alkyl nitroxides have been reported. Di-t-Butyl nitroxide(DBNO) complexes of Co(II)(18) and Pd(I)(19) are well characterized and the first appears to be tetrahedral 2:1 adduct of stoichiometry $CoX_2(DBNO)_2$ (Where X = Cl,Br,I) with magnetic moments suggesting the presence of only one unpaired electron. The Pd complexes are diamagnetic and have the general formula $(XPdDBNO)_2$ with the presence of bridging halogens. Studies have also been carried

out on the coordination of strong Lewis Acids with nitroxide radicals(20). More recently Eames and Hoffmann(21) investigated the acid-base complexes of the form $R_2NO:MX_3$ (M = B,Al,and X = F,Cl,Br) in solution. The nitroxide radical serves as a Lewis base and the acids are $AlCl_3$ and BX_3. It was found that the hyperfine interaction of the nitroxide ^{14}N nucleus increases upon complexation and depends on the electron-withdrawing strength of the particular Lewis acid in the complex. As Lewis-bases, the nitroxides have been used in nuclear magnetic resonance studies of transition metal compounds, particularly those of Cr(III), high-spin Fe(III) and Cu(II), which generally have long electron spin-relaxation times(20). In these complexes, spin relaxation is achieved by coordination of the nitroxide radical and rapid electron exchange between the complex and the paramagnetic molecule.

The method of spin labelling is indeed a large topic and the definition of this technique(as given earlier) could also include some applications of electron spin resonance to photochemistry. Such studies are usually undertaken to identify the free radicals produced during photochemical reactions, but some information regarding the environment of the radicals is frequently obtained from the ESR spectra. Thus although the classical techniques of photochemistry - the identification of reaction products, the method of chemical kinetics and the use of scavengers to detect the occurence of free radical intermediates - play a major part in the deter-

mination of photochemical mechanisms the most definitive information on the earlier stages of the process has come by and large from ESR and flash photolysis studies. A review of the applications of ESR to the photochemistry of organic molecules has been given by Kholmogorov(23), while the photochemical behaviour of the coordination compounds in reviewed and discussed in detail in the book by Balzani and Carassiti (24).

Many of the reaction mechanisms proposed in studies on the photolytic oxidation and reduction of transition metal ions involve free radicals and have been discussed in an early review by Uri(25). The possibility of using electron spin resonance to obtain information on such mechanisms was recognized by Ingram et al.(26).

Moorthy and Weiss studied the photooxidation of Fe^{2+} and I^- in frozen acid solutions(27) and the photoreduction of Ce^{4+} in frozen aqueous solutions(28). In the former case hydrogen-atom ESR signals were observed at 77°K. It is suggested that UV-irradiation leads to charge-transfer, giving in the first instance an excited state in which the electron is transferred to the hydration shell where it is bound in the field of the oriented water molecules around the ion. The electron in the excited state can therefore react with electron-acceptors present in the matrix e.g., acids, and their reaction leads to the formation of hydrogen atoms. In the case of the photoreduction of Ce^{4+} the reverse process

is suggested i.e., charge-transfer from the solvent molecules in the hydration shell to the ceric ion. The resulting hole in the matrix is trapped and exhibits a characteristic ESR spectrum.

In other investigations(29,30), however, some evidence has been reported in favour of a photoelectron production process during the UV-irradiation of acidic aqueous solutions of Fe^{2+} ($Fe^{2+}_{aq} \xrightarrow{h\nu} Fe^{3+}_{aq} + e^-_{aq}$). This process is similar to that obtained from the irradiation of $Fe(CN)_6^{4-}$ in alkaline glasses at 77°K where the formation of hydrated electrons is demonstrated by ESR(31,32) and the electron capture by one of the water molecules in the hydration shell is excluded.

Apparently the disagreement here is on the nature of the primary process i.e., whether the process is charge-transfer from metal to ligand(MLCT) or charge-transfer from metal to solvent(CTTS). While for several negative ions the process of photoelectron production has been definitively confirmed, completely convincing proofs for positive ions have not been reported up till now. On the other hand it is emphasized(33) that, from a theoretical point of view, the photoelectron production from a positive ion seems rather unplausible.

ESR techniques have also been used in studies of the photooxidation and reduction of cobalt complexes(34). In particular, during the UV-irradiation of frozen acidified

aqueous solutions containing trioxalatocobaltate(III) ion a primary charge transfer occurs, with formation of a C_2O_4H coordinated radical; then, a thermal reaction takes place which leads to the complete decomposition of the complex and the formation of hydrogen atoms.

The photolysis of a series of Pb^{4+} carboxylates has been studied by Heusler and Loeliger(35). UV-irradiation at 77°K in a solid benzene matrix leads to decarboxylation and production of alkyl radicals which were identified by ESR. A charge-transfer mechanism from oxygen to metal is suggested. Also, in solution, optical and ESR detection of radical intermediates in the photooxidation of organic molecules by transition metal ions(Ce(IV), U(VI), Cu(II), Fe(III), V(V)) has been carried out by Burrows et al.(36).

Finally, the effect of neighbouring nuclei on the ESR spectra of free radicals in solids produced by irradiation has been studied for hydrogen atoms(37,38,39) and some organic radicals in single crystals(40,41). This effect appears in the form of extra satellites accompanying the main absorption lines and it is attributed to a change in spin state of a nearby nucleus concurrent with the change in spin state of the unpaired electron. In such studies it is possible, under certain experimental conditions, to obtain an estimate of the average distance of the flipping nuclei from the nucleus on which the spin-density is concentrated.

CHAPTER II

THEORY

A. INTRODUCTION

Since its discovery more than 25 years ago, electron spin resonance has been developed rapidly and applied to a wide range of research problems. A large number of systems have been studied by ESR e.g., biological (nucleic acids, enzymes etc), chemical (polymers, catalysts),semiconductors, transition elements, free radicals, irradiated substances etc.

Essentially, ESR forms a branch of high resolution spectroscopy using frequencies in the microwave region. In terms of the observed phenomena, ESR studies the interaction between electron magnetic moments and magnetic fields. Being concerned with paramagnetic materials whose energy levels may be split by the application of a magnetic field (Zeeman effect), it may be said that ESR is the study of direct transitions between electronic Zeeman levels, i.e.study of the energy required to reorient electronic magnetic moments in a magnetic field. The principal information gained from ESR spectra is an evaluation of the various terms in the spin Hamiltonian of which the Zeeman and hyperfine terms are usually determined directly from ESR data. It is a sensitive technique and, being relevant only to paramagnetic systems, highly selective.

The theoretical principles of the ESR method may be found in several textbooks(42,43,44,45). However, the intention of this chapter is to emphasize the interpretative aspects of the subsequent chapters, and as such only a limited number of topics pertinent to the subject of this work are presented.

B. NUCLEAR HYPERFINE STRUCTURE

1. General: The spin Hamiltonian.

One of the most valuable aspects of ESR spectroscopy is the hyperfine structure of the spectra. This results from interaction of the magnetic moments of the unpaired electron with those of magnetic nuclei. The resulting hyperfine patterns are highly characteristic and, in many cases, can be related in some detail to the spatial distribution of the unpaired electron throughout the paramagnetic molecule.

The interaction between the unpaired electron and the nucleus arises in two ways. The first is essentially the classical interaction of two dipoles $\vec{\mu}_S$ and $\vec{\mu}_I$ separated by a distance $\vec{r}$. The combined spin and orbital angular momenta of the electron set up a field at the nucleus which depends on the shape of the electronic orbital and the average distance between electron and nucleus. Since the magnitude of this interaction depends on the angle between the radius vector (the line joining electron and nucleus) and the direction of the external field it is referred to as the "anisotropic" or "dipolar" interaction. The second type, known

as the "Fermi" or "contact" interaction, depends on the presence of a finite unpaired spin density at the position of the nucleus. This interaction is "isotropic" and is independent of the orientation of the paramagnetic species in the magnetic field. These interactions are combined into the third term of equation (2.1) which is the spin Hamiltonian for a free radical with one unpaired electron of spin S=1/2 and n nuclei of spin $\vec{I}_i$ in an external magnetic field $\vec{H}$.

$$\mathcal{H} = \beta \vec{S} \cdot \hat{g} \cdot \vec{H} - \sum_i^n g_{Ii} \beta_{Ii} \vec{I}_i \vec{H} + h \sum_i^n \vec{S} \cdot T_i \cdot \vec{I}_i \qquad (2.1)$$

In (2.1), β is the electronic Bohr magneton, g_{Ii} and β_{Ii} the g-factor and nuclear magneton for nucleus i, respectively, $\hat{g}$ is the g-matrix and T_i the hyperfine matrix for nucleus i. Nuclear quadrupole interactions have not been included in the above equation.

The first and second terms of (2.1) represent the electronic and nuclear Zeeman interactions, i.e., the interaction of the electron and nuclei with the external magnetic field. The g-factor anisotropy expressed by the g-matrix in the first term of (2.1) arises in the cases where the unpaired electron possesses orbital angular momentum which is strongly coupled with its spin. However, for most organic free radicals the orbital angular momentum is quenched and $\hat{g}$ has an almost isotropic value close to that of the free electron, therefore the term $\beta \vec{S} \cdot \hat{g} \cdot \vec{H}$ can be replaced by $\beta g \vec{S} \cdot \vec{H}$ where g is now a scalar quantity. In that case, equation (2.1)

is approximated for organic free radicals to equation (2.2).

$$\mathcal{H} = \beta g \vec{S}\cdot\vec{H} - \sum_i^n g_{I_i}\beta_{I_i}\vec{I}_i\vec{H} + h\sum_i^n \vec{S}\cdot T_i\cdot\vec{I}_i \qquad (2.2)$$

2. Isotropic hyperfine interaction: Organic radicals in solution.

In equation (2.2) the term representing the electron-nuclear hyperfine interaction $\vec{S}\cdot T\cdot\vec{I}$ may be decomposed into the sum of two terms

$$a\vec{S}\cdot\vec{I} + \vec{S}\cdot T'\cdot\vec{I} \qquad (2.3)$$

where a is the isotropic contact part, and T' is the magnetic dipolar tensor. In the solid state it gives rise to anisotropic splitting which will be examined in section (B-4). In the liquid phase, however, the average value of T' is zero and the observed hyperfine splitting gives the isotropic coupling constant a directly.

The term $a\vec{S}\cdot\vec{I}$ was introduced by Fermi in an early treatment of atomic hyperfine interaction and he showed that a is related to the unpaired spin density at the nucleus $\psi^2(0)$ by equation (2.4).

$$a = \left(\frac{8\pi}{3}\right) g\beta g_I\beta_I \left|\psi^2(0)\right| \qquad (2.4)$$

where $\psi^2(0)$ is only non-zero if the unpaired electron is in an s- or σ- orbital.

If for simplicity we consider a system with one unpaired electron and one nucleus of spin $\vec{I}$ in an external field

$\vec{H}$ then the spin Hamiltonian can be written as

$$\mathcal{H} = g\beta\vec{S}\cdot\vec{H} - g_I\beta_I\vec{I}\cdot\vec{H} + h\alpha\vec{S}\cdot\vec{I} \qquad (2.5)$$

where only the isotropic part of the nuclear hyperfine interaction is included (α is expressed in frequency units). In the absence of a magnetic field the hyperfine interaction term represented by $h\alpha\vec{S}\vec{I}$ results in a splitting of the electronic energy level into two hyperfine levels characterized by the quantum numbers I+1/2 and I-1/2 because the spin vectors $\vec{I}$ and $\vec{S}$ are coupled and the direction of quantization is that of their resultant

$$\vec{F} = (\vec{I}+\vec{S}) \qquad (2.6)$$

The energy difference between these two levels is given by (2.7)

$$\Delta E = (1/2)h\alpha(2I+1) \qquad (2.7)$$

When an external magnetic field $\vec{H}$ is applied, the coupling between $\vec{I}$ and $\vec{S}$ is progressively broken down as $\vec{H}$ increases until eventually both are independently quantized along the direction of $\vec{H}$. In this case the appropriate quantum numbers are M_S and M_I and the energy levels are given by

$$E_{M_S M_I} = g\beta M_S H - g_I \beta_I M_I H + h\alpha M_I M_S \qquad (2.8)$$

In (2.8) the first two terms represent the splitting due to the direct interaction of the electron and nuclear magnetic

moments respectively with the magnetic field, and the third represents the hyperfine splitting. The selection rules for transitions between these levels induced by an oscillating magnetic field perpendicular to the applied field are $\Delta M_S = \pm 1$ $\Delta M_I = 0$. The energy levels defined by equation (2.8) include the term $g_I \beta_I M_I H$ which implies a contribution for the direct interaction of the nucleus with the magnetic field. However, since the transitions observed occur between states with identical values of M_I this contribution cancels out, and in a first-order treatment the same values for the hyperfine splittings would be obtained if this term were omitted from the spin Hamiltonian, and equation (2.8) is reduced to eq.(2.9)

$$E_{M_S M_I} = g\beta M_S H + h a M_I M_S \qquad (2.9)$$

When more than one nucleus interacts with the unpaired electron the appropriate Hamiltonian is (2.2). The isotropic spectrum may be derived to first order by splitting the unperturbed electronic levels into $2I_i+1$ equally populated levels for nucleus i, then each of these levels is further split into $2I_j+1$ levels by nucleus j, and so on. Thus the total number of energy levels for a given value of M_S is $(2I_i+1)(2I_j+1)(2I_k+1)$ etc. Since transitions occur with no change in nuclear spin quantum number this is also the maximum number of observable absorption peaks. This is because in many radicals the symmetry of the orbital of the unpaired electron makes some of the interacting nuclei magnetically

equivalent, i.e. their hyperfine coupling constants are identical . In such cases some of the nuclear hyperfine levels are degenerate, e.g. the interaction of one unpaired electron with n equivalent protons results in n+1 absorption lines due to transitions originating from each of the n+1 hyperfine levels whose degeneracies (and hence the relative intensity of the lines) are proportional to the coefficients of the binomial expansion of $(1+x)^n$.

3. Electron spin densities

(a) Definitions

In equation (2.4) it is implied that contact interaction can only occur when the unpaired electron has a finite probability density at the nucleus, that is, the electron must have some s-orbital character. In the hydrogen atom there is a direct proportionality between the hyperfine splitting and the squared amplitude of the electronic wave function at the nucleus $\psi^2(o)$ which is the probability density for the hydrogen 1s orbital. In a molecular radical however, the unpaired electron is often distributed over many atoms and the probability that it is on a particular atom is quite small. The fraction of time that the unpaired electron spends in an orbital of a particular atom is often called the "unpaired spin density" in this orbital. According to this definition the unpaired spin density is a number representing the fractional population of unpaired electrons on an atom, and it is posi-

tive everywhere in the molecule since it is a one-electron function if it is assumed that the other electrons are perfectly paired together.

In fact, the spin density is a many-electron function, i.e., a molecule contains many electrons all of whose spins are coupled together but due to electron correlation effects the distributions of the paired electrons become "polarized" so that local unpairing of spins results. Therefore in order to define the spin density the complete wave function, ψ, of a molecule must be introduced. This is shown in equation (2.10)

$$\rho(x,y,z)=\int\psi^{*}\sum_{k}2\hat{S}_{zk}\delta(r_k)\psi\,dv \qquad (2.10)$$

where $\rho(x,y,z)$ is the spin density at the point (x,y,z), $\hat{S}_{zk}$ is the operator for the z-component of electron spin for electron k, and $\delta(r_k)$ is the Dirac delta function of the distance r_k between the electron k and the point (x,y,z). Since the operation of $\hat{S}_{zk}$ on ψ can have only two eigenvalues $\pm 1/2$ depending on whether the electron has α or β spin, $\rho(x,y,z)$ simply expresses the difference between the probability density of α spin and the probability density of β spin at the point (x,y,z). This implies that if at the point (x,y,z) an excess of electrons have β spin, the value of the spin density at this point will be negative.

Depending on the way that ψ is expressed in eq. (2.10) the spin density ρ can be formulated in terms of the elements ρ_{ij} of a molecular orbital spin density matrix, ρ if ψ is ex-

pressed as an antisymmetrized product of orthonormal molecular orbitals ϕ

$$\rho = \sum_{ij} \rho_{ij} \phi_i^* \phi_j \qquad (2.11)$$

or in terms of the elements $\rho_{\lambda\mu}$ of an atomic orbital spin density matrix ρ, if ψ is expressed in terms of a set of normalized atomic orbitals φ_λ

$$\rho = \sum_{\lambda\mu} \rho_{\lambda\mu} \varphi_\mu^* \varphi_\lambda \qquad (2.12)$$

In the linear combination of atomic orbitals (LCAO) approximation for the molecular orbitals, ρ_{ij}, $\rho_{\lambda\mu}$ and ϕ_i are related by equation (2.13)

$$\rho_{\lambda\mu} = \sum_{ij} \rho_{ij} a_{\mu j}^* a_{\lambda i} \qquad (2.13)$$

where

$$\phi_i = \sum a_{\lambda i} \varphi_\lambda \qquad (2.14)$$

The non-orthogonallity of the φ_λ orbitals implies that there will be nondiagonal elements in the matrix ρ. The diagonal elements $\rho_{\lambda\lambda}$ of the atomic orbital spin density matrix are just the atomic orbital spin densities defined as

$$\rho_i^{\varphi} = P_i^{\varphi}(\alpha) - P_i^{\varphi}(\beta) \qquad (2.15)$$

where $P_i^{\varphi}(\alpha)$ and $P_i^{\varphi}(\beta)$, are the probability densities of spin α and spin β in the atomic orbital φ, on the atom i.

(b) α-Proton hyperfine splitting: The McConnell relation

Isotropic proton hyperfine splittings can arise only

from a net spin density at the proton. In aromatic radicals the unpaired electron occupies a molecular π-orbital delocalized over the carbon atom framework of the molecule, and the protons lie in the nodal plane of the π-orbitals. Thus no hyperfine splittings are possible in zero order. However, proton hyperfine splittings are exhibited by π-electron free radicals. The apparent contradiction between theory and experiment was resolved when McConnell(46) and Weissman(47) showed that spin density could be induced at the proton via a mechanism called "spin polarization".

In terms of the molecular orbital theory the spin polarization can be described by considering the $\rangle\dot{C}$-H fragment for which the electronic configuration of the ground state has two electrons in the C-H σ_β bonding orbital and one electron occupies the $2p_z$ orbital π. The ground state wave function for the $\rangle\dot{C}$-H fragment is written as the Slater determinant

$$\psi_o = \| \sigma_\beta(1)\, \sigma_\beta(2)\, \pi(3) \| \alpha\beta\alpha \tag{2.16}$$

There are also two excited states with total spin S=1/2 and m_S=1/2 where one σ bonding electron is promoted into the σ **anti**bonding orbital σ_α. They are eigenfunctions of the operator $\hat{S}^2$ and therefore can be mixed with the ground state.

$$\psi_1 = \| \sigma_\beta(1)\, \sigma_\alpha(2)\, \pi(3) \| \frac{1}{\sqrt{2}} (\alpha\beta\alpha - \beta\alpha\alpha)$$

$$\psi_2 = \| \sigma_\beta(1)\, \sigma_\alpha(2)\, \pi(3) \| \frac{1}{\sqrt{6}} (2\alpha\alpha\beta - \alpha\beta\alpha - \beta\alpha\alpha) \tag{2.17}$$

However, since in the state described by ψ_1 the unpaired electron is still confined to the π-orbital, there is no need to consider it. The next, more accurate representation of the wave function Ψ for the $>\dot{C}$-H fragment will be an admixture of ψ_o and a small amount of the excited state ψ_2

$$\Psi = \psi_o + \lambda\psi_2 \qquad (2.18)$$

where the coefficient λ can be determined by means of the variation method. Ψ now, in containing ψ_2, possesses some s-orbital character which accounts for the proton hyperfine splittings.

The general theory of σ-π exchange interaction for hydrocarbon radicals has been formulated and solved using first-order perturbation theory(48,49). The final result relates the elements of the σ-electron spin density matrix, ρ^σ, to those of the π-electron spin density matrix, ρ^π, as follows:

$$\rho^\sigma_{ab} = Tr\left(\rho^\pi G^{ab}\right) = \sum_{l,m} \rho^\pi_{lm} G^{ab}_{ml} \qquad (2.19)$$

In equation(2.19) a and b designate σ-type orbitals (S_a and S_b) which form the basis set for the σ-spin density matrix; l and m, correspondingly, denote π-type orbitals (p_l and p_m) on carbon. The elements of the G matrix are given by

$$G^{ab}_{ml} = \sum_j{}' \sum_{c,d} \frac{\langle mc|dl\rangle \rho^\sigma(o\to j)_{cd} \rho^\sigma(j\to o)_{ab}}{\epsilon_j - \epsilon_o} \qquad (2.20)$$

where c, d are σ-type orbitals,

$$\langle mc|\,d1\rangle = \iint p_m^*(1)S_d(1)(e^2/r_{12})S_c^*(2)P_1(2)d\tau_1 d\tau_2 \qquad (2.21)$$

$\epsilon_j - \epsilon_o$ is the excitation energy to the jth excited configuration of the σ electrons, and $\rho^\sigma(o\rightarrow j)_{cd}$ is the cd matrix element of the σ-electron spin density between the ground and jth excited configuration.

The hyperfine splitting, a^H, for a particular proton in a radical can now be expressed as:

$$a^H = (8\pi/3)g_N\beta_N\sum_{a,b}\rho^\sigma_{ab}\,\alpha^*(o)b(o) \qquad (2.22)$$

where a^H (in gauss) is directly proportional to the σ spin density evaluated at the position of the nucleus (designated O). It is therefore obvious from equations (2.19) and (2.22) that in order to calculate the hyperfine splittings, ρ^π matrix as well as the numerous G^{ab} matrices should be evaluated for each radical. These difficulties were overcome however, when McConnell(48) suggested two approximations which considerably simplify the calculations of hyperfine splittings.

Considering that the proton of interest is located at the centre of the 1s-σ orbital designated c and that it is bonded to carbon atom k with π orbital p_k and σ orbital d, McConnell assumed that: (a) the main contribution to ρ^σ is from $G_{kk}\rho^\pi_{kk}$. Contributions of the off-diagonal terms of the G matrix, such as $G_{lm}\rho^\pi_{ml}$, are negligible as are the diagonal terms $G_{mm}\rho^\pi_{mm}(m\neq k)$. Then splitting at proton c is expressed

$$a_c^H = \left[(8\pi/3)\, g_N \beta_N \sum_{a,b} G_{kk}^{ab} \alpha^*(0)\, b(0)\right] \rho_{kk}^{\pi} \qquad (2.23)$$

(b) the term in the bracket in (2.23) can be considered approximately constant for all hydrocarbon radicals and is designated Q.

On the basis of the foregoing assumptions, eq.(2.23) is reduced to equation (2.24) known as the McConnell relationship,

$$a_c^H = Q\rho_{kk}^{\pi} \qquad (2.24)$$

in which the isotropic proton hyperfine splitting is related linearly to the π-electron spin density ρ^{π} on the adjacent carbon atom, Q is a constant and its value was estimated by Jarrett(50), on theoretical grounds, to be -28 gauss. The negative sign of Q indicates that the unpaired spin induced in the 1s orbital of the proton is opposite in sign to that induced in the carbon π-orbital. This has been confirmed experimentally by Gutowsky et al.(51), using broad line NMR.

There are some situations, where ρ^{π} is fixed by symmetry or can be reliably determined, and an estimate of the value of Q can be obtained. For instance, in the methyl radical $a^H = Q = -23.03$ G ($\rho^{\pi}=1$). Also, in the benzene negative ion $a^H = 3.75$ G, and since $\rho_{Ci}^{\pi} = 1/6$, this gives Q = -22.5 G. Thus, it appears that although the McConnell relationship holds approximately, Q is not a fixed constant but

does vary somewhat from one molecule to another. Several improvements have been made in this relationship(52-55), while for neutral radicals, Q in equation (2.24) may be taken as constant with a value of about -23 G. In any case, with a semiempirical value of Q, McConnell's relationship has proved quite successful in interpreting the proton hyperfine splittings and in the semiquantitative correlation of ESR data for hydrocarbon ions with π-electron theory.

(c) Hyperfine splitting from other nuclei

The relationship between spin density and hyperfine splitting due to other nuclei also has been studied theoretically and expermientally. Karplus and Fraenkel(56) developed the calculation for ^{13}C hyperfine splittings. In their treatment, which is essentially an extension of the valence bond calculation on the $>\dot{C}-H$ fragment, they considered the case of two four-atom fragments from an aromatic system

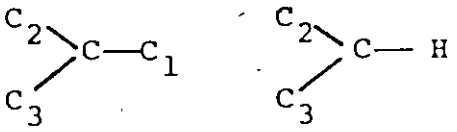

(I) (II)

The final result relates the hyperfine splitting produced by atom C to the π-spin densities on the C and Ci atoms as

$$a^C = 35.6\rho_C^\pi - 13.9\sum_i \rho_{Ci}^\pi \qquad (2.25)$$

$$a^C = 30.5\rho_C^\pi - 13.9\sum_i \rho_{Ci}^\pi \qquad (2.26)$$

where equation(2.25) and (2.26) apply for fragment (I) and

fragment (II), respectively.

In an analogous treatment, the ^{14}N hyperfine splittings for a nitrogen in an aromatic ring are related to the π-spin densities on the nitrogen and adjacent carbon atoms according to the equation (2.27), proposed by Henning(57)

$$a^N = Q_1\rho_N^\pi + Q_2(\rho_{C_1}^\pi + \rho_{C_2}^\pi) \qquad (2.27)$$

where $Q_1 = 19.1 \pm 1.7$ G and $Q_2 = 9.1 \pm 1.7$ G.

(d) β- and γ- Proton splittings: Hyperconjugation

The spectrum of ethyl radicals indicates that the protons of the methyl group interact with the unpaired electron to give hyperfine splitting of 26.9 G compared with 22.4 G for the α-protons. Also in other cases, such as the isopropyl and tert-butyl radical as well as aromatic radicals with methyl substituent groups, the β-proton interactions are comparable in magnitude with those of the α-protons.

Several theoretical treatments have been given in the literature(58,59,60) in order to describe the mechanism of interaction of β- and γ- protons with the unpaired electron. The possibility that some unpaired spin can find its way into the hydrogen 1s orbitals by a hyperconjugative mechanism is suggested, namely, the methyl protons lie in a plane parallel to the axis of the $2p_z$ orbital of the unpaired electron which is perpendicular to the C-C bond and therefore they are in a position such that their orbitals can overlap directly

with the carbon orbital possessing the unpaired electron. Such a process assumes that the unpaired electron in the carbon $2p_z$ orbital couples slightly with one electron in the C-H σ-bond (σ-π exchange interaction), leaving the other with a small positive spin density. In the molecular orbital treatment(60), considering the $\rangle\dot{C}\text{-}CH_3$ fragment the three protons are treated as a group in which linear combinations of the three hydrogen 1s orbitals (y_1,y_2,y_3) are combined with suitable orbitals on the carbon. Of the three possible combinations, $(y_1+y_2+y_3)$, $(y_1-\frac{1}{2}y_2-\frac{1}{2}y_3)$ and (y_2-y_3), the first has σ-symmetry (about the C-C bond) while the latter two have elements of π-symmetry (perpendicular to the C-C bond). So overlap of either of these π-type orbitals can lead to delocalization of the unpaired electron into the hydrogen 1s-orbitals.

It is found experimentally that the β-proton splitting is approximately equal to

$$a_\beta^H(\theta) = \left[B_o + B_2\cos^2\theta\right]\rho^\pi \qquad (2.28)$$

where θ is the dihedral angle between the axis of the $2p_z$ orbital and the projection of the C-H bond in the plane passing through this axis, and perpendicular to the C-C bond, B_o and B_2 are constants, and B_2 is at least an order of magnitude larger than B_o. The angular dependence of $a_\beta^H(\theta)$ indicated in (2.28) is expected if rotation of the methyl group about the C-C bond is restricted. If the methyl rota-

tion is free then an average over all θ's gives $\langle \cos^2\theta \rangle_{av} = \frac{1}{2}$ and for $\rho^{\pi} = 1$, equation (2.28) becomes

$$a_{\beta}^{H} = B_o + \frac{1}{2} B_2 \qquad (2.29)$$

with B_o = 4 G and B_2 = 50 G approximately.

(e) Spin density calculations

Using the relationships already given in the previous sections, the experimental spin distributions can be determined for many systems from the hyperfine coupling constants. The interpretation of the spin distributions in radicals has been made mostly in terms of the molecular orbital theory. The simple Huckel MO(62) treatment has been applied to many systems and good agreement between the observed and the estimated spin densities was found in certain systems.

In aromatic radicals, according to Huckel's MO theory each carbon atom has three trigonal sp^2 hybrid orbitals which form σ-bonds with other carbon and hydrogen atoms in the molecular plane, while the remaining $2p_z$ orbital on each carbon atom is used in the formation of π-molecular orbitals in which the π-electrons, it is assumed, move completely independently of one another and of the σ-electrons. These orbitals are taken to be linear combinations of the $2p_z$ orbitals

$$\psi_i = \sum_k a_{ki} \phi_k \qquad (2.30)$$

where, i and k refer to different molecular orbitals and different atoms respectively. When wave functions of this

type are used, then the spin density is the same as the unpaired electron density, i.e.,

$$\rho_k = \left| \alpha_{ki} \right|^2 \qquad (2.31)$$

where the unpaired electron is located in the molecular orbital ψ_i, and the spin density is being evaluated for the atomic orbital ϕ_k and α_{ki} is the coefficient of ϕ_k in the molecular orbital, ψ_i. Since the normalization of the wave function requires that the probabilities add up to one,

$$\sum_k \left| \alpha_{ki} \right|^2 = 1 \qquad (2.32)$$

the spin densities on the carbon atoms must also be normalized, namely,

$$\sum_k \rho_k = 1 \qquad (2.33)$$

Huckel MO treatment however, was found to be unsatisfactory in explaining the observed ESR spectra in many systems. One fundamental fault of this theory is its inability to predict negative spin densities, which were found to be important in many systems and this is because the molecular orbital wave function makes no allowance for the correlation of electrons with opposite spins.

In the Huckel MO treatment, the conventional single determinant wave function describing a radical with one unpaired electron and 2n other electrons paired in n molecular orbitals can be written as in equation (2.34),

$$\chi_o = \| \psi_1^2 \psi_2^2 \cdots \psi_n^2 \psi_o^\alpha \| \qquad (2.34)$$

in which 2n electrons occupy the orbitals $\psi_1 \ldots \psi_n$ in pairs, the odd electron of spin α (by convention) occupies ψ_o, and $\psi_o, \psi_1 \ldots \psi_n$ are expressed by equation (2.30).

In a simple wave function like (2.34) the spin density ρ is just equal to $|\psi_o|^2$ and is everywhere positive. However, the motions of electrons of α and β spins are affected in different ways by the odd electron and in order to allow for this difference a modified type of wave function, which automatically brings in negative spin densities, must be used.

Among the refined theoretical treatments McLachlan's self-consistent field MO treatment(63) has been used widely and successfully. McLachlan applied the self-consistent wave function (2.35) proposed by Pople and Nesbet(64) to calculate the spin distribution of the π-electrons in even alternant hydrocarbon ions and neutral odd radicals,

$$\Phi = \| \psi_1^\alpha \psi_1'^\beta \cdots \psi_n^\alpha \psi_n'^\beta \psi_o^\alpha \| \qquad (2.35)$$

In (2.35), electrons of α and β spin occupy independent sets of orbitals $\psi_o, \psi_1, \ldots \psi_n$ and $\psi_1' \ldots \psi_n'$. The orbitals are those which minimize the energy. In a wave function like (2.35) the effective field produced by the other electrons is different for electrons of different spin owing to the exchange term in the energy. Electrons of the same spin attract one another through the exchange force, and as a result high spin

density on a particular atom tends to induce a yet higher value on that atom, and negative values on the next neighbours. Therefore in this wave function the spin density ρ is

$$\rho = |\psi_o|^2 + \sum_1^n \left[|\psi_i|^2 - |\psi_i'|^2 \right] \qquad (2.36)$$

so that if $|\psi_i'|^2$ exceeds $|\psi_i|^2$ at the node of ψ_o, ρ becomes negative.

In his theory McLachlan applied the LCAO semiempirical method of Pariser and Parr(65) and the approximations of Pople and Brickstock(66) for the self-consistent orbitals, then use of perturbation theory gave for the spin density

$$\rho_r = c_{or}^2 - \tfrac{1}{2}\gamma \sum_s \pi_{rs}\, c_{os}^2 \qquad (2.37)$$

where π_{rs} is the mutual polarizability of the two atoms, the parameter γ is given by Pariser and Parr to be 10.53 eV and C_{or} is the coefficient for the atomic orbital ϕ_r in the molecular orbital ψ_o containing the unpaired electron. The mutual polarizability π_{rs} is calculated from the expression

$$\pi_{rs} = -4 \sum_i \sum_j \frac{C_{ri}\, C_{sj}\, C_{si}\, C_{rj}}{E_j - E_i} \qquad (2.38)$$

where i, j are occupied and vacant orbitals and E_i are the Hartree-Foch energy parameters.

The importance of the quantities in the expression (2.38) in the final result was tested by comparing the coefficients and energy parameters obtained by using self-consistent orbitals with those obtained when Huckel orbitals are

used. It is shown that although the relative energies are very different, the coefficients of the orbitals and especially the odd one are almost identical.

The use of Huckel orbitals in (2.38) instead of self-consistent ones, McLachlan proposed, will not make much difference since they are so alike provided that a proper choice of the resonance integral β is made so that the Huckel energies also can be safely used. According to the self-consistent theory, the resonance integral is

$$\beta_{rs}\ (\text{eff.}) = \beta_{rs} - \frac{1}{2} P_{rs}\gamma_{rs} \qquad (2.39)$$

where P_{rs} is the total bond order, β is taken to be the average of this quantity for all the bonds in the molecule and, using Pariser and Parr's parameters $\gamma = 10.53$ eV, $\beta_{12} = -2.39$, $\gamma_{12} = 7.30$ eV, β is about -4.5 eV in most cases, therefore

$$(\tfrac{1}{2})\,\gamma/\beta = -1.2 = -\lambda \qquad (2.40)$$

The spin densities deduced in this way by the perturbation theory with self-consistent and Huckel energies are almost identical and McLachlan finally concluded that the Huckel approximation gives just as reliable results as the more elaborate methods and adopted instead of the complicated expression (2.37) the simple formula

$$\rho_r = c_{or}^2 - \lambda \sum_s \pi_{rs}\, c_{os}^2 \qquad (2.41)$$

where π_{rs} is the numerical value (without β) of the mutual

polarizability of atoms r and s, C_{or} is the Huckel coefficient of the odd orbital on atom r, and the only adjustable parameter is λ. If a computer is used for the solution of the secular equations, the calculation of π_{rs} (directly) is not necessary, but ρ can be found from equation (2.36) written in its explicit form as

$$\rho_r = C_{or}^2 + \sum_{i=1}^{n} \left[|C_{ir}|^2 - |C'_{ir}|^2 \right] \qquad (2.42)$$

where C'_{ir} are the coefficients of the ordinary Huckel orbitals $\psi'_1 \ldots \psi'_n$ on atom r, and C_{ir} are the coefficients for the orbitals $\psi_1 \ldots \psi_n$ calculated with β_{rs} unchanged but the Coulomb integral α_r adjusted by $\alpha_r = + 2\lambda C_{or}^2 \beta$.

4. Anisotropic hyperfine interactions: Organic radicals in solids

(a) The spin Hamiltonian: Energy levels

In section (B-1) it was mentioned that the anisotropic interaction is due to the coupling between the magnetic moments of the electron and nucleus which is analogous to the classical interaction of two dipoles $\vec{\mu}_S$ and $\vec{\mu}_I$ separated by a distance $\vec{r}$.

For a system with one unpaired electron and one nucleus of spin $\vec{I}$ in an external field $\vec{H}$ the spin vectors $\vec{I}$ and $\vec{S}$ are fully decoupled so that each has its axis parallel to the field $\vec{H}$ and the Hamiltonian corresponding to the anisotropic or dipolar interaction for this system is given as

$$\mathcal{H}_d = g_s g_I \beta_s \beta_I \left[\frac{\vec{I}\cdot\vec{S}}{r^3} - \frac{3(\vec{I}\cdot\vec{r})(\vec{S}\cdot\vec{r})}{r^5} \right] \qquad (2.43)$$

where the anisotropy arises from the orientation dependence of the vector $\vec{r}$, the distance between the dipoles. This term can also be written in the scalar form as in equation (2.44)

$$\mathcal{H}_d = g_s g_I \beta_s \beta_I \left[\frac{1 - 3\cos^2\phi}{r^3} \right] \vec{I}\cdot\vec{S} \qquad (2.44)$$

where ϕ is the angle between the axis of the dipoles and the line joining them. Since in an atom or molecule the electron is not localized but is distributed over the region of space represented by the orbital wave function, the orientation dependent term in equation (2.44) must be replaced by its average over the whole spatial distribution of the unpaired spin, i.e., $\left\langle (1-3\cos^2\phi)/r^3 \right\rangle_{av}$. The total spin Hamiltonian therefore, analogous to (2.5) for the isotropic interaction, can be written as in equation (2.45)

$$\mathcal{H} = g_s \beta_s \vec{S}\cdot\vec{H} - g_I \beta_I \vec{I}\cdot\vec{H} + h\alpha' \vec{I}\cdot\vec{S} \qquad (2.45)$$

where

$$\alpha' = g_s g_I \beta_s \beta_I \left\langle \frac{1 - 3\cos^2\phi}{r^3} \right\rangle_{av} \qquad (2.46)$$

is the orientation dependent term.

Solution of equation (2.45) gives for the energy levels,

$$E_{M_I M_S} = g\beta M_S \vec{H} - g_I \beta_I M_I \vec{H} + h\alpha' M_I M_S \qquad (2.47)$$

The result is of exactly the same form as equation (2.8),

describing the isotropic interaction and the selection rules $\Delta M_S = \pm 1$, $\Delta M_I = 0$, are identical. Consequently, when g is isotropic and $M_S = \pm \frac{1}{2}$, the hyperfine spectrum resulting from this dipolar interaction consists of 2I + 1 equally spaced and equally intense lines, symmetrically distributed about the field H, where $H = h\nu/g_S\beta_S$. But now the line separations are dependent on the relative orientation of the orbital of the unpaired electron and the applied field and transitions occur at fields given by equation (2.48)

$$H_{M_I} = H + M_I a'/g_S\beta_S \qquad (2.48)$$

where $M_I = I, I-1, \ldots\ldots -I$.

When, as is usual, isotropic and anisotropic interactions both contribute to the hyperfine spectra, they are added to give the total hyperfine coupling constant A which will take the same symmetry properties as a'. Therefore, in the first-order treatment can be written

$$A = a + a' \qquad (2.49)$$

If A is measured along three orthogonal axes x,y,z, it is always possible to separate the isotropic and anisotropic components since $A_x = a + a'_x$, etc. For convenience, the tensor notation is used for representing experimental values of A_x, A_y, A_z, etc. In that case the tensor representing the total hyperfine interaction of a given nucleus may be separated into isotropic and anisotropic terms as follows:

$$\begin{vmatrix} A_x & & \\ & A_y & \\ & & A_z \end{vmatrix} = \begin{vmatrix} \alpha & & \\ & \alpha & \\ & & \alpha \end{vmatrix} + \begin{vmatrix} \alpha'_x & & \\ & \alpha'_y & \\ & & \alpha'_z \end{vmatrix} \qquad (2.50)$$

where the dipolar tensor has zero trace so that $(\alpha'_x+\alpha'_y+\alpha'_z)$ vanishes and α is just the average of the principal values A_x, A_y, A_z,

$$\alpha = (1/3)(A_x+A_y+A_z) \qquad (2.51)$$

The interpretation of anisotropic hyperfine coupling constants is based on calculations of $\left\langle \frac{1-3\cos^2\phi}{r^3} \right\rangle_{av}$ from the known wave functions of s-, p-, d-, etc., orbitals so that α' can be calculated from equation (2.46). It should be noted that this function vanishes for spherically symmetrical orbitals and hence s-electrons cause no anisotropic interactions while p-electrons cause hyperfine interactions with cylindrical symmetry, etc.

In order to make a reliable measurement of the components of the anisotropic tensor it is necessary to study a single crystal in which all the radicals are similarly oriented. In that case it is possible to extract from experimental observations the magnitude and direction of the principal axes of the coupling tensor and hence the orientation of the paramagnetic unit in the crystal.

(b) Dipolar line-broadening: Radicals in glassy solids

The interaction of electron and nuclear moments in isolated atom has been examined in the previous section(B-4a). In general, interaction between dipoles which belong to different atoms or molecules can also take place, and depending on the experimental conditions, such interactions may cause broadening of the absorption line to a greater or lesser extent. The magnetic field at a distance r from a dipole whose magnetic moment is $\vec{\mu}$ is approximately $\vec{\mu}/r^3$. Consequently in a real system to which an external field H_z is applied, the actual field experienced by a particular spin is the resultant of H_z and contributions from all other spins in the sample

$$H_{total} = H_z + H_{local} \qquad (2.52)$$

In order to determine the effect on the spin transitions which will occur when $h\nu = g_s \beta_s H_{total}$, it is necessary to estimate $\sum H_{local}$ and study its variation with time. Considering the system of two spins A and B separated by a distance r to which an external field H_z is applied, then B produces at A a magnetic field which can be resolved into a steady field with a constant component along the direction of the external field H_z and a rotating component perpendicular to H_z. The static component parallel to H_z is given by

$$H_{Bz} = \mu_{Bz}(1-3\cos^2\theta)/r^3 \qquad (2.53)$$

where μ_{Bz} is the z-component of the magnetic moment of B, and θ is the angle between $\vec{r}$ and $\vec{H}_z$.

In general, several neighbouring spins will contribute to the H_{local} according to equation (2.54)

$$H_{local} = \sum_i \mu_{iz}(1-3\cos^2\theta_i)/r_i^3 \qquad (2.54)$$

where i represents the ith spin. Since the total field at A is now $H_z + H_{local}$ the Larmor frequency of A will be shifted by an amount corresponding to H_{local}. In a random system, e.g., an amorphous solid, each spin will have a different environment, experiencing a different H_{local} and therefore absorption from a radiation field (of constant frequency) will take place over a range of magnetic field corresponding to H_{local} and the observed line may therefore be considered as an envelope of much narrower lines, each corresponding to transitions of spins subjected to a particular H_{local}. The distribution of H_{local} in a random system is approximately gaussian, therefore the observed line will be gaussian in shape when dipolar interactions are the main source of broadening.

Since the magnetic moment of an electron is about a thousand times greater than that of most nuclei it is clear that neighbouring unpaired electrons will have the dominant effect. However, for dilute solid systems, e.g., free radicals produced by irradiation and trapped in a glassy matrix, it is possible for neighbouring nuclei to cause line-broad-

ening while the contribution from electron dipole-electron dipole interactions may be less than one gauss.

In general, modulation of the dipole-dipole interactions in a solid system is caused by vibrations of a semi-rigid lattice, and displacements from the equilibrium configuration are small. Hence, the angular dependent interaction (with terms in $1-\cos^2\theta$) is not averaged completely and in randomly oriented solid samples would cause considerable line-broadening. In a fluid medium however, molecules move in a completely random manner with respect to one another and to the direction of the external field and if the rate of tumbling of radicals in solution is fast enough only the isotropic components of A [eq.(2.50)] are left with negligible line-broadening.

(c) Second order transitions

The first-order analysis of nuclear hyperfine spectra will be found quite adequate for most purposes and one finds a very great measure of agreement with theory for almost all radicals in solution and in the description of the main features of the spectra observed in single crystals. Such interpretations are based on a number of assumptions, i.e., the independent quantization of electron and nuclear magnetic moments along the direction of the applied field, the validity of the selection rules $\Delta M_S=\pm 1$, $\Delta M_I=0$, and the neglect of the direct interaction of nuclear spins with the magnetic field.

However, there are a number of cases in which extra satellite absorption lines not predicted by first-order treatment appear in the ESR spectra of radicals in solid matrices or in solution. In particular, the satellite lines observed in the hyperfine components of trapped hydrogen atoms(37,39) were attributed to the flipping, in conjunction with the electron spin, of neighbouring protons to which the electron spin is weakly coupled through dipole-dipole interaction. A theoretical treatment of these transitions has been given by Trammel, Zeldes, and Livingston(38). A more general theory of second-order transitions which includes the case for strong coupling as is observed in the CH fragment, has been developed by Miyagawa and Gordy(67).

In the case of weak coupling, Trammel et al.(38) assumed the interaction of the electron with the applied field to be much stronger than interaction involving nuclei, the orbital angular momentum of the electron is assumed to be either zero or completely quenched, and internuclear dipole-dipole interactions are neglected. Including the nuclear Zeeman term, the energy eigenvalues to first-order are given as

$$E_{Me,Mi} = g_e\beta_e Me\,\vec{H} - \sum_i g_i\beta_N Mi\left|\vec{H}+\vec{h}_{ei}(Me)\right| \qquad (2.55)$$

where e and i refer to electron and nuclei, respectively, $\vec{H}$ is the applied field (taken in the z direction), and $\vec{h}_{ei}(Me)$ is the field of the electron in state $Me(\pm 1/2)$ at the ith

nucleus. The important new feature in (2.55) is that both the magnitude and the direction of $[\vec{H}+\vec{h}_{ei}(Me)]$ depend on the direction of the electron spin. The magnetic fields at a nucleus are indicated vectorially:

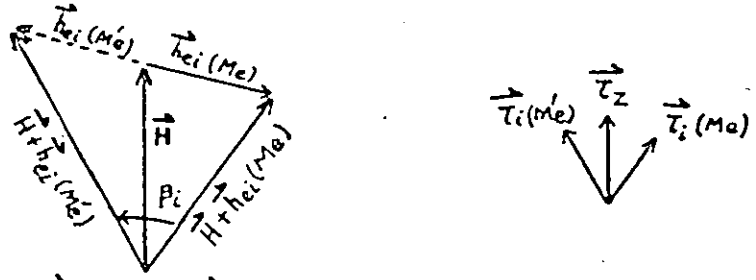

where $\vec{\tau}_i(Me)$, $\vec{\tau}_i(Me')$, $\vec{\tau}_z$, are the corresponding unit vectors. If an oscillating field of the proper frequency is applied to a sample containing some electrons, transitions are induced between the levels with energies given by equation (2.55). The transition probabilities between levels of the same Me but with one Mi differing by one unit are proportional to $g_i^2\beta_N^2[H_\omega(\perp\vec{\tau}_i)]^2$, where $H_\omega(\perp\vec{\tau}_i)$ is the component of the oscillating field which is perpendicular to $\vec{\tau}_i$. In general $\vec{\tau}_i$ is not in the direction of $\vec{H}$ (the z direction) and transitions can be induced by an oscillating field along $\vec{H}$. The transitions observed in ESR are for levels of different Me. Here the transition probabilities are proportional to $g_e^2\beta_e^2[H_\omega(\perp\vec{H})]^2$, where $H_\omega(\perp\vec{H})$ is the component of the oscillating field perpendicular to $\vec{H}$. When the transition is made each $\vec{\tau}_i$, in general, changes direction. This change in the direction of quantization for $\vec{S}_i$ (nuclear spin vector) permits changes in Mi to occur. In particular, the transition probability from state $|Me,Mi\rangle$ to $|Me',Mi'\rangle$, where Me' is different from Me, is given

by equation (2.56)

$$T_{Me\ Mi;Me'\ Mi'} = \frac{g_e^2\beta_e^2[H_\omega(\perp\vec{H})]^2}{4\omega\hbar^2}\prod_i\left|D^{Si}_{MiMi'}(\beta_i)\right|^2 \qquad (2.56)$$

where D^{Si} is the rotation matrix for a particle of spin Si, β_i is the angle between $\vec{\tau}_i(M_e)$ and $\vec{\tau}_i(M_e')$, and $2H_\omega(\perp\vec{H})$ is the strength of the sinusoidal magnetic field perpendicular to $\vec{H}$ and oscillating at angular frequency ω. For β_i small then

$$D^S_{MM'} \propto \beta_i^{|M-M|} = \left|\frac{2hi_\perp H}{H^2-h_{ei}^2}\right|^{|M-M'|} \qquad (2.57)$$

where $hi_\perp$ is the component of $\vec{h}_{ei}$ perpendicular to $\vec{H}$. In that case (β_i small) according to eqs.(2.56) and (2.57) the most prominent transitions are the ones in which $\Delta M=0$ for the nucleus, while transitions for which $\Delta M\neq 0$ will be reduced in intensity by a factor $\beta^{2|\Delta M|}$. According to equation (2.57), for β_i to be small it is sufficient for h_{ei} to be small compared to H, but not necessary since $hi_\perp$ may be small. This situation is realized for nuclei sufficiently far from the electron.

For the case in which the unpaired electron is concentrated on a single atom the field, $\vec{h}_{ei}$, of the electron at the ith nucleus is given as

$$\vec{h}_{ei} = Me\ g_e\beta_e\left[\frac{3(\vec{r}_i\cdot\vec{\tau}_z)\vec{r}_i}{r_i^3} - \vec{\tau}_z\right] \qquad (2.58)$$

The above equation put in the scalar form is expressed as

$$h_{ei}^2 = Me^2\, g_e^2\beta_e^2 \cdot \frac{1}{r_i^6}[(1-3\cos^2\theta_i)^2+9\cos^2\theta_i\sin^2\theta_i]$$

$$hi_{\perp} = Me\, g_e\beta_e \cdot \frac{1}{r_i^3}\,(3\cos\theta_i\sin\theta_i) \qquad (2.59)$$

$$hi_{\parallel} = Me\, g_e\beta_e \cdot \frac{1}{r_i^3}\,(3\cos^2\theta_i-1)$$

where $\vec{r}_i$ is the vector distance between the ith nucleus and the nucleus of the atom containing the unpaired electron, and θ_i is the angle between this vector and $\vec{H}$. Since the only magnetic nuclei in the system are protons, the appropriate rotation matrix is

$$D^{(1/2)} = \begin{vmatrix} \cos(\beta/2) & -\sin(\beta/2) \\ \sin(\beta/2) & \cos(\beta/2) \end{vmatrix} \qquad (2.60)$$

hence, for h_{ei} small according to the equation (2.55) the satellites will be spaced at $\pm g_i\beta_N H$ from a central line at $g_e\beta_e H$.

Now from equations (2.56), (2.57), (2.59) and (2.60)

$$\frac{T_1}{2T_2} \cong \frac{9}{8}\cdot\sum_i \frac{g_e^2\beta_e^2}{H^2 r_i^6}\,\sin^2\theta_i\cos^2\theta_i \qquad (2.61)$$

where the ratio of intensity of either satellite line, T_1, to that of the two superimposed central lines, $2T_2$, is given. For a large number of randomly oriented systems, such as would be found on measurements of polycrystalline or glassy materials, equation (2.61) is reduced to equation (2.62)

$$\frac{\overline{T}_1}{2\overline{T}_2} \cong \frac{3}{20} \left\langle \sum_i \frac{g_e^2 \beta_e^2}{H^2 r_i^6} \right\rangle_{av} \qquad (2.62)$$

Therefore, from the experimental ratio $\overline{T}_1/2\overline{T}_2$ it is possible to calculate an effective single-proton distance defined as

$$r_{eff.} \equiv \left[\left\langle \sum_i \frac{1}{r_i^6} \right\rangle_{av} \right]^{1/6} \qquad (2.63)$$

It should be noted that the satellite intensity, being proportional to $1/r^6$, is insensitive to all but the nearest protons. If observations were made with a spectrometer of sufficient sensitivity, a second set of satellites ($1/r^{12}$ intensity dependence) can be observed corresponding to two neighbouring protons concurrently changing state.

CHAPTER III
EXPERIMENTAL

The spectrometer

The apparatus and experimental techniques used for the observation of ESR spectra are by now well established and an overall summary and bibliography of both the theoretical and the practical aspects of the instrumentation can be found in the reference book by Poole(68).

In general, the essential features of any ESR spectrometer are (a) a source of microwave radiation of constant frequency and variable amplitude,(b) a means of applying the microwave power to the paramagnetic sample,(c) a means of measuring the power absorbed from the microwave, and(d) a homogeneous but variable magnetic field.

Although most ESR spectrometers employ radiation of frequency about 9,500 MHz corresponding to the microwave X-band, measurements can also be made at Q-band (~35,000 MHz), or K-band (~25,000 MHz). The principal object of varying the frequency is to sort out the frequency-dependent and the frequency-independent terms in the Hamiltonian. Hyperfine structure intervals will be independent of frequency, and anisotropic g-factors will produce separations which vary linearly with the frequency. Also, the higher frequency Q-band spectrometers offer a very significant improvement in sensitivity in the cases where the sample size is limited,e.g.,

in single crystal studies or in studies at very low temperatures where the sample usually saturates readily and it is not possible to use the maximum available power. Otherwise X-band is usually more convenient, particularly for liquid phase studies. The usual source of radiation of this frequency is a klystron oscillator, delivering 30-300 mW of power. The energy is transmitted by means of a waveguide of dimensions appropriate to the wavelenght of the radiation and the sample is placed inside a resonant cavity whose purpose is to concentrate energy on to the sample by multiple reflections of the travelling microwave from the two end walls. Detection is generally performed by a semiconducting crystal detector which acts as a rectifier, converting the microwave power into direct current. Finally, the steady field is generally produced by an electromagnet so arranged that the steady field H and the oscillating field of the microwave radiation, $2H_1 \cos \omega t$, are mutually perpendicular.

In this study, the ESR experiments were conducted with a JEOLCO-JES-3BS-X spectrometer system operating at a frequency 9,400 MHz (X-band). The magnetic field was modulated at 100 KHz. The spectrometer employed a cylindrical cavity operating in the TE_{011} cylindrical mode. The cavity resonator could be applied in combination with a variety of accessories. The variable temperature accessory was used to cover the range from -185°C to -100°C, and the low-temperature control was achieved by feeding evaporated cold nitro-

gen gas at regulated flow rate to the vicinity of the sample. The temperature was checked with a thermocouple with an estimated precision of $\pm 2°$ C. For measurements at liquid nitrogen temperatures (-196° C), an insertion-type dewar vessel was used. The lower portion of this vessel, which is inserted into the cavity resonator, is made of transparent quartz, thus enabling exposure of the sample to ultraviolet rays. A window for ultraviolet application is provided in the cavity and UV-radiation can reach the sample through the window during measuring operation. All UV-irradiations were performed directly into the cavity with a PHILIPS SP-500W (directed radiation) high-pressure mercury lamp whose beam was applied effectively to the sample through a condenser lens

For all UV-irradiation experiments at low temperatures, quartz-glass sample tubes (3mm outside diameter) were used and the field was calibrated by simultaneous recording of the spectrum of the sample and that of an ESR marker consisting of MgO powder which contained a small quantity of thermally dispersed Mn^{2+} ions (69).

In the liquid phase, all the experiments were carried out at room temperature ($\sim$25° C.) Although the radical species employed here were air-stable it was found necessary, in most cases, to record the ESR spectrum after the samples had been thoroughly deoxygenated in order to observe well-resolved hyperfine structure. This was achieved by using standard vacuum techniques. In general, solvents with low

dielectric constants were used and therefore the effect of the sample volume on sensitivity was negligible. In this case, the 5mm (o.d.) quartz tubes, employed for these experiments, allowed for large volumes of very dilute radical solutions and therefore optimum resolution could be achieved. The field calibration was performed by recording simultaneously the ESR spectrum of the sample and that of a dilute aqueous solution of peroxylamine disulfonate ion-radical, $(SO_3)_2\dot{N}O^{2-}$, based on the ^{14}N coupling constant, α_{NO}^{N} = 13 G, given by Windle and Wiersema(70).

Finally, all NMR spectra were recorded with a Varian HA 100 spectrometer. The calculations mentioned in this work were carried out on a CDC 6400 computer.

CHAPTER IV

SPIN-LABELLED LIGANDS

A. INTRODUCTION

Spin-labelled ligands have been used in inorganic chemistry in a number of solution studies of metal complexes by ESR and/or NMR, though with limited success. The intention of this chapter is to present the use of the spin-labelled ligand approach in a study of metal-ligand bonding. This technique may prove to be generally useful for such studies provided that a proper choice of the radical ligand is made.

A spin-labelled ligand is defined as a molecule containing two functional groups, one of which possesses an electron pair suitable for donation to a metal. The other functional group must possess the unpaired electron necessary to produce an ESR signal. It is the radical function which is used as a probe for electronic changes at the Lewis base site at the other end of the molecule.

Ideally, the two functions must be connected, but not too closely connected. If the unpaired electron is too well removed from the site of interaction with the metal it will obviously be an insensitive probe. If on the other hand the Lewis base and radical functions are combined in the same

group, the ligand-metal bonding may be very different from that of the unlabelled ligand. A number of ESR studies involving radical ligands of this latter type have been quoted in Chapter I, i.e. o-semiquinones(15), alkyl nitroxides(18,19, 20,21), where the unpaired electrons remain essentially localized on the ligand. In other cases, e.g., o-phenanthroline(14) negative ion and dithiolate(71) ions, the interactions with the metal are sufficiently strong to lead to complete delocalization of the electron and it is not clear whether the compound should be described as a complex of a radical with a metal ion in a high oxidation state or a complex of a non-radical ligand with a metal in a lower oxidation state. Thus, for example, V(dipyridyl)$_3$ could be described as a complex of V^{3+} with three radical anions, a complex of V° with three neutral diamagnetic ligands or any intermediate combination.

In general however, previous ESR work on this field does not include any instances in which a conscious attempt has been made to separate the Lewis base and radical functions. In the present study, pyridine was chosen for the Lewis base part of the molecule and both the semidione groups and nitroxide groups were used to provide the spin label.

The radical ligands, 4-pyridylpropane-1,2-semidione (I) and 4-pyridyl-t-butyl nitroxide (II) have been prepared and their metal complexes studied.

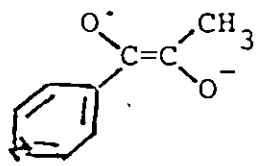

(I)

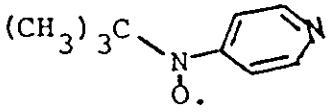

(II)

The use of spin-labelled ligands with structures (I) and (II) is advantageous in a number of ways.

(a) Pyridine can readily form complexes with a wide variety of metal ions. It also possesses a π-system which can form a link with the radical group.

(b) The extent of electron delocalization is sufficiently strong to allow for high sensitivity to electronic changes at the Lewis base site, however, the major fraction of the unpaired electron is concentrated on the radical function and hence the spin-labelled ligand is only slightly perturbed.

(c) Both semidione groups and nitroxide groups are capable of forming relatively stable radicals (in particular, the radical ligand (II) is indefinitely stable).

(d) Their ESR spectra show well-resolved hyperfine structure and therefore detailed information about the redistribution of the spin density within the ligand due to the complexing of the metal can be obtained.

(e) Radical (II), being soluble in a variety of polar as well as non-polar solvents, can be studied in the presence of metal ions whose solubility is limited only to certain solvent systems.

B. EXPERIMENTAL

1. Synthesis of Ligands

(a) 4-Pyridylpropane-1,2-Semidione

One method of generating semidiones is to expose a solution of a monoketone in dimethyl sulfoxide(DMSO) containing potassium t-butoxide [$(K^+ \ ^-OC(CH_3)_3$] to a trace of oxygen. The mechanism by which reactions of this type lead to the formation of semidione radicals has been discussed by Russell(72).

In the present case, a few drops of commercially available 4-pyridylethyl ketone () were added to DMSO or DMSO/THF mixtures (THF=tetrahydrofuran) which contained potassium t-butoxide. After a few minutes of exposure to atmospheric oxygen the solution became red indicating the formation of the radical. This technique involves the diketone as an intermediate which can then be reduced to semidione by $^-OC(CH_3)_3$= B^- or the anion of the diketone, namely,

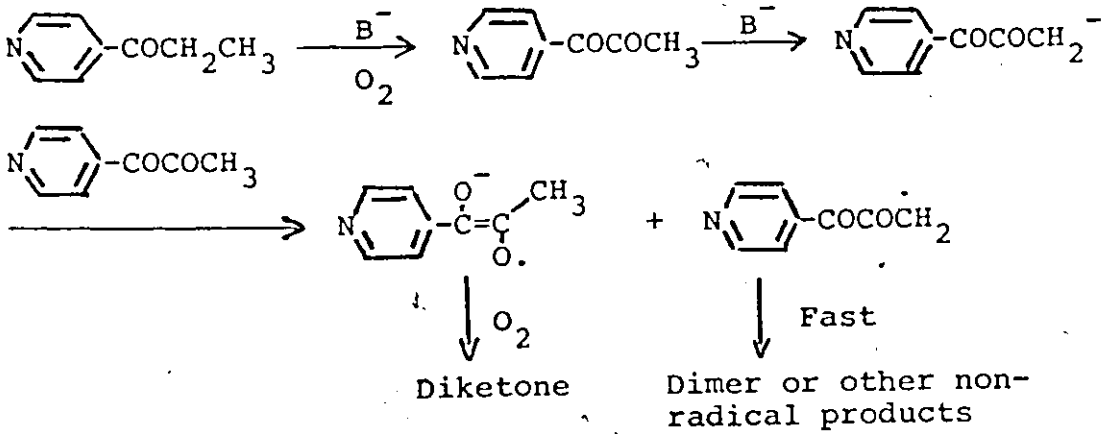

The radical obtained in this way was not isolated but used in the reaction mixture.

(b) 4-Pyridyl-t-Butyl Nitroxide

This radical was prepared by the reaction sequence:

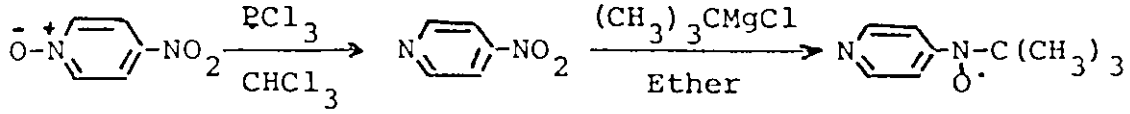

The preparation of the analogous p-tolyl radical has been reported by the reaction of t-butyl magnesium chloride with p-nitrotoluene(73).

As indicated above, the first step in preparing radical (II) is the preparation of 4-nitropyridine(74). Commercially available 4-nitropyridine 1-oxide was further purified by recrystallization from acetone. To 1 g of pure 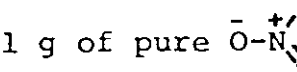 (m.p. 159°C) suspended in 15 ml of ice cold chloroform, 1.9 ml of phosphorous trichloride were added and the mixture was heated for 1 hour at 70°-80° C. The mixture was cooled, diluted with water, made alkaline with sodium hydroxide, and 4-nitropyridine extracted with chloroform. The organic phase was then dried over anhydrous sodium sulfate and the chloroform solution was evaporated to dryness. The residue, recrystallized from petroleum ether, gave 4-nitropyridine as pale yellow crystals of melting point 48° C which was further checked for impurities by NMR. The final step for the preparation of the radical involves the reaction of 4-nitro-

pyridine with t-butyl magnesium chloride. This step was carried out as follows: A solution of 1.24 g of 4-nitropyridine in 100 ml of dry ether was added dropwise and with constant stirring to an ice cold, freshly prepared ethereal solution containing 0.03 moles of t-butyl magnesium chloride(75). After neutralization of the reaction mixture with a solution of ammonium chloride (non-saturated), the radical was extracted with ether and the organic phase dried over anhydrous sodium sulfate. Finally, the ethereal solution containing the radical was concentrated under vacuum and the product stored over anhydrous sodium sulfate at room temperature.

2. Procedure for Preparing Samples

The semidione radical, as mentioned earlier, was not isolated from the reaction mixture. Since the solvents used in the preparation of this radical (DMSO or DMSO/THF) have high dielectric constants, it was necessary to reduce the sample volume so that the adverse effect of the solvent on sensitivity could be compensated. For this purpose, capillary sample tubes were used in this case. On the other hand, the high oxygen content in the sample did not have any effect on the resolution of the ESR spectra; therefore, by adjusting the radical concentration so that line-broadening from this source could be avoided, the ESR spectra were recorded without previous deoxygenation of the samples.

In the case of the nitroxide radical the samples were prepared as follows: One part of the concentrated

ethereal solution containing the radical was diluted with the particular solvent by a factor about 100. The low dielectric constants of the solvents used (Benzene, 1,4-dioxane, or benzene/THF and 1,4-dioxane/THF mixtures) allowed for large sample size and strong ESR signals coupled with good spectral resolution could be achieved. In this case, however, the samples had to be thoroughly deoxygenated before recording their ESR spectra.

Finally, the samples used for recording the ESR spectra of the nitroxide radical in the presence of metal compounds were prepared in the following manner: First, a clear, saturated solution of the particular metal compound in THF was prepared. One part of the THF solution was added to ten parts of either 1,4-dioxane or benzene (depending on the solubility of the metal compound) and the resulting mixture filtered (if not clear). Then, one part of the ethereal solution of the radical was added to 100 parts of the benzene/THF or 1,4-dioxane/THF solvent system. The final mixture, containing now the radical and excess of the metal compound, was placed in the ESR tube, deoxygenated on the vacuum line and its ESR spectrum recorded at room temperature.

C. RESULTS

1. ESR Spectra of Ligands

The ESR spectrum of radical (I) is shown in Figure IV-1. 45 of the possible 108 lines are resolved and the analysis

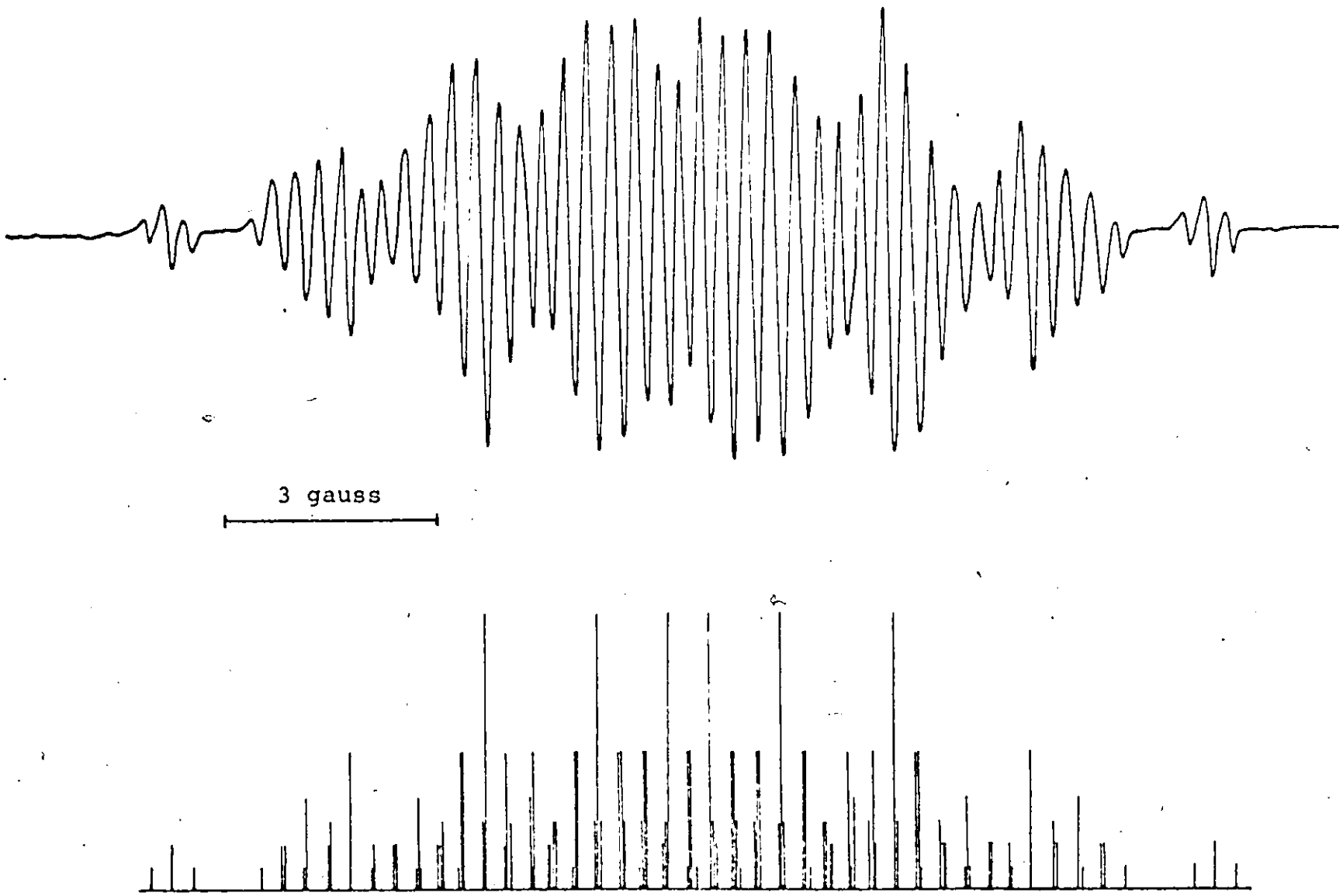

FIGURE IV-1. ESR spectrum of 4-pyridyl propane-1,2-semidione radical in DMSO solution.

is straightforward as shown also in Figure IV-1. This spectrum arises from splittings by two sets of two equivalent protons (I=1/2), one set of three equivalent protons (methyl group) and one ^{14}N nucleus of spin I=1. The derived hyperfine coupling constants for this radical may be compared with those reported for the radical containing a phenyl group rather than a pyridyl group and are shown in Table IV-1. The coupling constants corresponding to the phenyl compound have been shown to be consistent with spin densities calculated by the McLachlan method(63) and the similarity with those obtained for radical (I) confirms the correctness of the assignment. Although these calculations predict zero spin-density at the position 11, however, the large splittings arising from the methyl protons are consistent with a hyperconjugation mechanism for β interaction which has been discussed in Chapter II, section B-3d.

The analysis of the spectrum in Fig.IV-1, showing the equivalence of protons 3,5 and 2,6 in pairs as well as the equivalence of the three protons of the methyl group, implies that the semidione group rotates freely about the N  -C bond and the methyl group about the C-CH_3 bond. It may also be assumed by analogy with the phenyl compound that radical (I) has a trans configuration. Chelation of a metal ion with the semidione oxygens is therefore unlikely.

The ESR spectra of radical (II) are also well-resolved and analysis is again straightforward. No splitting is ob-

TABLE IV-1

Hyperfine coupling constants (gauss) of 1-phenylpropane-1,2-semidione and 4-pyridylpropane-1,2-semidione[a].

Radical	a(Position)[b]				Ref.
	12	3	1,5	2,4	
$(C_6H_5C(O.)=\dot{C}(\bar{O})CH_3)$	3.43	1.84	1.59	0.53	72
$(C_5H_4NC(O.)=C(\bar{O})CH_3)$	2.6	1.6	1.9	0.3	

[a] Values obtained in DMSO solution at room temp.

[b] Numbering system:

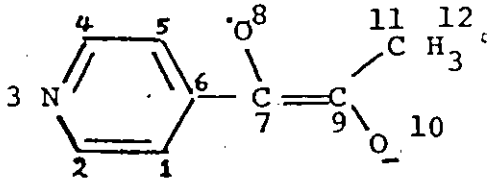

TABLE IV-2

Hyperfine coupling constants (gauss) of 4-pyridyl-t-butyl nitroxide radical.

Radical	a(Position)				Solvent
	a^N_2	a^N_6	$a^H_{4,8}$	$a^H_{5,7}$	
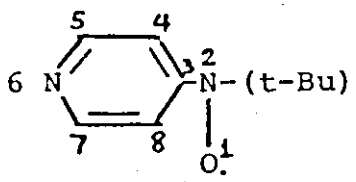	10.57	1.26	2.17	0.63	Benzene
	10.70	1.23	2.16	0.63	1,4 Diox.
	10.52	1.23	2.16	0.64	Benz./THF (11:1)
	10.74	1.23	2.16	0.63	Diox./THF (11:1)

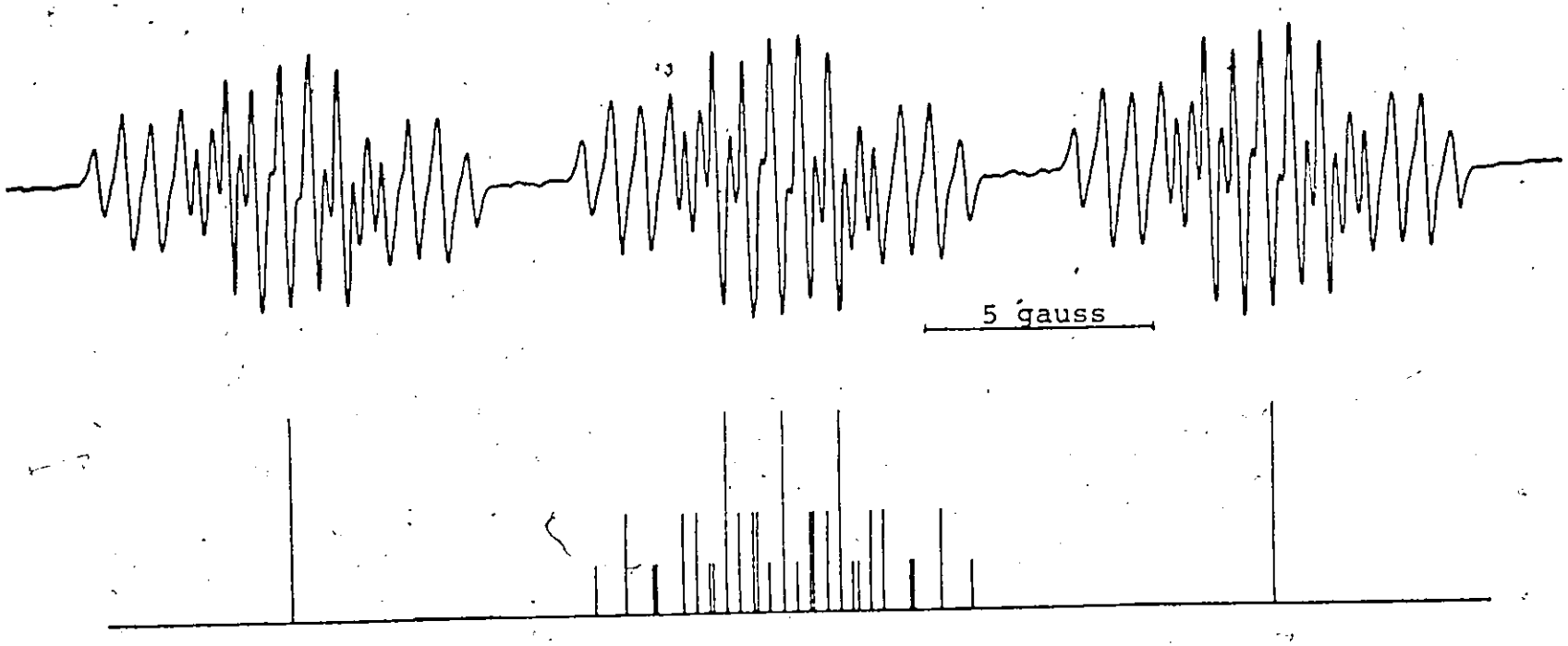

FIGURE IV-2. ESR spectrum of 4-pyridyl-t-butyl nitroxide radical in benzene/THF mixture.

served from the protons of the t-butyl group. 69 of the predicted 81 lines (arising from two sets of two equivalent protons and two non-equivalent ^{14}N nuclei) are resolved. Here again the nitroxide group is rotating freely about the C-N bond. A typical spectrum is shown in Figure IV-2. It proved convenient to prepare metal complexes of this radical in several different solvents. The extent of the variation of hyperfine constants with solvent was therefore checked by recording the spectra of the free radical in several solvent systems. The results are shown in Table IV-2.

It should be mentioned that the semidione radical ESR signal is sufficiently strong for observation for a period of 12-15 hours, while the nitroxide radical is indefinitely stable.

2. Complexing of Radicals with Metal Ions

Only very limited success was achieved in forming metal complexes of the semidione radical. Addition of the ether and trimethylamine complexes of the very strong Lewis acid BF_3 to a solution of the radical in DMSO lead to the observation of the ESR spectrum of Figure IV-3. Although this spectrum could not be resolved, the additional lines however, indicate that complexation of BF_3 with the spin-labelled ligand does occur but more than one paramagnetic species are present. There is no evidence as to where complexation occurs. The pyridine nitrogen or the semidione oxygen atoms are both possible.

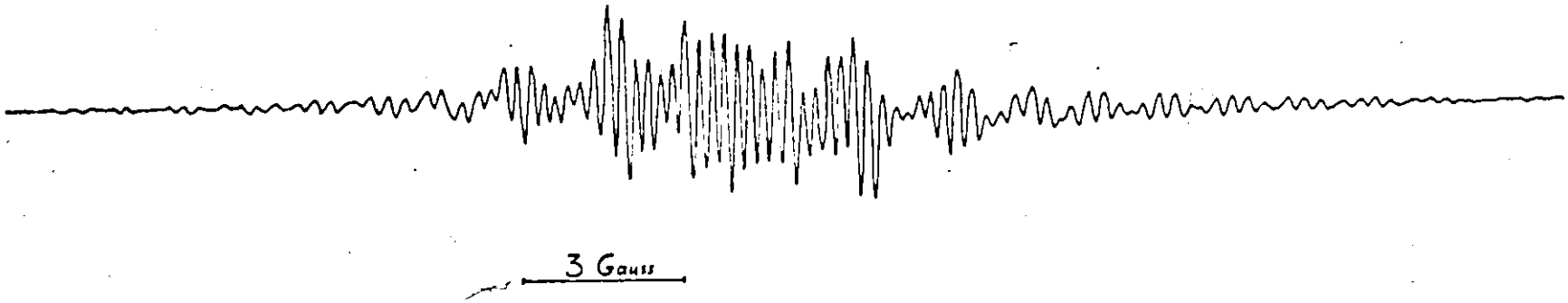

FIGURE IV-3. ESR spectrum of 4-pyridyl propane-1,2-semidione radical ion obtained in the presence of excess $(C_2H_5)_2OBF_3$ in DMSO solution.

A number of attempts were made to produce zinc complexes of the semidione radical by adding various zinc salts and labile complexes to the radical in DMSO or DMSO/THF mixtures. These experiments lead to destruction of the radical. The problem probably lies in the ready oxidation of semidiones except in strongly basic solution (see mechanism in Sec. B-1a). Addition of metal ions removes the base [$(CH_3)_3CO^-$] followed immediately by oxidation of the radical. This occurs even in solutions which have been carefully deoxygenated on a vacuum line. An attempt was also made to produce complexed radicals by oxidation of the compound $Zn(N\langle\rangle\text{-}COCH_2CH_3)_2(SCN)_2$ but this also proved unsuccessful.

Experiments with the nitroxide labelled ligand proved more fruitful. The stability of this radical is unaffected by the presence of metal compounds except in one or two special cases. The results obtained fall into six different classes.

(1) Addition of the metal compound leads to no change in the ESR spectrum of the radical. In this class fall complexes such as $Co(acac)_3$ (acac=acetylacetone) for which replacement of the chelating acetylacetonate would not be expected. Any change due to the presence of the spin-labelled ligand in the second sphere is apparently too small to observe. Similarly, the radical will not replace phosphine in $Pd(P\phi_3)_2Cl_2$ (ϕ=phenyl) or pyridine in $Co(Py)_3(NCS)_2$ Cl to any observable extent. Also, no evidence could be found for in-

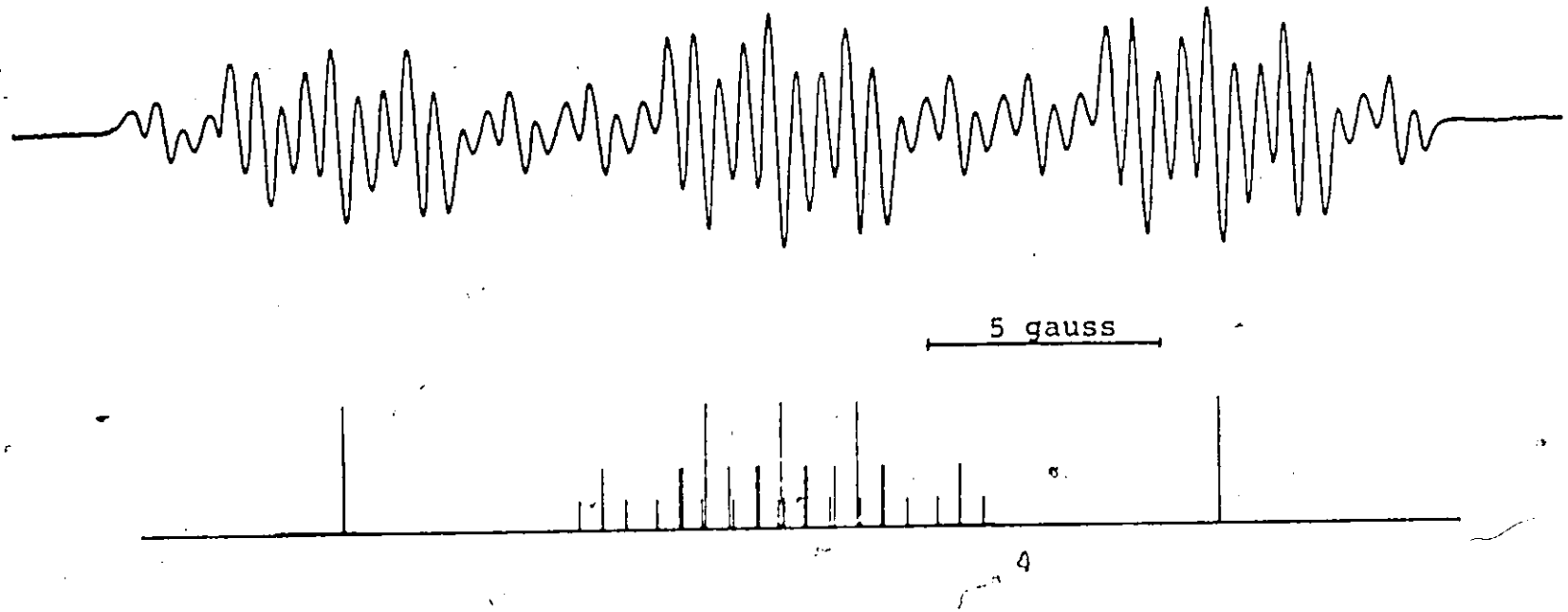

FIGURE IV-4. ESR spectrum of 4-pyridyl-t-butyl nitroxide radical in the presence of excess $ZnCl_2$ in benzene/THF mixture.

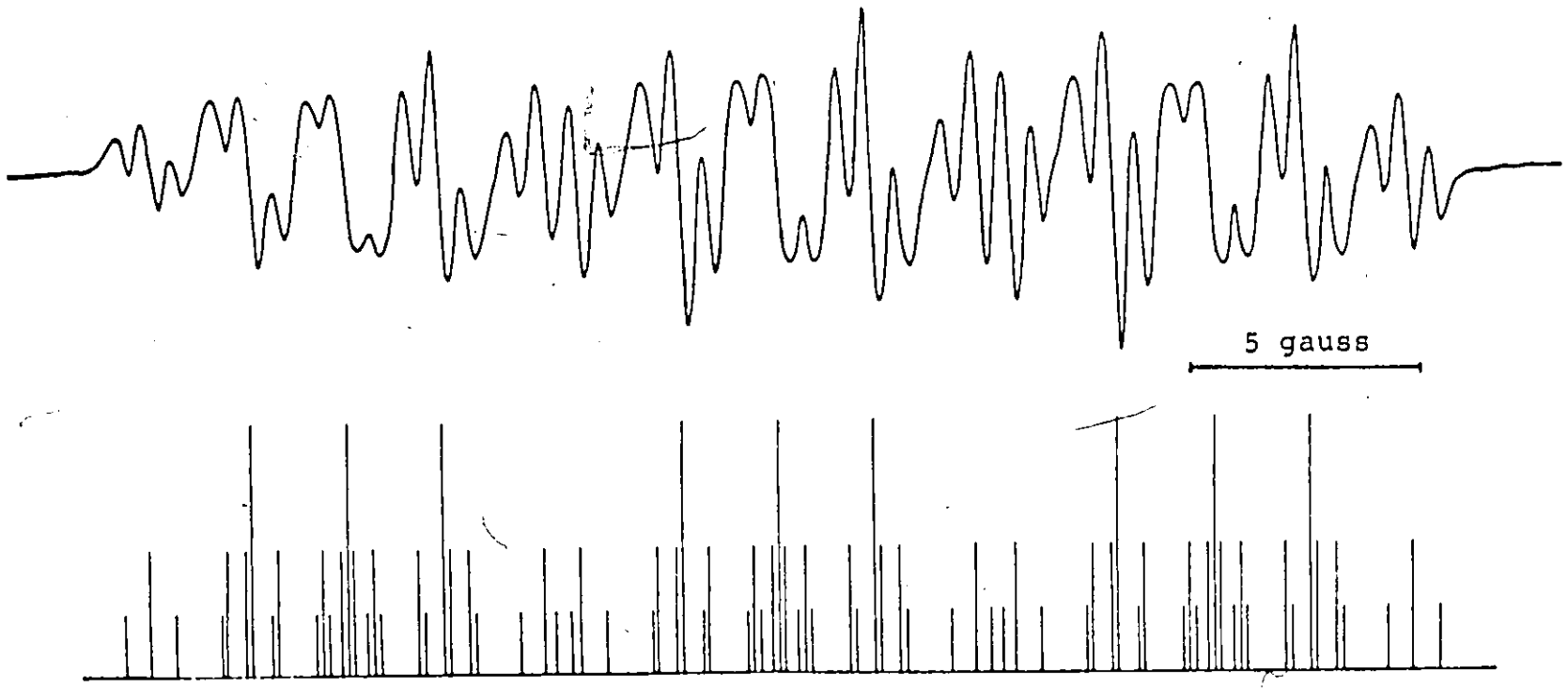

FIGURE IV-5. ESR spectrum of 4-pyridyl-t-butyl nitroxide radical obtained in the presence of excess $Pd(NO_3)_2$ in benzene/THF mixture.

crease in the metal coordination number on the addition of $Pt(acac)_2$, $Pd(acac)_2$ or zinc phthalocyanine.

(2) Addition of excess of the metal compound leads to complete complexation of the spin-labelled ligand. In these cases, well resolved and analyzable spectra are obtained. Results in this class were obtained with a variety of zinc compounds, with mercury halides, with cadmium iodide and with palladium hitrate. Representative example of the spectra obtained with Zn, Cd, and Hg compounds is shown in Fig. IV-4. Also, the type of spectrum obtained with palladium nitrate is shown in Fig. IV-5.

The hyperfine coupling constants derived from the analysis of the several spectra in this class are given in Table IV-3.

(3) Complexation of the spin-labelled ligand definitely occurs but more than one radical species are present. The ESR spectra obtained are complex and generally unsymmetrical about the centre of the spectrum. Analysis of such overlapping spectra is not feasible. This type of spectrum was observed on the addition of $Zn(\phi NH_2)_2I_2$, $Zn(Py)_2Br_2$, $Zn(Py)_2(SCN)_2$, $Pd(hfac)_2$ (hfac=hexafluoroacetylacetone), $Zn(hfac)_2(H_2O)_2$ and $Pd(tfac)_2$ (tfac=trifluoroacetylacetone). In most cases a mixture of free and complexed ligands is probably present but two different environments for complexed ligand represents another possibility. The spectrum of

TABLE IV-3

Hyperfine coupling constants(gauss) and experimental spin-densities of 4-pyridyl-t-butyl nitroxide in the presence of metal compounds.

Metal compound	a(position)[a]				ρ_2^N (Exper.)[b]
	a_2^N	a_6^N	$a_{4,8}^H$	$a_{5,7}^H$	
-	10.52[c]	1.23[c]	2.16[c]	0.64[c]	0.207[c]
$Zn(TU)_2Cl_2$[e]	9.47	1.60	2.12	0.49	0.142
CdI_2	9.38	1.63	2.15	0.51	0.136
$ZnCl_2$	9.28	1.60	2.12	0.49	0.130
$ZnBr_2$	9.24	1.60	2.12	0.49	0.127
ZnI_2	9.14	1.63	2.13	0.49	0.121
$HgCl_2$	9.85	1.55	2.14	0.57	0.165
HgI_2	9.87	1.56	2.16	0.57	0.167
$Pd(NO_3)_2$	9.14	2.03	2.16	0.54	0.121
$Zn(\phi NH_2)_2Cl_2$[d]	9.25	1.60	2.12	0.49	0.128
$Zn(\phi NH_2)_2Br_2$[d]	9.20	1.60	2.12	0.49	0.125

[a] Obtained in benz./THF, 11:1 mixture. Numbering system as in Table IV-2.

[b] Calculated using eq. (4.1)

[c] H.C.C's of the uncomplexed radical

[d] Obtained in 1,4 dioxane/THF (10:1)

[e] TU=Thiourea

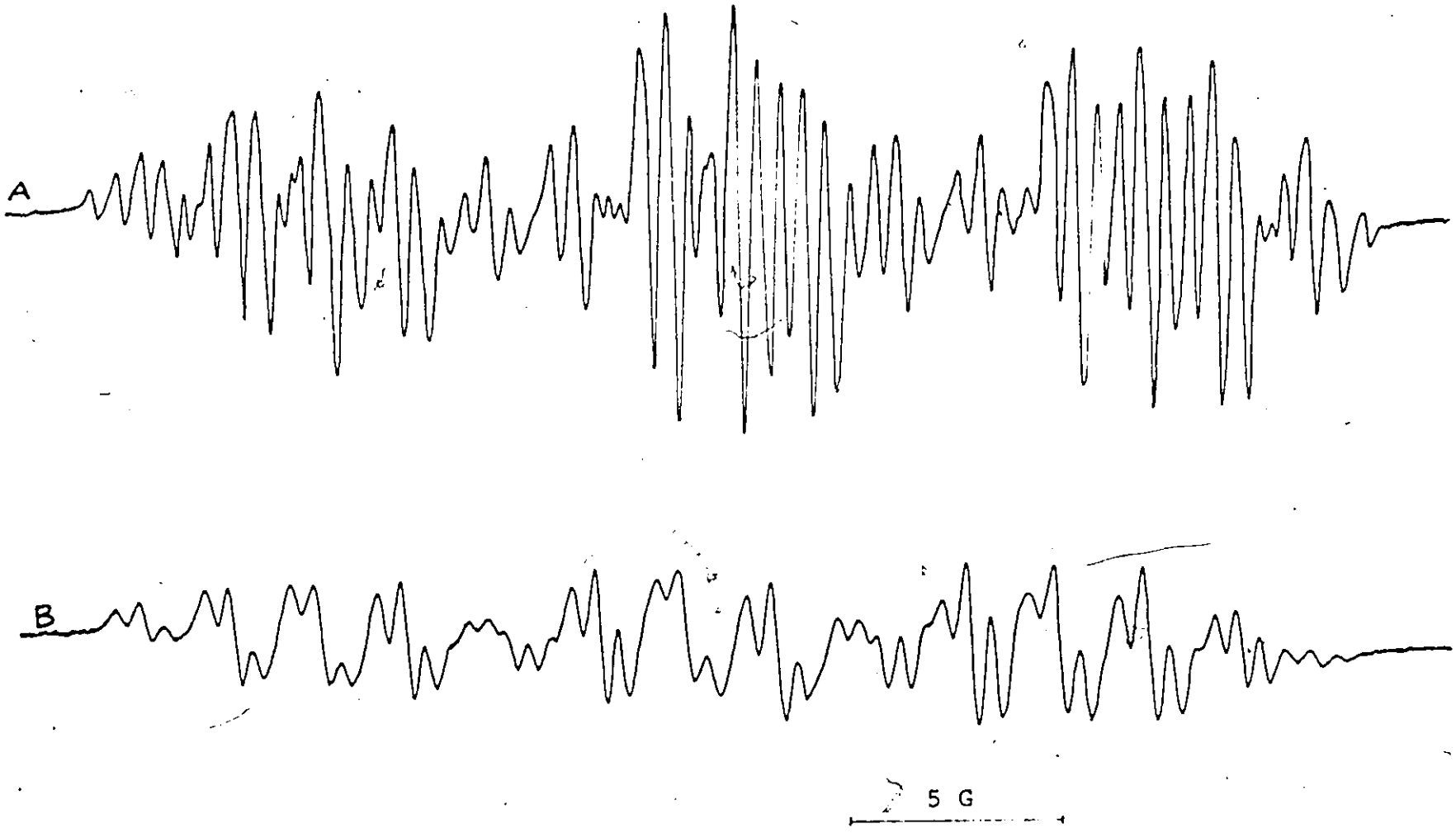

FIGURE IV-6. ESR spectra of 4-pyridyl-t-butyl nitroxide radical obtained (A) in the presence of excess $Zn(py)_2Br_2$, (B) in the presence of excess $Pd(hfac)_2$, in 1,4 dioxane/THF mixtures.

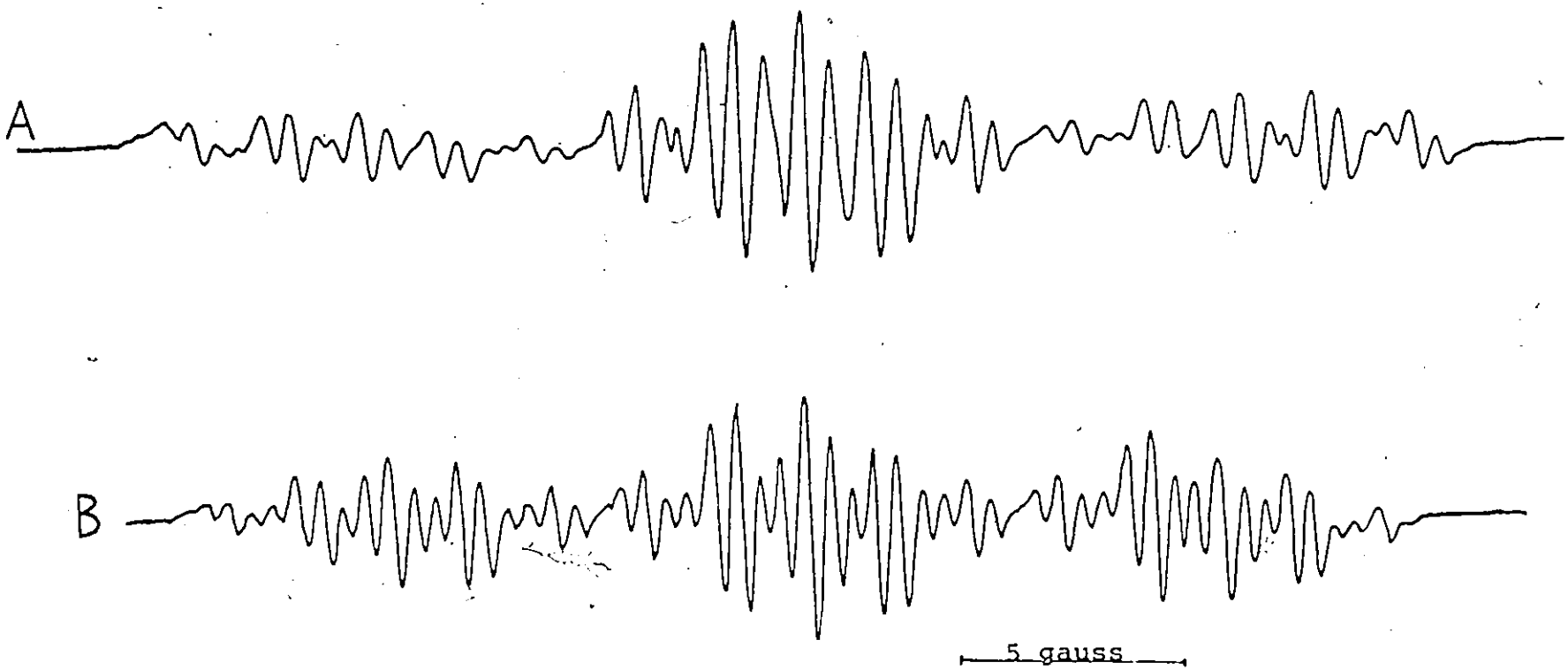

FIGURE IV-7. ESR spectra of 4-pyridyl-t-butyl nitroxide radical obtained (A) in the presence of excess $Zn(acac)_2H_2O$ in benzene/THF mixture, (B) in the presence of excess $ZnCl_2$ in benzene/THF mixture plus a few drops of DMSO.

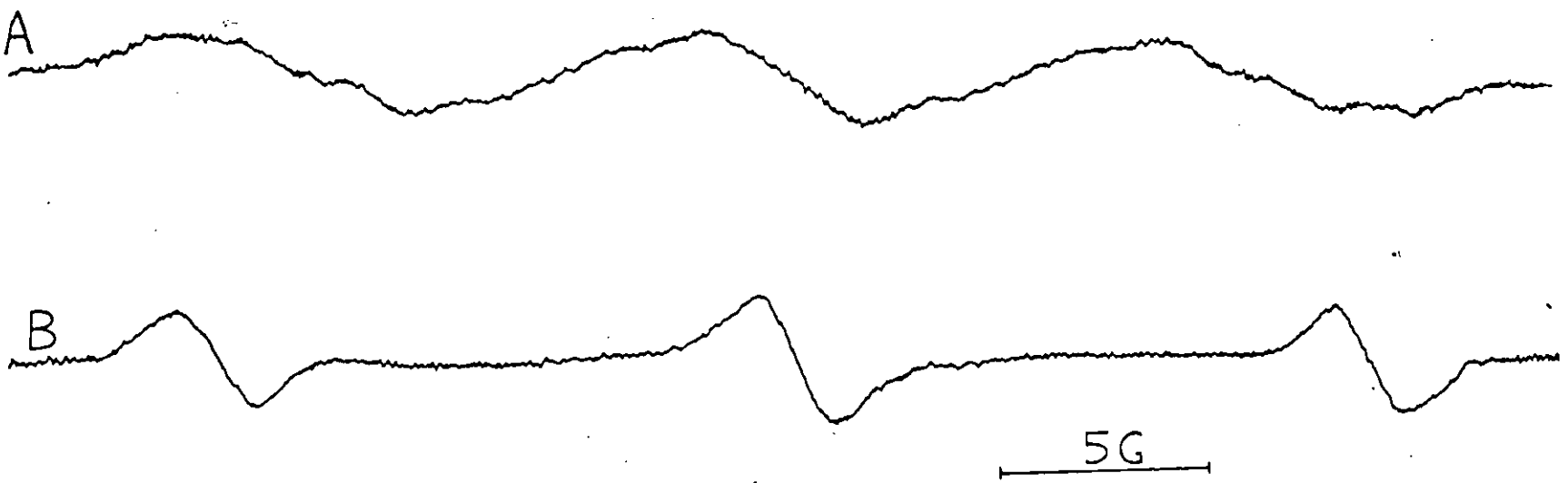

FIGURE IV-8. ESR spectra of 4-pyridyl-t-butyl nitroxide radical obtained in benzene, (A) in the presence of excess $Co(hfac)_2$, line separations 12 gauss, (B) in the presence of excess $Ni(hfac)_2$, line separations 14 gauss.

Fig. IV-6A is an example of the former case. The total line-width in this spectrum is that of the free ligand, also, some of the lines are identified with those of the uncomplexed radical. The situation is different however, with the spectra obtained on the addition of $Pd(hfac)_2$ [Fig. IV-6B]. In this case the total line width of the spectrum is somewhat smaller than that of the free radical. It is also unsymmetrical about the centre. This would imply that complete complexation occurs but different environments for the complexed ligand lead to this spectrum.

(4) Exchange between free and complexed ligands is fast on the ESR time scale. If this is the case, line broadening of some lines in the ESR spectrum will occur. Examples of such spectra are shown in Fig. IV-7. $Zn(acac)_2H_2O$ and $Zn(Py)_2(CNO)_2$ show this effect. Very rapid ligand exchange of this type probably implies addition of a fifth or sixth ligand rather than replacement of a ligand already present.

(5) If the metal compound to which the spin-labelled ligand is attached is already paramagnetic, interaction between the unpaired electron of the ligand and those on the metal must be anticipated. Both changes in the coupling constants and in the electron spin relaxation time can occur. Fig. IV-8 shows the ESR spectra obtained by addition of Ni(II) hexafluoroacetylacetonate and Co(II) hexafluoroacetylacetonate to the spin-labelled ligand.

(6) With some very strong Lewis acids such as BF_3 and $AlCl_3$ it appears that catalytic rearrangement of the radical occurs. These rearrangement reactions will be discussed in Chapter V.

D. DISCUSSION

Hyperfine coupling constants and spin densities obtained from the analysis of spectra in the second class in the above summary are shown in Table IV-3. It is apparent that there are significant changes in the spin density distribution of the radical due to the complexing of the metal. Most notably the ^{14}N coupling involving the nitroxide nitrogen has diminished by approximately one gauss and the ^{14}N coupling of the pyridine nitrogen has increased by around 0.4 gauss. This behaviour may be compared with that observed for metal complexes formed with the nitroxide oxygen(20,21,76). In these cases the hyperfine coupling with the nitroxide nitrogen has been markedly increased due to enhanced contribution of the valence bond structure (II).

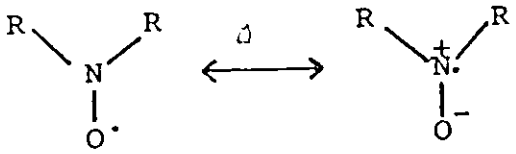

(I) (II)

The present spectra, showing the opposite effect, i.e., diminished coupling from the nitroxide nitrogen, clearly arise from complexing with the pyridine nitrogen of the spin-label-

led ligand. As a further check, the phenyl-t-butyl nitroxide radical was prepared by the reaction of t-butyl magnesium chloride with nitrobenzene (according to the method of Sec. B-1b). The ESR spectrum of this radical was examined in the presence and absence of metal compounds. In no case did the metal compound cause any observable change in the ESR spectrum demonstrating that the pyridyl nitrogen is necessary for complex formation. This conclusion has been further confirmed by molecular orbital calculations of the spin density distribution using the McLachlan method(63), already described in Chapter II, Sec. B-3e. The model used is based on the premise that complex formation removes charge from the pyridine nitrogen thereby increasing its effective Coulomb integral but that the remaining parameters are unchanged. Similar models have been used for such calculations in previous cases, e.g., Gendall, Freed, and Fraenkel(77) treated the solvent effect in the semiquinone case by using the Huckel molecular orbital theory and adjusting the Coulomb integral of the oxygen atom. Also, Eaton(15) treated similarly the effects of the complexing of metals with semiquinones by adjusting the Coulomb integral of the semiquinone oxygen atoms. Interpretation of small perturbations in the hyperfine splittings of hydrocarbon negative ions due to positive ions (counterion effect) has also been based on a similar model(78). In the present case, spin density calculations were carried out for the isolated 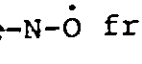
fragment using the parameters -

$\delta_{(O)}=0.84$, $\delta_{(N)}=1.19$ for the Coulomb integrals of oxygen and nitrogen atoms of the nitroxide group, respectively, $\gamma_{CN}= 1.29$, $\gamma_{NO}= 1.10$ for the resonance integrals of the nitroxide group (79), and $\gamma_{CN}= 1.00$ for the resonance integral of the ring nitrogen - unchanged, while varying the Coulomb integral, $\delta_{(N)_{Ring}}$, of the pyridine nitrogen from $\delta_{(N)_{Ring}}= 0.50,...1.00$ at 0.05 intervals. The results of these calculations are shown in Table IV-4 (values obtained with $\lambda=1$ are in better agreement with experiment than those obtained with $\lambda= 1.2$).

Such adjustment of the Coulomb parameter indeed predicts (at least in qualitative terms) the observed trend the spin densities of the spin-labelled ligand due to complexation. Increasing the Coulomb integral on the pyridine nitrogen clearly decreases the spin density on the nitroxide nitrogen (ρ_2 in Table IV-4). Hoffmam and Eames (21) have related this spin density to the ^{14}N hyperfine coupling constant by the equation

$$a^{N}_{N-O} = Q\,\rho^{\pi}_{N} + q \qquad (4.1)$$

where Q=16 gauss and q=7.2 gauss. Using this formula the nitroxide nitrogen spin density falls from about 0.21 to about 0.15 on complexation (Table IV-3) and this drop in spin density corresponds to a change of more than 0.5β in the pyridine nitrogen Coulomb integral (Table IV-4). The smallest ^{14}N coupling constant can therefore be associated with the largest amount of electron withdrawal by the metal ion from the pyri-

TABLE IV-4

Theoretical spin densities [a] and corresponding hyperfine coupling constants[b] in 4-pyridyl-t-butyl nitroxide as a function of the Coulomb integral, $\delta_{(N)\,(Ring)}$, of the pyridine nitrogen atom.

λ [c]	$\delta_{(N)}$ Ring	ρ_1^π	ρ_2^π	ρ_3^π	$\rho_{4,8}^\pi$	$\rho_{5,7}^\pi$	ρ_6^π	a_6^N (Theor)
1.20	0.50	.6253	.2459	-.0557	.0890	-.0388	.0843	-
"	0.55	.6281	.2410	-.0529	.0866	-.0362	.0834	-
"	0.60	.6310	.2368	-.0503	.0842	-.0337	.0822	-
"	0.65	.6336	.2314	-.0473	.0816	-.0310	.0810	-
"	0.70	.6364	.2268	-.0444	.0793	-.0284	.0797	-
"	0.75	.6389	.2221	-.0415	.0768	-.0257	.0782	-
"	0.80	.6417	.2176	-.0388	.0744	-.0230	.0767	-
"	0.85	.6443	.2130	-.0358	.0719	-.0201	.0750	-
"	0.90	.6447	.2084	-.0329	.0695	-.0174	.0733	-
"	0.95	.6489	.2041	-.0299	.0671	-.0146	.0718	-
"	1.00	.6514	.1998	-.0269	.0645	-.0117	.0700	-
1.00	0.50	.5909	.2383	-.0421	.0925	-.0313	.0902	1.15 G
"	0.70	.6017	.2215	-.0319	.0838	-.0217	.0849	1.23 G
"	1.00	.6179	.1968	-.0166	.0707	-.0073	.0769	1.34 G

[a] McLachlan calculations (Ref.63). Numbering as in Tbl.IV-2.

[b] Values obtained using eq. (4.2), (Ref.57).

[c] Values obtained with λ=1.00 agree better with exper.

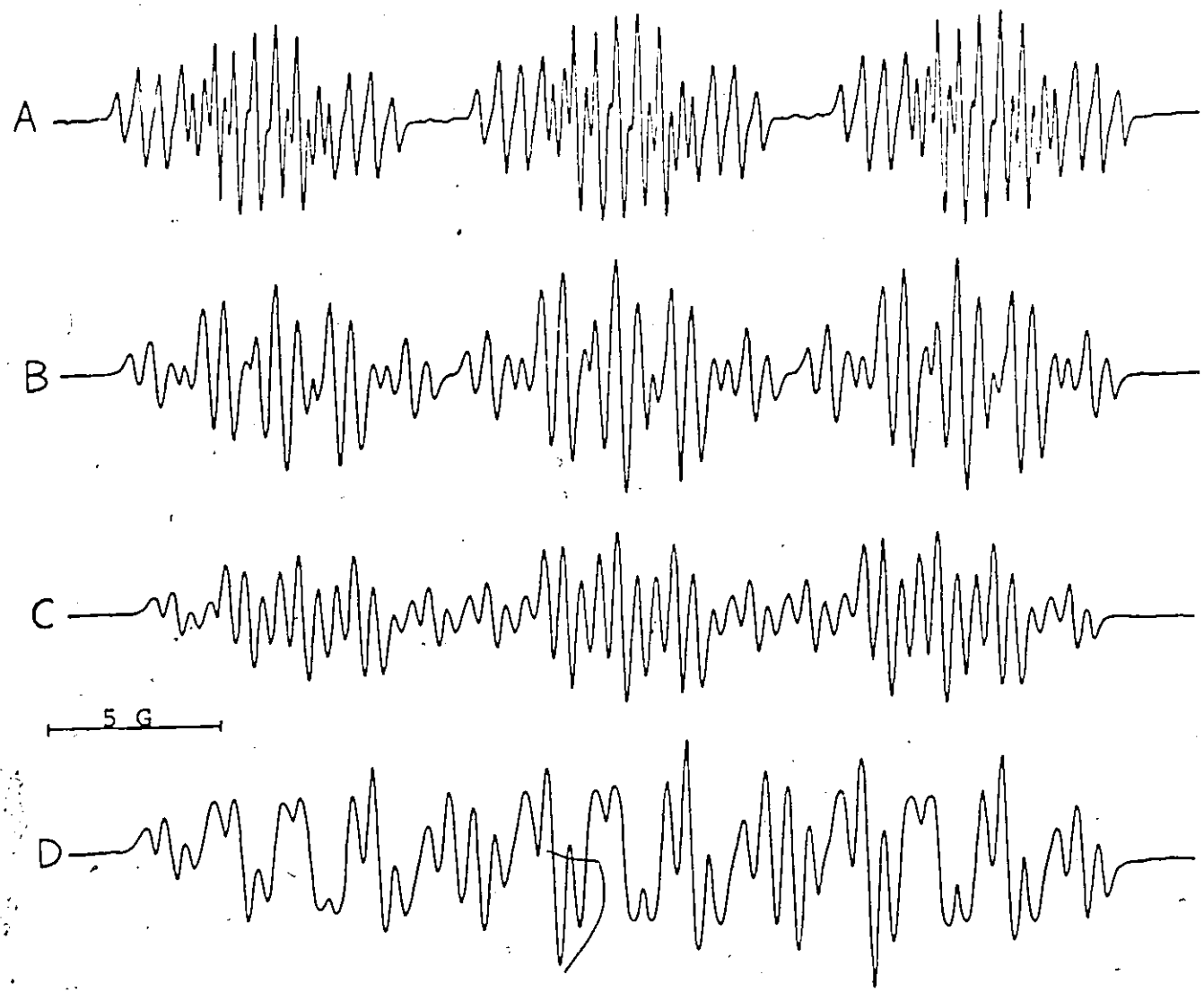

FIGURE IV-9. ESR spectra of 4-pyridyl-t-butyl nitroxide in benzene/THF mixture, (A) free radical, (B) radical + excess $HgCl_2$, (C) radical + excess $ZnCl_2$, (D) radical plus excess $Pd(NO_3)_2$.

dine nitrogen.

The differences among the various metal complexes are significant. This is illustrated in Figure IV-9. The sequence, $a^{N}_{NO}(Hg\ I_2)$ = 9.87 gauss, $a^{N}_{NO}(CdI_2)$ = 9.38 gauss, $a^{N}_{NO}(Zn\ I_2)$ = 9.14 gauss (Table IV-3), is particularly noted. Clearly, zinc withdraws electrons more effectively than cadmium which in turn is more effective than mercury as would be anticipated from the electronegativities of the elements. The various zinc compounds are presumably solvated by THF under the conditions employed. Replacement of THF by thiourea apparently decreases the electron affinity of zinc as might be anticipated on the basis that a Zn-S bond is likely to be more covalent than Zn-O bond. The sequence of the a^{N}_{NO}'s for the zinc halides, Cl > Br > I, is opposite to what might have been expected on the basis of the electronegativity of the halogens. However, anomalous orders for the halogens have also been observed in nuclear magnetic resonance studies of the electron withdrawing abilities of complexed metal ions and it is apparent that simple considerations of electronegativities do not always suffice to account for charge density distributions in complexes of this type.

The results also indicate that the palladium compound has a very small a^{N}_{NO} and hence a large metal electron affinity. Planar Pd coordination must be assumed in this case, since the metal salt is diamagnetic and the results should perhaps not be compared directly with those for tetrahedral

zinc compounds. The spin density distribution within the pyridyl ring of the spin-labelled ligand differs somewhat from that of the other complexes, most notably in the high value for the pyridyl nitrogen coupling constant (position 6, in Table IV-3). It is possible that metal-ligand π-bonding is important for a square planar complex in which case a calculation based simply on adjusting the Coulomb integral of the pyridine nitrogen would be inappropriate. It is apparent that with the present small number of compounds examined, extensive discussion of trends in the charge distributions is inappropriate and that these results merely serve to illustrate the potentialities of the method.

Changes in the pyridine nitrogen hyperfine coupling constants have also been noted. Experimentally a_6^N (Tab. IV-3) changes from 1.23 gauss in the uncomplexed radical to up 1.63 gauss in the complexes. The interpretation here is a little more complicated since such coupling constants depend on the spin densities on both the nitrogen and the adjacent carbon atoms. Henning(57) has studied a number of nitrogen containing aromatic radicals and proposed the equation (4.2) in which the ^{14}N hyperfine splittings for a nitrogen in an aromatic ring are related to the π-spin densities on the nitrogen and adjacent carbon atoms as follows:

$$a^N = Q_1\rho_N^\pi + Q_2(\rho_{C_1}^\pi + \rho_{C_2}^\pi) \qquad (4.2)$$

where $Q_1 = 19.1\pm1.7$ gauss, $Q_2 = 9.1\pm 1.7$ gauss and C_1, C_2

refer to the adjacent carbon atoms. The spin density calculations in Table IV-4 show that both ρ_N (position 6) and ρ_{C_i} (positions 5,7) of the adjacent carbons decrease with increasing nitrogen Coulomb integral. The carbon spin densities are however negative so that, by using equation (4.2), the net result is that the calculated hyperfine coupling constant, a_6^N, increases from 1.15 gauss to 1.34 gauss for an increase of 0.5β in the pyridine nitrogen Coulomb integral, i.e., a change of approximately 20%. The absolute calculated values of a_6^N are somewhat low, but from the experimental increase on complexation of approximately 30% it would again be deduced that, on complexation, an increase in the nitrogen Coulomb integral better than 0.5β occurs. Thus the changes in the pyridine nitrogen coupling are entirely consistent with those of the nitroxide nitrogen. The nitroxide nitrogen however, obviously provides a more sensitive probe of the charge withdrawing properties of the metal ion.

Finally, the line broadening effects, illustrated in Fig.IV-7, are attributed to rapid exchange between free and complexed ligand. Line broadening due to rate processes has been extensively discussed in the ESR literature and has been used to study cases of restricted rotation, electron transfer, proton transfer, counterion interactions, solvent interactions etc. In particular, the "alternating line width effect" with applications to most of the above cases has been reviewed by Sullivan and Bolton(80). In the present case the central set

of lines arising from transitions for which m_I for the nitroxide nitrogen is zero, is much less broadened than the outer sets of lines for which $m_I = \pm 1$. This effect is clearly shown in Fig. IV-7A. A modulation of the nitroxide nitrogen hyperfine coupling by the exchange process is implied. Since free and complexed ligand have substantially different ^{14}N coupling constants, ligand exchange is indicated. It is necessary that the complexed ligand should have a lifetime of the order 10^{-8} - 10^{-9}sec, therefore implying very rapid ligand exchange. The correctness of this interpretation is further confirmed by the observation that broadened spectra can also be obtained by adding small amounts of water or DMSO to solutions of the nitroxide radical complexed to zinc chloride. This effect is illustrated when the spectrum in Fig.IV-7B is compared with that in Fig. IV-4 which represents the case of the ligand-zinc complex in the absence of water or DMSO. It is therefore clear that in the presence of coordinating solvents, the exchange is between complexed ligand and the added coordinating solvent.

There is precedence for the observation of extremely fast ligand exchange for pyridine ligands. Thus Corden and Rieger(10) have studied the broadening of the ESR spectra of Cu(II) bis(di-n-butyldithiocarbamate) on the addition of amines. Also, Farmer, Herring and Tapping(11) have reported a study of a similar process using Cu(II) bis(diethyldithiocarbamate). Both groups consider an equilibrium of the type

$$ML_2 + B \underset{k_d}{\overset{k_f}{\rightleftharpoons}} ML_2B \qquad (4.3)$$

(A) (B)

where ML_2 is the metal bis chelate, B the Lewis base and both ML_2, ML_2B species are paramagnetic. For fast rates of exchange (10^7 to 10^9 sec^{-1}) such an equilibrium can be treated as a "two jump" system on the ESR time scale. In the limit of fast exchange, the problem is treated by the modified Bloch equations leading to a single exchange signal centered at a mean frequency

$$\langle\omega\rangle = P_A\omega_A + P_B\omega_B \qquad (4.4)$$

with line widths given by

$$1/T_2 = P_A/T_{2A} + P_B/T_{2B} + P_A^2P_B\tau_B(\omega_A - \omega_B)^2 \qquad (4.5)$$

where $1/T_{2A}$, I/T_{2B} are the line widths for site A and B in the absence of their mutual interconversion, P_A, P_B are the fractional populations of sites A and B, ω_A, ω_B are the Larmor frequencies of sites A and B and τ_B is the mean lifetime of site B. Using such equations, both groups arrived at values for τ_B, the lifetime of complexed ligands, of the order of 10^{-9}sec. In the present case, the inverse of these experiments was performed, i.e., the exchange is between a paramagnetic ligand and a diamagnetic metal rather than between a diamagnetic ligand and a paramagnetic metal. An implication of this model is that, according to equation (4.4),

the smaller hyperfine coupling constants of the exchanging spectra should be intermediate between those of the free and complexed ligand. Analysis of the central multiplet of the spectrum in Fig. IV-7A shows that this is true.

In conclusion, the intent of the present work was to utilize the spin-labelling concept in a study of metal-ligand bonding and also to investigate the potential utility of this approach in inorganic chemistry. Three of the areas uncovered seem to have potential.

(a) It has been demonstrated that the hyperfine coupling constants of a complexed radical are sensitive to the Lewis acid involved and that they may be used as a measure of the strength of this Lewis acid. Further, this can be done using ligands only slightly perturbed, from those commonly occuring in a large variety of metal complexes. Also, the observation with the Palladium complex suggests that more detailed studies of metal-ligand bonding, e.g., evaluations of the importance of π-bonding, may be possible.

(b) A method for the study of very fast ligand exchange reactions is suggested. Such studies need not be confined to paramagnetic metals as is the case with previous ESR work, or to simple ligands in aqueous solution suitable for temperature jump or ultrasonic relaxation techniques. Potentially, the spin-labelled ligand approach has also a number of practical advantages in the form of sharper lines, the absence of quadrupolar broadening and of effects due to anisotropy in

the g tensors. It should be possible in favourable conditions to measure rapid ligand exchange rates almost to the diffusion controlled limit.

(c) It has been shown that coordination of the spin-labelled ligand to a metal already paramagnetic affects the electron spin relaxation time. The use of basic stable free radicals, containing nitrogen donor atoms for instance, to study the NMR of transition metal complexes may therefore prove to be generally useful.

CHAPTER V

LEWIS ACID CATALYZED REARRANGEMENTS OF NITROXIDE RADICALS

A. INTRODUCTION

In Chapter IV, the synthesis and use of certain radicals as spin-labelled ligands was described. In particular, interactions of a molecule in which a pyridine moiety acted as the Lewis base and t-butyl nitroxide group provided the spin label were studied with a variety of metal compounds.

In the large majority of cases the resulting ESR spectrum could be interpreted in terms of complexing of the pyridine nitrogen with the metal. In the case of the strong Lewis acids $AlCl_3$ and BF_3 however, the ESR spectra obtained could not be readily interpreted along these lines. Also, the stability of the radical in the presence of $AlCl_3$ or BF_3 was greatly affected. It seemed therefore possible that with strong Lewis acids, interaction with the oxygen of the nitroxide group was occuring. ESR studies of such complexes have indeed been reported(20,21,76), but their relevance to the interpretation of the spectra mentioned above was not clear. The reactions of several nitroxide radicals with strong Lewis acids was therefore further investigated using ESR and NMR

techniques. In the course of these studies it became apparent that some of the ESR spectra observed did not arise from the nitroxide radical introduced into the system. In the present chapter therefore, evidence for Lewis acid catalyzed rearrangements of nitroxide radicals is presented.

B. EXPERIMENTAL

1. Synthesis of Nitroxide Radicals

Nitroxide radicals with structures (I), (II) and (III) have been prepared.

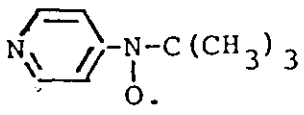

(I)

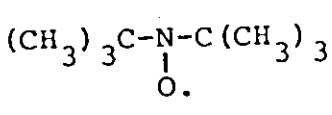

(II)

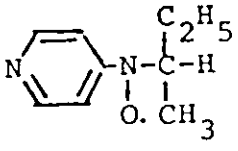

(III)

The preparation of radical (I) has been described in Chapter IV, sec. B-1b. This method was also applied for preparing the analogous sec-butyl radical (III). In this case however, the final step of the preparation involves the reaction of 4-nitropyridine with sec-butyl magnesium chloride (75) rather than t-butyl magnesium chloride.

Radical (II) was obtained by the reaction of metallic sodium with t-nitrobutane in 1,2-dimethoxyethane (DME) according to the method described by Hoffmann et al.(81). Di-t-butylnitroxide was redistilled at 54°C and 11 mm. Radical (III) is stable indefinitely at room temperature.

2. Prccedure for Preparing ESR Samples

In general, a similar method to that described in Chapter IV, sec. B-2 was used to prepare samples in this case. First, a dilute radical solution (to avoid exchange broadening) in 1,4-dioxane was prepared. Separately, solutions of $(C_2H_5)_2OBF_3$ in 1,4-dioxane (1:10 ratio), and dry $AlCl_3$ in THF were also prepared. To the radical solution, the mixture containing the required Lewis acid was added in small amounts. The final product was then placed in the ESR sample tube, deoxygenated and its ESR spectrum recorded immediately at room temperature. It proved convenient to use di-t-butyl nitroxide as a field calibration standard based on the line separations, a_{NO}^{N}=15.36 gauss, given by Faber et al.(82).

3. NMR Experiments

NMR spectra were obtained using a Varian HA 100 spectrometer. The solvent (benzene) used for the preparation of the samples was of spectro-grade quality. Magnetic susceptibility measurements were performed using the NMR method devised by Evans(83).

C. RESULTS

Radical (I) was initially used in these studies.

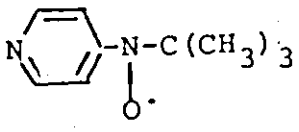

(I)

The ESR spectrum of the free radical is shown in Fig. IV-2.

Also, the ESR spectra of this radical in the presence of a variety of metal compounds have been discussed in Chapter IV. These spectra could be interpreted in terms of complexing of the pyridine nitrogen with the metal and, in most cases, their analysis is straightforward.

In the case of the strong Lewis acids $AlCl_3$ and BF_3 the situation is different. First, the ESR spectrum of radical (I) in the presence of $AlCl_3$ consists of fourteen broad lines with intensity ratios, approximately, 1:4:6:6:5:5:6:6:5:5:6:6:4:1. This spectrum is shown in Fig. V-1A. In the presence of BF_3 the spectrum is essentially similar except that an additional quartet splitting with intensity ratios 1:3:3:1 is observed. This can be reasonably assigned to coupling with three equivalent fluorine atoms (I=1/2). This latter spectrum is shown in Fig. V-1B. These spectra are anomalous in two respects:

(a) All attempts to find a reasonable combination of hyperfine coupling constants [including possible couplings with ^{27}Al (I=5/2) or ^{11}B(I=3/2)] which, allowing for overlapping lines, would reproduce the pattern of the observed ESR spectra failed. The basic problem here is that radical (I) should give a spectrum with an odd number of lines whereas the observed spectra clearly have an even number of lines.

(b) The ESR spectra are much weaker than those obtained with other metal complexes and the spectrum decays

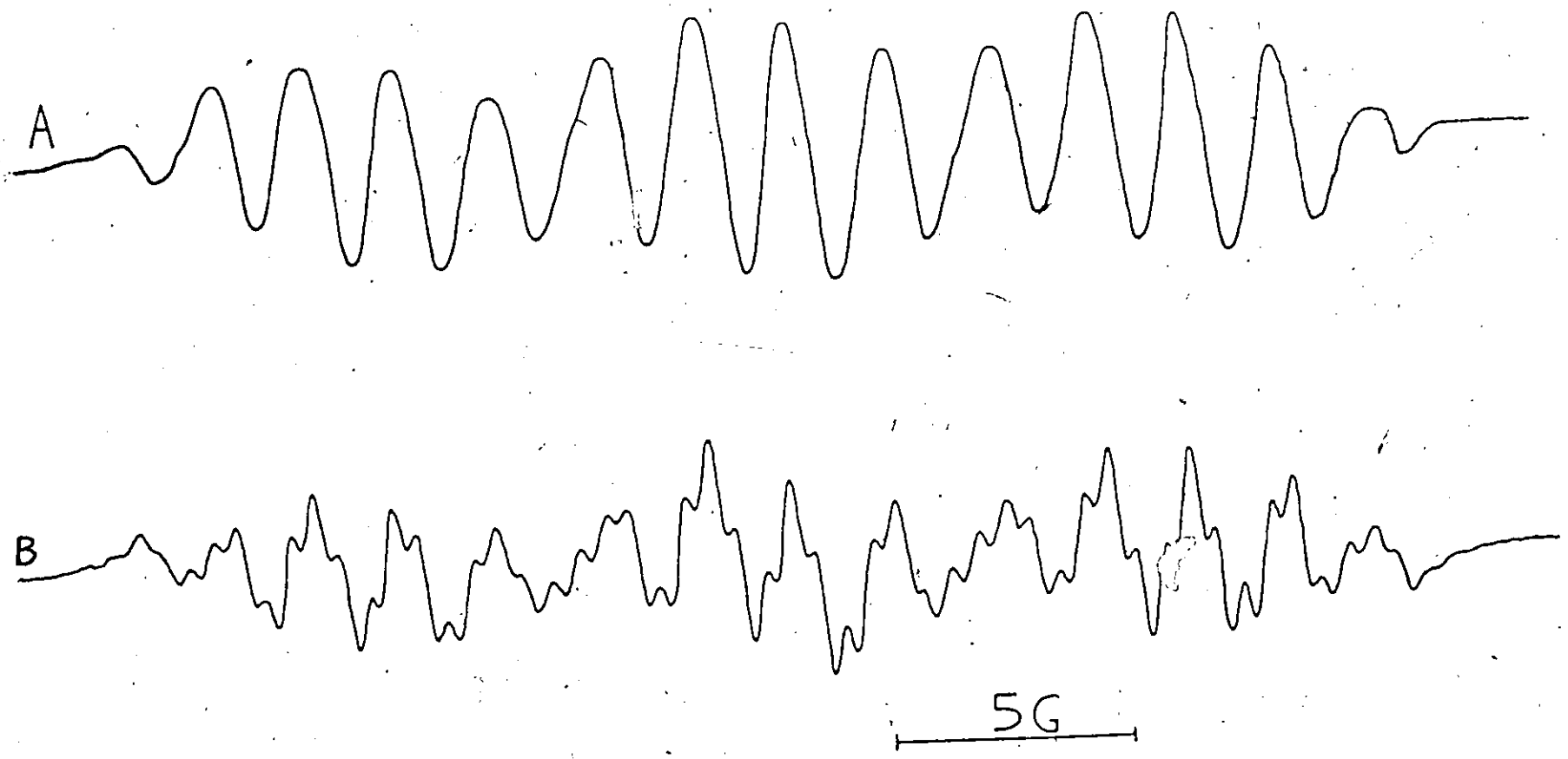

FIGURE V-1. ESR spectrum of 4-pyridyl-t-butyl nitroxide radical obtained in 1,4 dioxane/THF mixture, (A) in the presence of excess $AlCl_3$, (B) in the presence of excess $(C_2H_5)_2OBF_3$.

with time. Other complexes seem quite stable. In order to clarify these results the spectrum of the simpler radical (II) was investigated in the presence of BF_3 and $AlCl_3$.

$$(CH_3)_3C\text{-}N(O\cdot)\text{-}C(CH_3)_3 \qquad \text{(II)}$$

In this case only complexing with the oxygen of the nitroxide group is possible.

The ESR spectrum of radical (II) comprises a simple triplet which is shown in Fig. V-2A. Hoffmann and Eames(21) have described the preparation of complexes of this radical with BF_3 using a technique of distilling excess BF_3 into a solution of the radical in toluene. However, in order to duplicate the conditions used to obtain the spectrum of Fig. V-1B, a rather different approach was adopted (sec. B-2). Initially, a solution of the diethyl ether addition compound of boron trifluoride in 1,4-dioxane was added incrementally to a solution of radical (II) in the same solvent. It was observed that the ESR spectrum of radical (II) decreased in intensity with the addition of BF_3 but that a new weaker spectrum appeared. This second spectrum consists of three triplets and is shown in Fig. V-2B. With a large excess of BF_3, this latter spectrum also disappeared. The original spectrum with approximately its original intensity can be regenerated by adding triethylamine to the final solution. In the experiments in which triethylamine was added to the solution

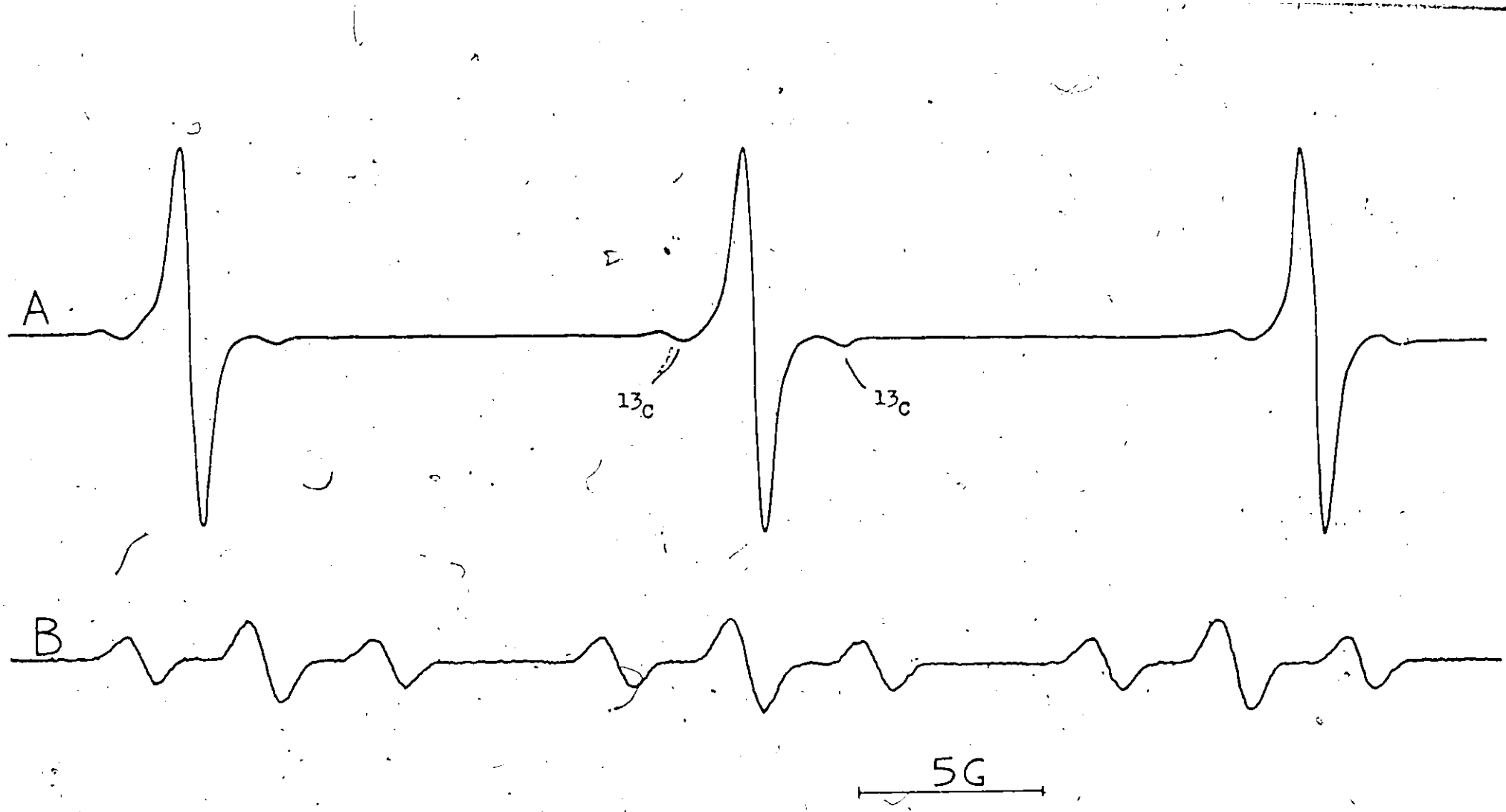

FIGURE V-2. (A) ESR spectrum of $(t\text{-BU})_2NO^{\cdot}$ radical in 1,4 dioxane. (B) ESR spectrum obtained by adding excess $(C_2H_5)_2OBF_3$ to a solution of $(t\text{-BU})_2NO^{\cdot}$ in 1,4 dioxane.

with excess BF_3, no regeneration of the second ESR spectra was observed but since radical (II) is much more intense than the second spectrum, the latter may still be present. Presumably triethylamine, a strong base, preferentially complexes with BF_3 and restores the status quo.

The rate of reaction of radical (II) with BF_3 appears to be relatively slow since the intensity of the ESR signal continues to fall for some time after an aliquot of BF_3/ether solution is added. This is illustrated in Fig. V-3. The second line beginning from the low field side of the spectrum is identified with the low field line of radical (II), indicating that a small amount of this radical is still present. However, during the time interval (~7 mins) required to sweep the field by approximately 15 gauss, the radical has already decayed since the central line does not appear in the spectrum.

It seemed likely that the solution with excess BF_3 was diamagnetic. This was confirmed by measuring the magnetic susceptibility using the NMR method described in sec. B-3. The susceptibility falls from ~1.45 BM to zero on adding BF_3/ether solution. As expected this solution also gave a sharp-line NMR spectrum shown in Fig. V-4A. This proton spectrum shows the CH_2 and CH_3 groups of the diethylether and an additional peak assigned to the t-butyl protons originating from radical (II). The ether chemical shifts have reverted from their positions in the BF_3/ether complex (Fig. V-4B) towards

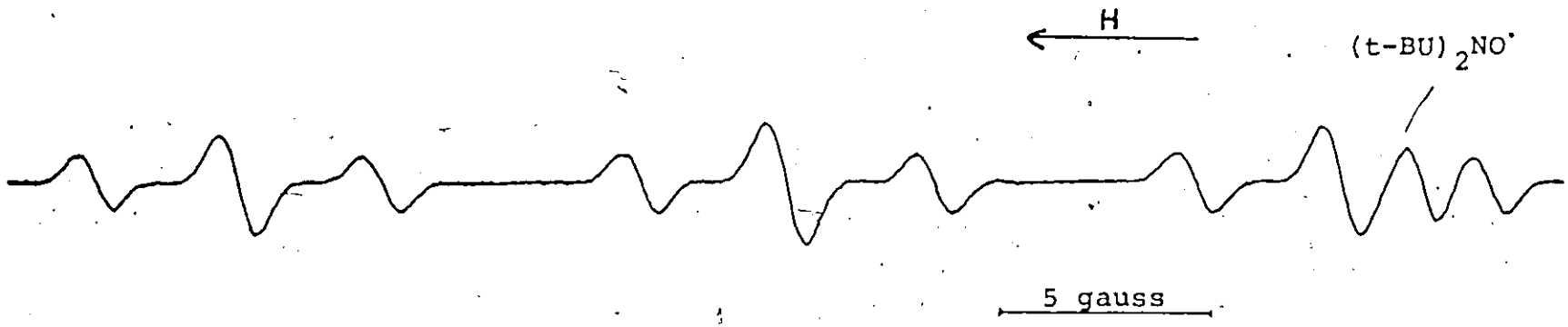

FIGURE V-3. ESR spectrum obtained immediately after the addition of excess $(C_2H_5)_2OBF_3$ to a solution of $(t\text{-BU})_2NO^\cdot$ in 1,4 dioxane. The spectrum is attributed to a mixture of $(t\text{-BU})_2NO$ and $(s\text{-BU})_2NO^\cdot$ radicals.

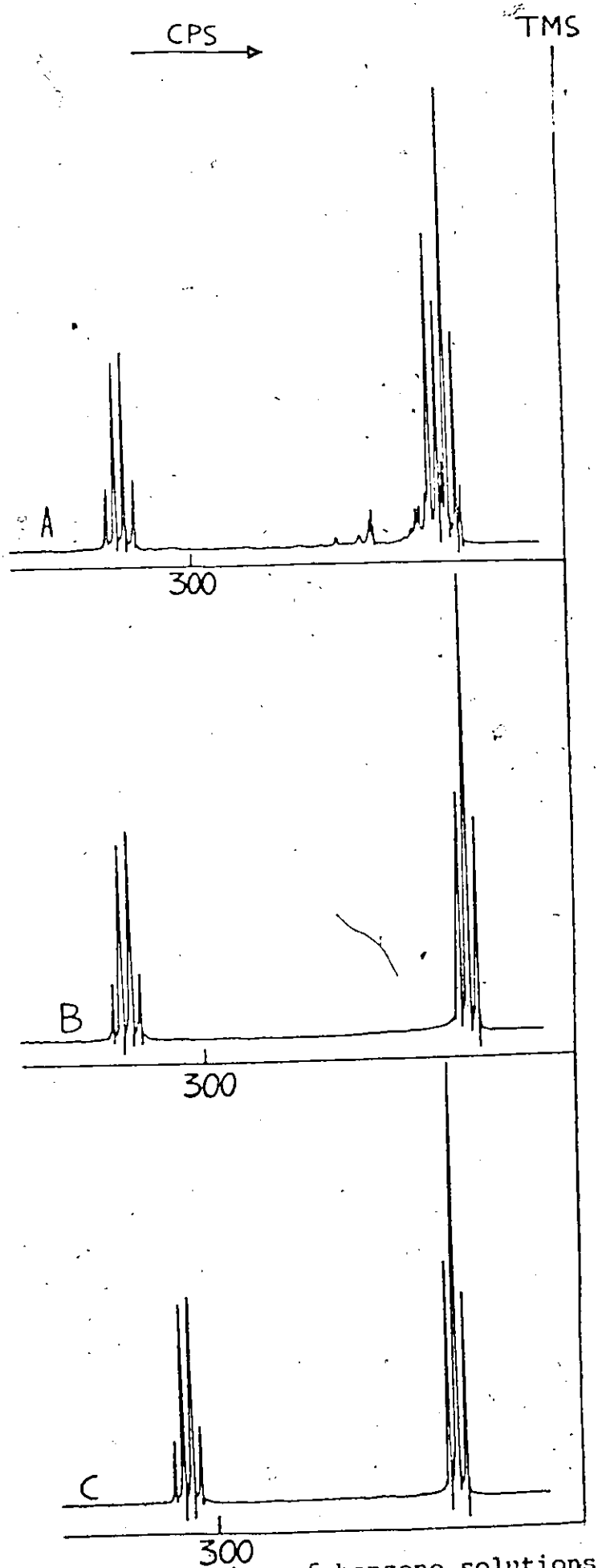

FIGURE V-4. NMR spectra of benzene solutions containing, (A) $(t\text{-BU})_2NO^{\cdot} + (C_2H_5)_2OBF_3$, (B) $(C_2H_5)_2OBF_3$, (C) $(C_2H_5)_2O$.

the positions found for free ether (Fig. V-4C) confirming that the reaction proceeds by displacement of the ether of the BF_3/ether complex.

Similar experiments were carried out with $AlCl_3$. In this case it proved more convenient to use tetrahydrofuran as a solvent. The ESR results were exactly analogous to those with BF_3 including the observation of the spectrum of Fig.V-2B. However, some further information resulted from an attempt to examine the ESR spectra in CCl_4. An excess of $AlCl_3$ was added to a solution of the radical in CCl_4. A yellow precipitate appeared immediately. After decanting the CCl_4 this precipitate was found to be soluble in benzene. On standing, the solution separated into two layers, the upper layer being yellow in colour and the lower layer deep red. The yellow solution was found to be diamagnetic but the red solution gave the ESR spectrum shown in Fig. V-5. This spectrum has 18 lines of equal intensity and can be readily analyzed on the basis of a ^{14}N hyperfine coupling constant of 20.1 gauss and a ^{27}Al ($I = 5/2$) hyperfine coupling constant of 11.5 gauss. It is in fact the spectrum of the $AlCl_3$ complex reported by Hoffmann and Eames(21). The significant observation is that reaction with $AlCl_3$ leads to two products only one of which is paramagnetic. It is reasonable to assume the formation of a complex between the Lewis acid and the free radical is the initial reaction and that rapid precipitation from CCl_4 made the isolation of this intermediate possible. The $AlCl_3$ complex

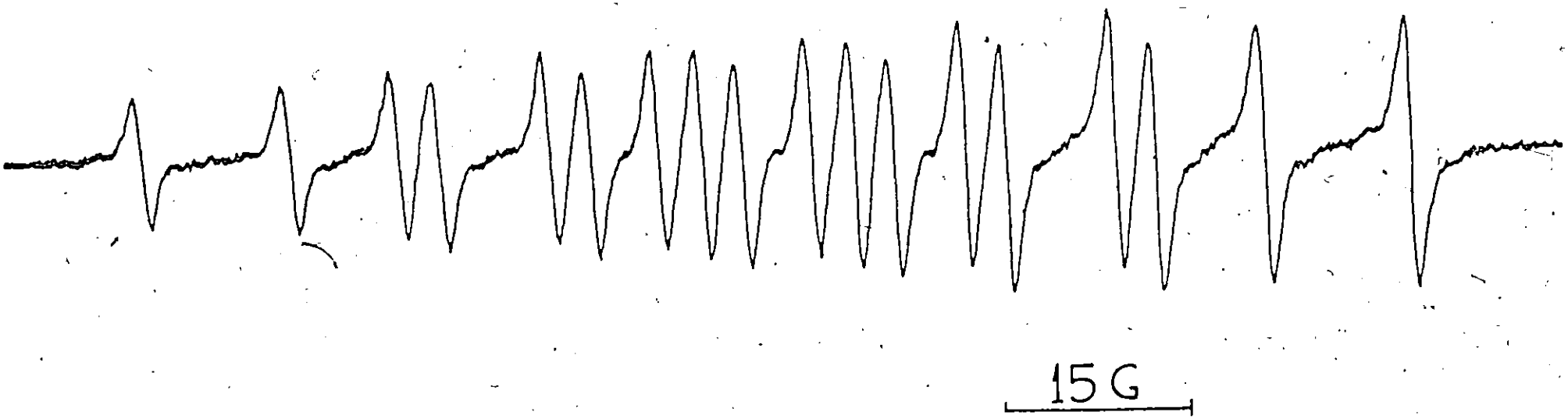

FIGURE V-5. ESR spectrum of $(t\text{-BU})_2\dot{N}O \rightarrow AlCl_3$ complex in benzene.

has only limited stability in benzene since the spectrum disappears in 45-60 minutes.

There remains the question of the assignment of the spectra shown in Fig. V-1 and Fig. V-2B. The possibilities in the second case are quite limited. It is obviously a nitroxide radical showing hyperfine coupling with the nitrogen and two additional nuclei of spin 1/2. The latter can only be protons. Protonation of di-t-butyl nitroxide has been reported(84). The proton is located on the oxygen atom and gives rise to a hyperfine coupling of 3.3 gauss. However, this would only account for coupling with one proton and it is accompanied by a large increase in the ^{14}N coupling constant. In our case coupling with <u>two</u> protons and a <u>decrease</u> in the ^{14}N coupling constant is observed. Coupling to protons on the carbon adjacent to the nitrogen is therefore suggested. The observed couplings to a CH_2R group in this position vary from 8-10 gauss(85), whereas those for CHR_2 groups are in the range 3-4 gauss(85). A value of 3.62 gauss is found in this case. These arguments suggest the di(sec-butyl) nitroxide radical (IV).

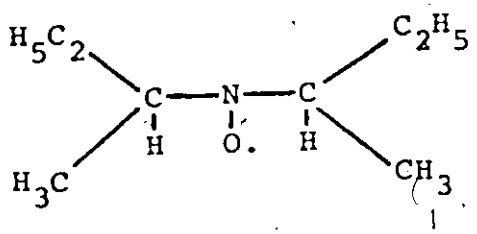

(IV)

The ESR spectrum of this radical has been reported

in the literature(86). The reported coupling constants, a^N_{NO}= 13.4 gauss and a^H= 3.8 gauss (observed in benzene), agree satisfactorily with those found in the present experiments - a^N_{NO}= 13.2 gauss and a^H= 3.62 gauss (obtained in 1,4-dioxane). No other assignment of the radical seems plausible. The hyperfine coupling constants derived from the various spectra of t-butyl nitroxide obtained in the presence of BF_3 and $AlCl_3$ are shown in Table V-1.

By analogy the spectra obtained with the pyridine nitroxide radical (I) might be expected to be derived from (III).

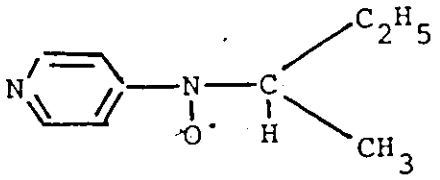

(III)

This radical has not been reported previously and it was therefore synthesized by the reaction of 4-nitropyridine with sec-butyl magnesium chloride according to the method described in sec. B-1. It was obtained only in low yield and the incompletely resolved spectrum is shown in Fig. V-6. This spectrum cannot be analyzed in detail, however, the nitrogen coupling constant of 9.4 gauss can be readily picked out and assigned to the nitroxide group. Some difficulty was experienced obtaining reasonable spectra of this radical in the presence of metal compounds since the initial radical spectrum is relatively weak. A fairly well resolved spectrum was however obtained with zinc chloride. This spectrum proved to be

TABLE V-1

Data[a] on the reaction of $(t\text{-Bu})_2\dot{N}O$ radical with $AlCl_3$ and BF_3 in 1,4 dioxane.

Original Radical + MX_3	Radical product	Hyperfine Coupling Constants (gauss)			Figure
		a^N_{NO}	a^H_{CH}	a^{Al}	
$(t\text{-Bu})_2\dot{N}O$ + BF_3	$(s\text{-Bu})_2\dot{N}O$	13.2	3.62	-	V-2B
" + $AlCl_3$	"	13.2	3.62	-	
" + "	$(t\text{-Bu})_2\dot{N}O \rightarrow AlCl_3$[b]	20.1[b]	-	11.5[b]	V-5
$(s\text{-Bu})_2\dot{N}O$ ——	——	13.39[c]	3.84[c]	-	
$(t\text{-Bu})_2\dot{N}O$ ——	——	15.2	-	-	V-2A

[a] Data obtained at room temperature

[b] Isolated intermediate. H.c.c's obtained in benzene

[c] Values reported in Ref.(86) in benzene

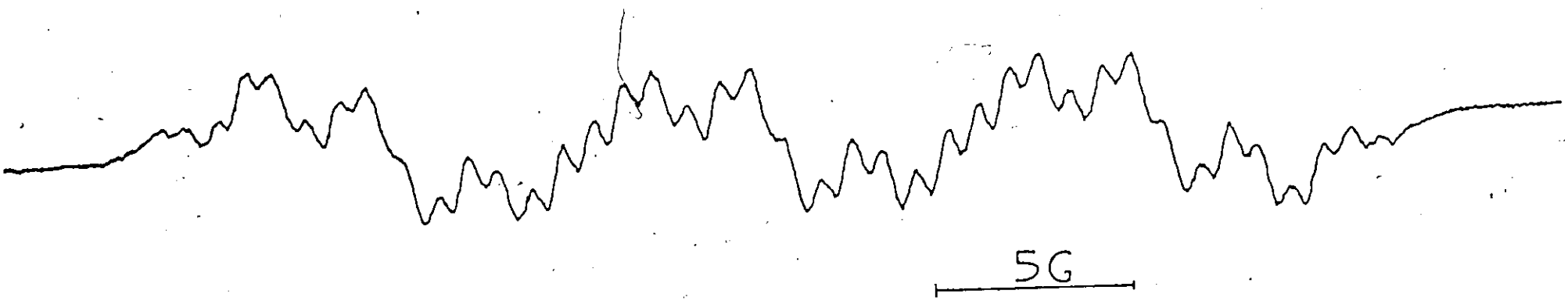

FIGURE V-6. ESR spectrum of 4-pyridyl-s-butyl nitroxide radical in 1,4 dioxane.

virtually identical to that obtained initially with radical (I) and $AlCl_3$. The two are shown together in Fig. V-7. In both cases the nitrogen hyperfine coupling constant has been reduced to ~8.3 gauss as expected for metal complexing on the pyridine nitrogen. The spectrum of Fig. V-1A can therefore be assigned to

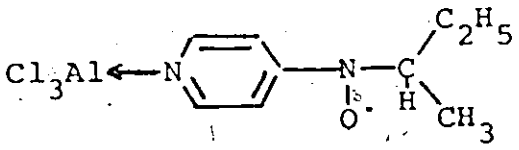

and the spectrum of Fig. V-1B to the analogous BF_3 adduct with some confidence. Both spectra can be reasonably analyzed on this basis since an even number of lines is predicted. The approximate values of the coupling constants obtained from the analysis of these spectra are presented in Table V-2.

D. DISCUSSION

It is apparent that strong Lewis acids can interact with nitroxide radicals in several ways. The present studies provide evidence for three different reactions namely:

(1) The formation of paramagnetic adducts of the type reported by Hoffmann and Eames (21).

(2) The formation of diamagnetic adducts presumably involving dimers or polymers of the radical.

(3) Rearrangement of the alkyl groups to give different radicals.

The third type of reaction is established by the iden-

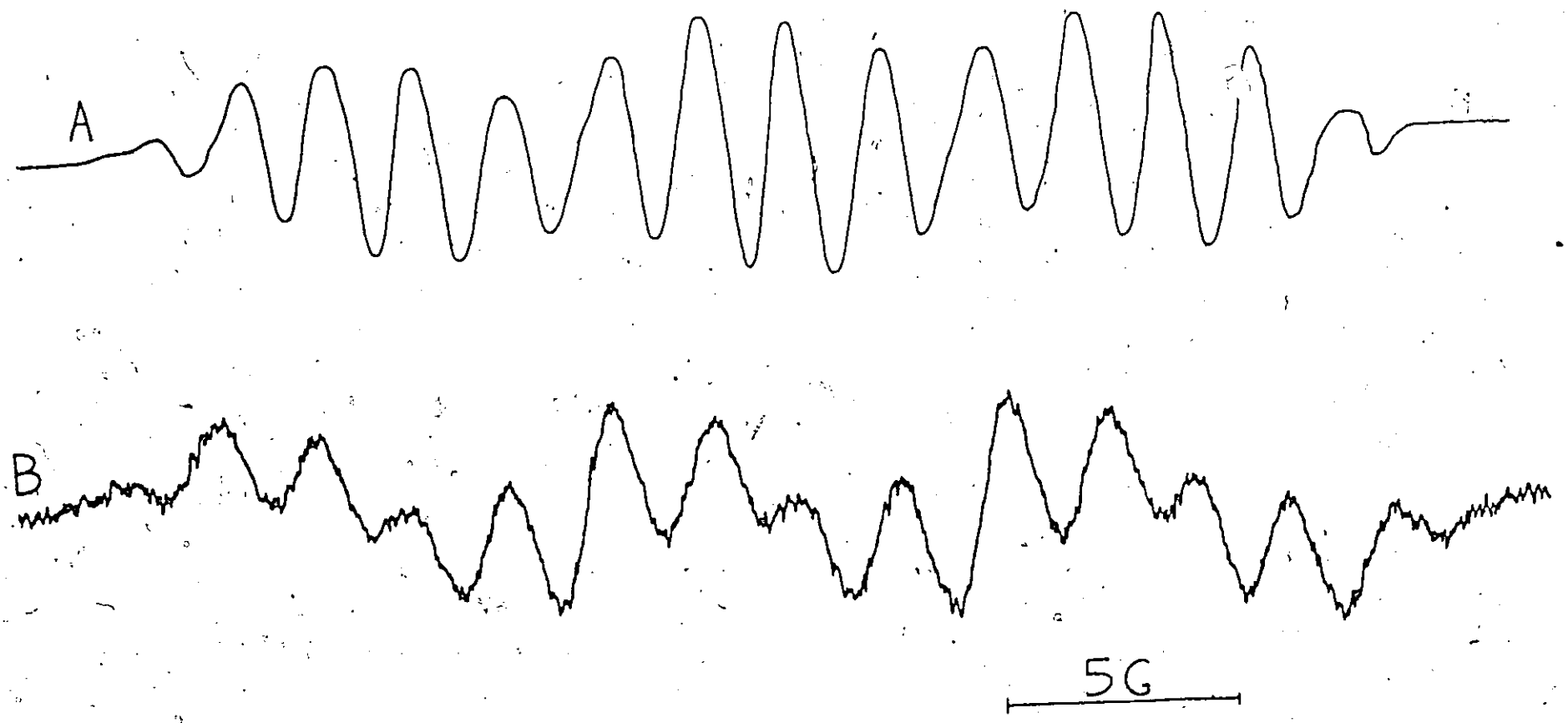

FIGURE V-7. (A) ESR spectrum of 4-pyridyl-t-butyl nitroxide radical in the presence of excess $AlCl_3$ in 1,4 dioxane. (B) ESR spectrum of 4-pyridyl-s-butyl nitroxide radical in the presence of excess $ZnCl_2$ in 1,4 dioxane.

TABLE V-2

Data[a] on the reaction of (py)-N(O·)-(t-Bu) radical with BF_3 and $AlCl_3$ in 1,4-dioxane.

Original radical	+ Lewis acid	Radical product	Hyperfine coupling constants (gauss) a^N_2	a^N_6	$a^H_{4,8}$	$a^H_{5,7}$	a^H_{CH}	a^{Al}	a^B	a^F	Fig.
(Py)-N(O·)-(t-Bu)	+ $AlCl_3$	Cl_3Al←N(py)-N(O·)-(s-Bu)	8.3	~2	~2	Not obs.	~2	Not obs.	-	-	V-1A
"	+ BF_3	F_3B←N(py)-N(O·)-(s-Bu)	8.3	~2	~2	"	~2	-	Not obs.	~.5	V-1B
(Py)-N(O·)-(s-Bu)	+ $ZnCl_2$	Cl_2Zn←N(py)-N(O·)-(s-Bu)	~8.5	~2	~2	"	~2	-	-	-	V-7B
"	—	—	~9.4	NOT RESOLVED							V-6

[a] Data obtained at room temperature. Numbering system:

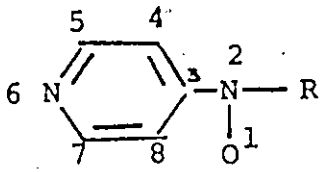

tification of ESR spectra arising from radicals containing sec-butyl groups. The possibility that such radicals might have been present as impurities in the original t-butyl radicals was considered. Samples of di-t-butyl nitroxide were examined very carefully to check this possibility. Several of the lines of the sec-butyl radical occur in positions well away from the ESR lines of the t-butyl radical. No signs of absorption at these frequencies could be observed. In the spectra used, the ^{15}N satellites of di-t-butyl nitroxide were observed with a signal to noise ratio better than 10:1. ^{15}N has a spin of 1/2 and an isotopic adundance of 0.365%. Each line therefore corresponds to an abundance of 0.18%. It was deduced therefore that any sec-butyl impurity is present in a concentration of less than 0.03%. This is insufficient to account for the observed spectra.

It is reasonable that the initial reaction in each case is formation of an adduct with the Lewis acid, e.g.,

$$R_2\dot{N}O + AlCl_3 \longrightarrow R_2\dot{N}O{\rightarrow}AlCl_3$$

Abakumov et al.(20) suggested that such adducts involved π-bonding to the N-O bond but Hoffmann and Eames(21,76) and other authors(22) prefer a σ donor bond. The latter seems more reasonable.

The electronic structure of such adducts can be discussed either in terms of valence bond theory or molecular orbital theory. In the former terms the radical has two

principal contributing structures:

(A) (B)

Complexation with a Lewis acid greatly increases the contribution of structure (B). This is manifested by a large increase in the ^{14}N hyperfine coupling constant, e.g., from 15.2 to 20.1 gauss in the case of the aluminum chloride adduct with di-t-butyl nitroxide (Table V-2).

In molecular orbital terms the effect of complexation may be represented by an increase in the Coulomb integral of the oxygen and a Huckel calculation reproduces the increase in the nitrogen spin density quite satisfactorily. The results of these calculations are shown in Table V-3. Increasing the Coulomb integral of the oxygen clearly increases the spin density on the nitrogen atom. Hoffmann and Eames(21) have consideredthe molecular orbital diagram in more detail and have calculated N spin densities from the equation (4.1) (Ch. IV). The experimental spin densities shown in Table V-4) on the nitrogen atom of the free and complexed radical (II) obtained by using equation (4.1) compare favourably with those calculated by the Huckel method. It is therefore suggested that the increased polarity of the N-O bond provides a rationale for the subsequent reactions.

TABLE V-3

Theoretical[a] spin densities in $R_2NO^{\cdot}$ as a function of the Coulomb integral, $\delta(O)$, of the nitroxide oxygen atom.

$\delta(O)$	ρ_N^{π}	ρ_O^{π}
0.84	0.46	0.54
2.00	0.67	0.33

[a] Huckel calculations with $\gamma_{NO}=1.10$, $\delta(N)=1.19$ (Ref. 79)

TABLE V-4

Experimental[a] spin densities in $(t\text{-Bu})_2NO^{\cdot}$ and $(t\text{-Bu})_2NO\rightarrow AlCl_3$

Radical	ρ_N^{π}	ρ_O^{π}
$(t\text{-Bu})_2NO^{\cdot}$	0.50	0.50
$(t\text{-Bu})_2NO\rightarrow AlCl_3$	0.80	0.30

[a] Values obtained from the hyperfine coupling constants of Table V-1 using eq. (4.1).

A possible reaction to give a diamagnetic species is:

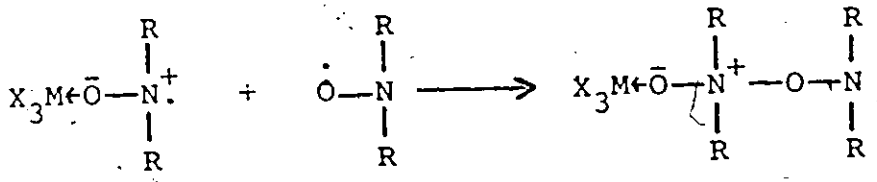

The Lewis acid must be involved in the diamagnetic complex since the NMR experiments show that ether is no longer bound to BF_3. More than one radical could be complexed to $AlCl_3$ but not to BF_3. Although the NMR shows only a single peak for the t-butyl group, this observation does not necessarily have structural significance since there may be exchange processes operative which are fast on the NMR time scale. Since nitroxide radicals show little or no tendency to dimerize in the absence of Lewis acids it seems reasonable to attribute the process to the enhanced dipole of the N-O bond which results from complexation.

Rearrangements of alkyl groups catalyzed by strong Lewis acids are well known. They frequently occur for example during the alkylation of benzene using the Friedel-Crafts reaction with $AlCl_3$ as a catalyst. Perhaps the most pertinent report is that of Roberts, McMahon and Hine(87) who observed the isotope position rearrangement of t-butyl chloride on treatment with $AlCl_3$. They proposed a carbonium ion mechanism with the secondary butyl carbonium ion acting as an intermediate, i.e.,

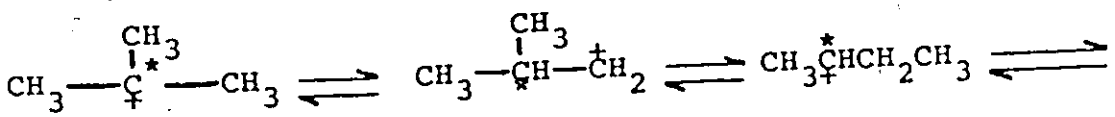

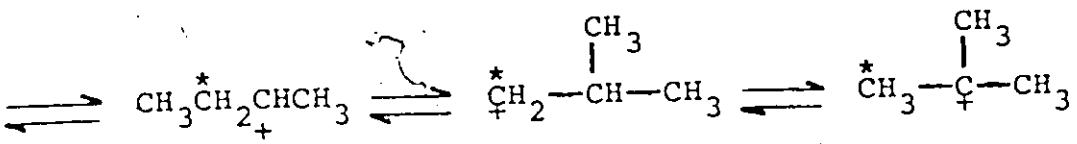

The existence of carbonium ions in solutions of alkyl halides with $AlCl_3$ and BF_3 seems to be uncertain. Thus Olah(88), referring to studies with t-butyl chloride comments on the basis of NMR evidence that the shifts "could be attributed only to weak-donor-acceptor complexes and not to carbonium ions". Alkyl fluorides and very strong Lewis acids such as SbF_5 unambiguously produce carbonium ions and the rearrangements of these ions have been directly studied by NMR(89). In any event whether $AlCl_3$ produces discrete carbonium ions or not it seems clear that its key function in catalyzing alkyl rearrangements is to withdraw charge from the carbon atom.

In the present case the ESR data clearly show that complexation with $AlCl_3$ withdraws a substantial amount of charge from the nitrogen. The change in spin density calculated from equation (4.1) suggests that this withdrawal amounts to approximately 1/3 of an electron. This effect will certainly be reflected in a more positive charge on the adjacent carbon. Rearrangement of the alkyl group can then proceed in a manner exactly analogous to that suggested by Roberts et al. (87) for t-butyl chloride except that only the first two steps are necessary. The present results do not provide any further

evidence as to whether there is any carbonium ion intermediate. Any mechanism which suffices to explain the $AlCl_3$ catalyzed rearrangement of alkyl halides will suffice to explain the present rearrangement.

The following reaction scheme, to describe the interaction of Lewis acids with nitroxide radicals, is therefore postulated.

$$R_2NO + MX_3 \overset{1}{\rightleftharpoons} R_2NOMX_3 \overset{2}{\rightleftharpoons} (R_2NO)_{2n}(MX_3)_m$$

$$\Big\Vert \uparrow 5$$

$$R'_2NO + MX_3 \overset{3}{\rightleftharpoons} R'_2NOMX_3 \overset{4}{\rightleftharpoons} (R'_2NO)_{2n}(MX_3)_m$$

The species observed depend on the equilibrium constants for these various reactions and the rate at which equilibrium is attained. The observations are consistent with the equilibrium constant for complex formation (reaction 1) being smaller in polar solvents such as 1,4-dioxane than in non-polar solvents such as benzene or toluene. In particular, the effect of the solvent on the equilibrium constant for complex formation is quite spectacular in the case of DMSO. Addition of this solvent to a diamagnetic $(t\text{-butyl})_2NO/AlCl_3$ solution in benzene, regenerates the ESR spectrum of the di-t-butyl nitroxide radical. It also appears that reactions 1, 3 and 5 are fast but 2 and 4 are relatively slow and solvent dependent. Thus in 1,4-dioxane the dimerization reaction is fairly fast and this factor, combined with the smaller equi-

librium constant for complex formation, does not allow sufficient buildup of the intermediate paramagnetic complex to permit observation by ESR. In the less polar solvents the equilibrium is more favourable and dimerization is apparently much slower so that ESR spectra are observed although they decay slowly with time. The same considerations apply to the isomeric sec-butyl compounds. The latter differ however in the important respect that the overall equilibrium of reactions 3 and 4 is significantly further to the left than that of reactions 1 and 2. Thus under conditions in which sufficient $AlCl_3$ has been added to convert di-t-butyl nitroxide completely to the diamagnetic dimer there is still sufficient di-sec-butyl nitroxide present to give a reasonably intense ESR spectrum. It is this latter factor which allows the isomerization to be observed in spite of the fact that the equilibrium concentration of the sec-butyl isomer is considerably less than that of the t-butyl isomer. It is also inferred that the isomer with the t-butyl and one sec-butyl group has equilibrium constants similar to those of the di-t-butyl compound and is not observed for this reason.

Finally, the original observations involving the pyridyl radical (I) can now be explained on the basis of similar considerations but with the additional complication that complexing to the pyridine nitrogen can also occur. Apparently, the addition to radical (I) of sufficient $AlCl_3$ or BF_3 to form the pyridine complex also suffices to com-

pletely dimerize the compound. The ESR spectrum of the expected complex was therefore not observed. However, a smaller amount of the sec-butyl isomer has been formed by rearrangement and, as this is less susceptible to dimerization, sufficient free radical is present to form a pyridyl complex. It is also interesting to note that the ESR characteristics of the radicals obtained by interaction of the Lewis acid with the pyridine nitrogen mirror those of complexes involving the nitroxide group. Thus, with the BF_3-pyridine complex the coupling constant of the nitroxide nitrogen is reduced, ^{19}F coupling is observed but no ^{11}B coupling occurs. For the nitroxide complex, the ^{14}N coupling is enhanced, ^{11}B coupling is quite large but ^{19}F coupling is absent. Assignment of the Lewis base site is therefore unambiguous.

CHAPTER VI

ESR STUDIES OF THE PHOTOLYSIS OF METAL ACETATES

A. INTRODUCTION

Inorganic photochemistry is considerably less well developed than its organic counterpart. Photochemical studies of metal complexes in particular, present a number of experimental and theoretical difficulties over and above those encountered with most organic molecules. Theoretically, the principal problem lies in the large number of excited states of differing spin multiplicities and characters available for potential photochemical reactions. In organic molecules only a restricted number of low lying singlet and triplet states usually require consideration. Experimentally, problems arise because many metal complexes readily undergo ligand exchange and oxidation-reduction reactions in their ground states and it is not always easy to disentangle the photochemical reactions from the thermal ones. As a result of this latter restriction, the bulk of the earlier work on the photochemistry of metal complexes was concerned with the relatively inert Cr(III) and Co(III) compounds. There has however been considerable expansion of the field in the last few years which is reflected in several recent reviews(90,91,92,93) and a mono-

graph(24) published in 1970.

It is usual to classify the electronic absorption spectra of coordination compounds as arising from ligand field transitions, charge transfer transitions and internal ligand transitions(24). The second category can be subdivided into metal to ligand and ligand to metal charge transfer bands. Irradiation in a charge transfer band of a metal complex can be reasonably expected to result in one-electron oxidation or reduction of the metal ion accompanied by concurrent production of free radicals from the ligand. Such processes have indeed been frequently postulated and the resulting free radicals detected indirectly by means such as their ability to initiate the polymerization of organic monomers(94). In a few cases, the free radicals have been detected directly by ESR(27,28,34,95,96). Recently, Janzen and Blackbourn(97) have reported an interesting variation of the ESR method in which the primary radicals are trapped as more stable nitrone radicals which can be identified by analysis of their ESR spectra. There has however been little systematic study of the relative susceptibility of different metal salts or complexes to photochemical oxidation or reduction.

In the present study a series of metal acetates have been irradiated with ultra-violet light and the resulting radicals examined by ESR. Most of the radicals expected to be formed are reactive species with lifetimes too short for detection by solution ESR at room temperature. The experi-

ments are therefore performed in frozen solution at liquid nitrogen temperature. Under these conditions spectral resolution is relatively low and only simple radicals can be unambiguously identified. This factor dictated the choice of anion.

Relatively little work has been reported on the photochemistry of acetic acid and acetates. The lowest lying excited state of acetic acid is an n- π^* transition which in the vapour phase occurs around 2100 Å(98). Aushoos and Steacie(99) examined the products of the photochemical decomposition of acetic acid vapour and concluded that four primary reactions may occur, namely.

$$CH_3COOH \xrightarrow{h\nu} CH_4 + CO_2 \qquad (6.1)$$

$$CH_3COOH \xrightarrow{h\nu} CH_3COO^{\cdot} + H^{\cdot} \qquad (6.2)$$

$$CH_3COOH \xrightarrow{h\nu} CH_3CO^{\cdot} + OH^{\cdot} \qquad (6.3)$$

$$CH_3COOH \xrightarrow{h\nu} \dot{C}H_3 + \dot{C}O_2H \qquad (6.4)$$

Sufficient energy is available for any of these processes. In addition, they found evidence for the secondary reaction

$$CH_3COOH + \dot{C}H_3 \longrightarrow CH_4 + \dot{C}H_2COOH \qquad (6.5)$$

Earlier studies had been reported by Farkas and Wansborough-Jones(100), Cusius and Schanzer(101) and Burton(102). The latter author demonstrated the presence of free radicals by a metal mirror technique. Reaction (6.1) does not lead to

radical products and cannot therefore be studied by ESR. The remaining reactions all give rise to radicals which can be distinguished by their ESR spectra.

The initial intent of this work was to investigate which, if any, of the above reactions occur with metal acetates and whether there is variation of the photochemistry with differing metal ions. Both transition and non-transition metal ions have been employed. It seemed reasonable that metal ions capable of one-electron oxidation or reduction might favour radical formation. The investigations of Sheldon and Kochi(103) on the photochemistry of Ce(IV) carboxylates support this view. A second objective concerned acetates capable of two-electron oxidations or reductions. Thus Kochi and Bethea(104) have studied the photochemistry of Tl(III) carboxylate and postulated Tl(II) intermediates. Such compounds should be paramagnetic and observable by ESR. Similar possibilities exist for Pb(IV) compounds and a recent paper by Heusler and Loeliger(35) has made use of ESR. Both primary and secondary radicals were observed but no paramagnetic lead species could be detected.

B. EXPERIMENTAL

Commercially available metal acetates were used in the present studies. The large majority of metal compounds were irradiated in frozen acidified aqueous solution (except in one or two cases where the irradiation was performed in frozen benzene) with a PHILIPS SP-500W mercury lamp. In particular,

0.1 M solutions of the metal acetates in 10% H_2SO_4 were used and, in most cases, both irradiation and ESR experiments were carried out at 77°K. For this purpose an insertion-type dewar vessel was employed. Warming experiments, in order to establish secondary reactions, were also performed. In this case, the variable temperature accessory of the spectrometer was used so that monitoring of the shape of the ESR spectra as a function of temperature could be achieved. Description of the several accessories employed in the present experiments is given in Chapter II.

C. THE IDENTIFICATION OF THE RADICALS OBSERVED

The initial problem in studies of the present type is the identification of the radicals produced. This problem becomes increasingly more severe as the radicals become more complex. As indicated above, only a restricted number of simple radicals are expected from the photolysis of acetates and this factor influenced the choice of systems. Hydrogen atoms are the simplest paramagnetic product. In acidified ice they display an ESR spectrum consisting of a doublet with a large hyperfine separation of around 1415 MHz (~502 gauss)(105). This hyperfine splitting is somewhat variable(106) but this causes no ambiguity in the identification of the species. The methyl radical gives rise to a quartet with 1:3:3:1 intensities and a 23 gauss splitting(107). This again presents no problem in identification. The hydroxyl radical should show a doublet with an isotropic splitting of approximately 41 gauss(106).

Both the g value and the hyperfine coupling are significantly anisotropic so a somewhat distorted spectrum would be expected in a polycrystalline matrix. In the present experiments, this radical has not been observed but its identification should not present a problem if it were present. The formyl radical $HCO^{\cdot}$ gives rise to a doublet with 128 gauss separation(108). The anisotropy of the g value and hyperfine coupling broadens the higher field component more than the lower field component and imparts a characteristic appearance to this spectrum. The acetyl radical ($CH_3CO^{\cdot}$) resembles methyl in giving a quartet ESR spectrum. However, its coupling constant (16.8 gauss) is sufficiently different(109) to allow it to be distinguished. It could however be difficult to detect in the presence of larger amounts of $\dot{C}H_3$ and $\dot{C}H_2COOH$. This latter radical(110) or its ionized form $\dot{C}H_2COO^-$(111) is expected to give rise to a triplet spectrum with splitting 21 - 22 gauss and relatively broad lines owing to the anisotropy of the coupling. This is conveniently different from the sharp quartet produced by $\dot{C}H_3$. Finally, either of the radicals $\dot{C}O_2^-$(112) or $\dot{C}O_2H$(113) will show a relatively sharp singlet at the centre of the spectrum close to g = 2. The proton in the latter species apparently does not cause appreciable splitting(113). Since many free radicals give a single line close to g = 2 this is in some respects an unsatisfactory identification and some unsuccessful efforts to locate ^{13}C satellites to confirm the assignment were made. However, there is no other non-hydrogen containing

radical which can result in any simple manner from the photolysis of acetate solutions and therefore CO_2^- (or $\dot{C}O_2H$) is postulated whenever a single g = 2 resonance is observed. The radical $CH_3CO_2^{\cdot}$ does not appear to have been reported and there is no evidence for its occurrence in the present studies.

D. RESULTS AND DISCUSSION

The majority of photolyses have been performed in frozen aqueous solution acidified to prevent hydrolysis of the acetates. It is necessary to compare the resulting spectra with those obtained from acetic acid alone. Fig. VI-1 shows the spectrum resulting from the photolysis of 0.2 M sodium acetate in 10% sulfuric acid. The two radicals present are $\dot{C}H_3$ and $\dot{C}O_2H$ (Fig. VI-1B). It appears that the predominant reaction is that shown in equation (6.4) above and that reactions (6.2) and (6.3) do not occur to any significant extent. This result could be rationalized on the basis that the carbon-carbon linkage is the weakest bond in the acetic acid molecule and hence, other things being equal, the most likely to break. It is also noted that in these circumstances there is no production of secondary radicals by reaction (6.5). Relatively few radicals are produced and the spectrum of Fig.VI-1A required 30 mins. of irradiation. It has also been demonstrated that frozen solutions of acetic acid in benzene give the same radicals but with the added complication that secondary radicals (probably $\dot{C}_6H_5$) are produced by reaction of the $\dot{C}H_3$ with

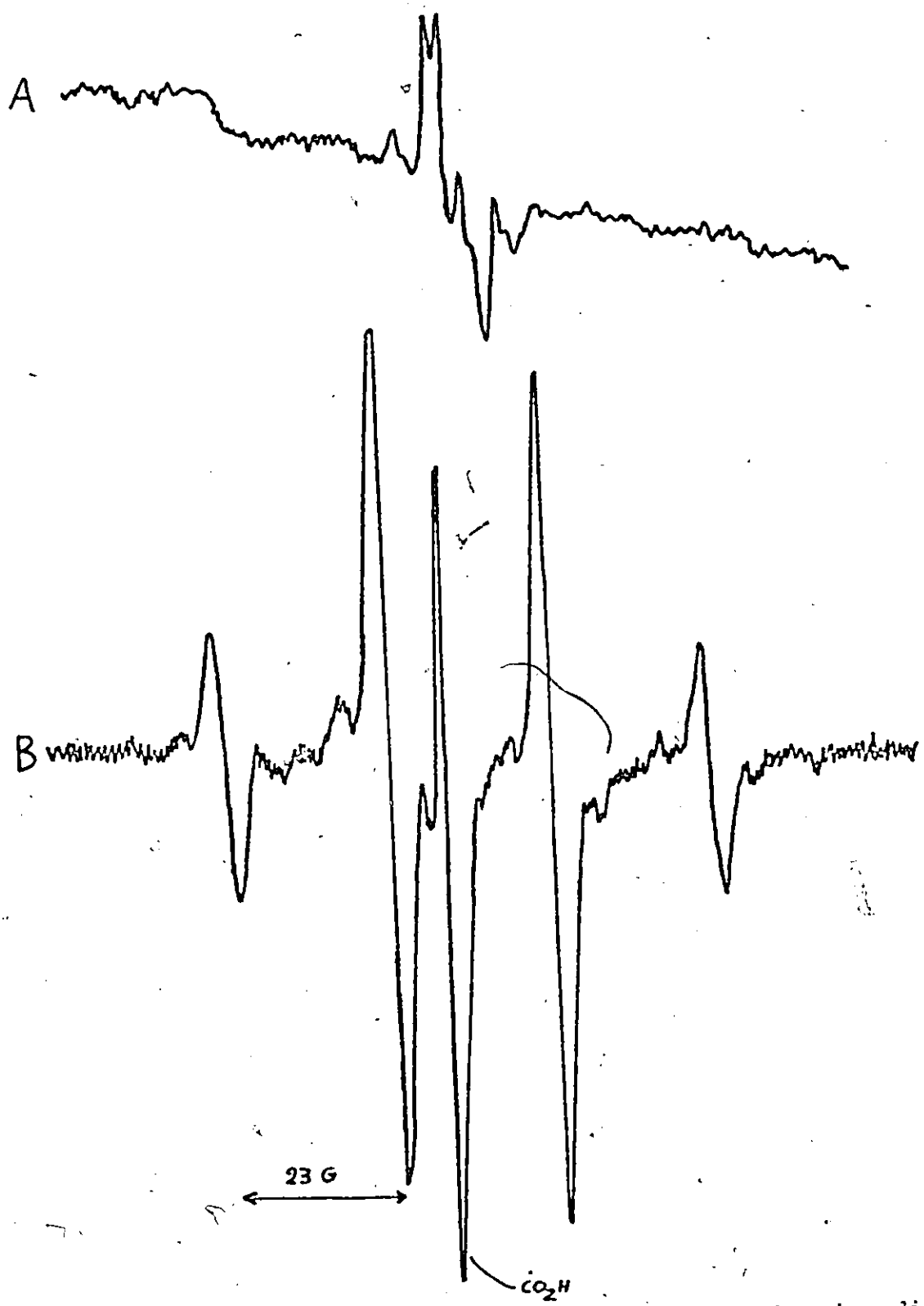

FIGURE VI-1. (A) ESR spectrum obtained after 30 mins. irradiation of a solution of 0.2 M sodium acetate in 10% H_2SO_4 at 77°K. (B) Central part of the same spectrum after two hours irradiation. The quartet lines, separated by 23G, represent methyl radicals.

the solvent. Acetic acid shows very little absorption at wavelengths longer than 250 m (114). The acetate ion has more intense absorption but at even shorter wavelengths(114). The UV spectra of some of the metal acetates involved in this study have been examined. The UV absorption of Zn(II) and Co(II) acetates, for example, moves to shorter wavelengths but is relatively more intense than that of the acetate ion. On the other hand, for some acetates e.g., Tl(III) additional absorption presumably of a charge transfer nature appears at longer wavelengths. For those acetates showing no obvious charge transfer band the greater intensity of the acetate ion absorption might be expected to lead to increased production of free radicals even if the mechanism for radical formation is unchanged. This indeed occurs. Thus, irradiation of solutions of Zn(II), In(III), Ni(II) and Co(II) acetates in 10% sulfuric acid leads to increasingly intense ESR signals along this series. In all these cases, CH_3 and CO_2H are the principal radical species, but on passing along the series increasing amounts of two new radical species, H and CHO, are observed indicating new photochemical reactions.

Photolysis of Hg(II) and Pb(II) acetates also give rise to considerably more intense ESR spectra than are obtained with acetic acid alone, but in these cases, only CH_3 and CO_2^- are observed. Figure VI-2A shows a spectrum obtained with Zn(II) acetate. The spectrum of Fig. VI-2B is obtained with Co(II) acetate and that of Fig. VI-3 with Pb(II) acetate. In all these cases, the concentration of the metal

FIGURE VI-2. ESR spectra obtained after 30 mins irradiation at 77°K of (A) 0.1 M solution of Zn(II) acetate in 10% H_2SO_4, (B) 0.1 M solution of Co(II) acetate in 10% H_2SO_4. The lines representing $CHO^{\cdot}$ are separated by 128 G. The hydrogen atom splitting is 503 G.

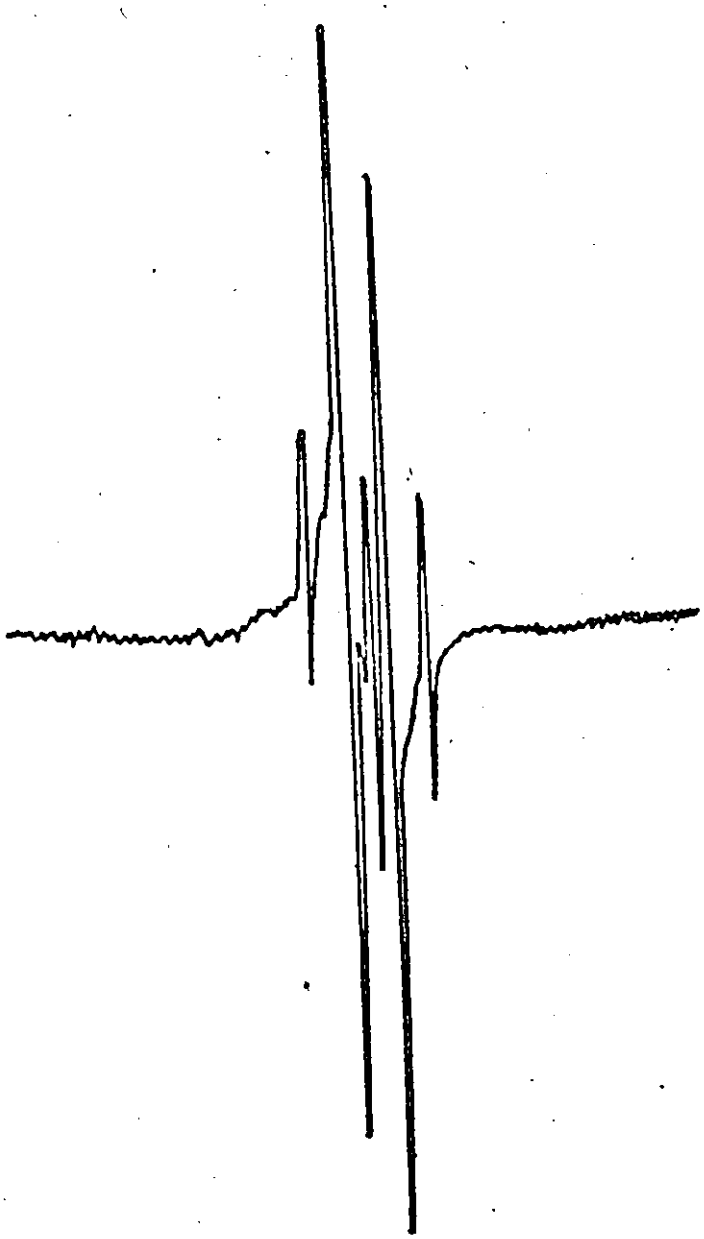

FIGURE VI-3. ESR spectrum obtained after 30 mins irradiation of a solution of 0.1 M Pb(II) acetate in 10% H_2SO_4 at 77°K.

acetate was 0.1 M and the irradiation time 30 mins.

None of the reactions (6.1) - (6.4) lead to H· and CHO·. In the case of Co(II) hydrogen atoms have been shown to be produced by a photoreaction involving the metal ion and complexed water, i.e.,

$$Co^{2+}(H_2O) \xrightarrow{h\nu} Co^{3+} + OH^- + H\cdot$$

However, this does not occur with the other metal ions in this series, as shown by irradiation of similar solutions containing the chlorides rather than the acetates, and even with Co(II) it was reported(34) that the hydrogen atom spectra were significantly more intense with the acetate than with the chloride. An additional photochemical process is therefore indicated. The most reasonable possibility would seem to be reaction (6.2) followed by rapid decarboxylation of the acetate radical(115), i.e.,

$$CH_3COOH \xrightarrow{h\nu} CH_3COO\cdot + H\cdot$$

$$CH_3COO\cdot \longrightarrow \dot{C}H_3 + CO_2$$

The formyl radical cannot be a primary product and presumably arises from reaction of hydrogen atoms with free or complexed acetic acid as suggested previously(34), i.e.,

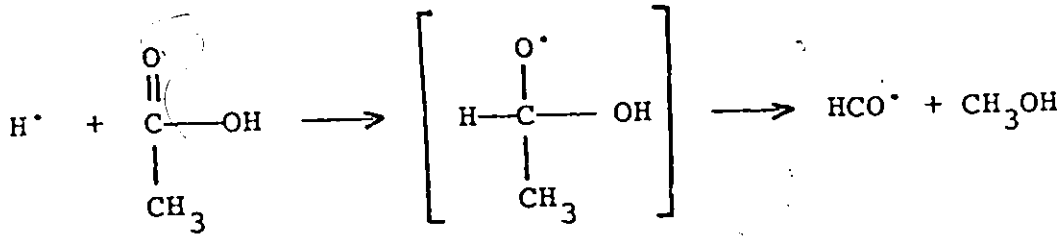

In agreement with this, DCO is formed if the photolysis is carried out in D_2O.

We turn now to the spectra obtained from the photolysis of Tl(III)acetate. As mentioned above, it was hoped to be able to detect Tl(II) species in this experiment since they had been postulated as intermediates by Kochi and Bethea(104). Experimentally, a very strong $\dot{C}H_3$ signal is observed but no other paramagnetic species. A spectrum is shown in Fig. VI-4. The satellite lines shown, arise from simultaneous electron spin/nuclear spin transitions and will be discussed in Chapter VII. It is to be noted that these spectra are much more intense than those discussed above and require only a few seconds irradiation. Clearly a different photochemical process is involved. Tl(III) acetate shows absorption throughout the ultra-violet with the tail of the band extending to 360 mμ(104). Kochi and Bethea(104) consider that this absorption is in part charge transfer in origin. The decomposition products are therefore a methyl radical and a neutral carbon dioxide molecule rather than a methyl radical and a $\dot{C}O_2^-$ or $\dot{C}O_2H$ radical. The process can therefore be written as follows:

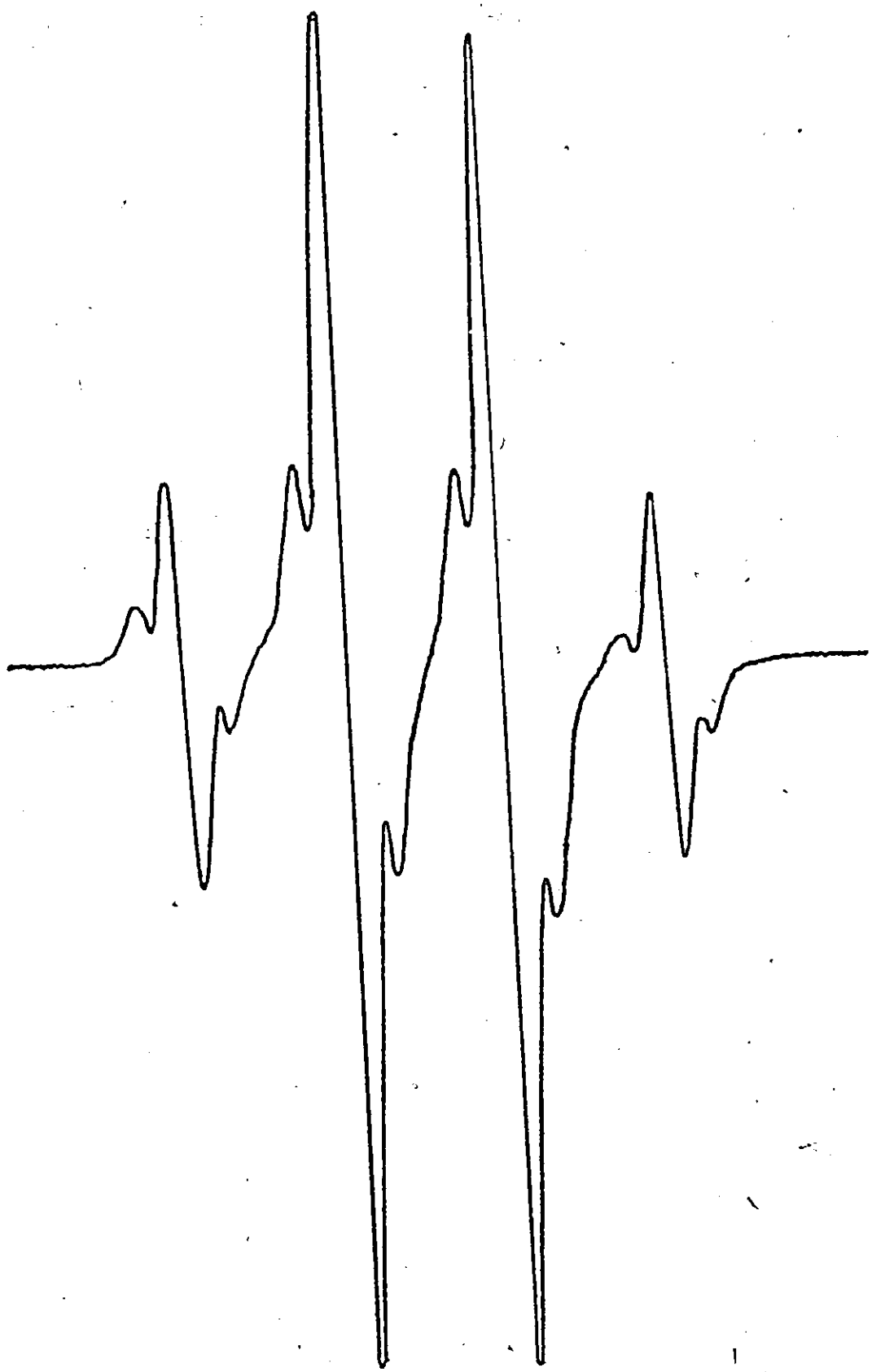

FIGURE VI-4. ESR spectrum obtained after 3 mins irradiation of 0.1 M Tl(III) acetate in 10% H_2SO_4 at 77°K. The satellites are attributed to second order transitions.

$$(CH_3CO_2)_3Tl \xrightarrow{h\nu} (CH_3CO_2)_2Tl + \dot{C}H_3 + CO_2$$

$$(CH_3CO_2)_2Tl \xrightarrow{fast} (CH_3CO_2)Tl + \dot{C}H_3 + CO_2$$

The second step may be either thermal or photochemical but is, in any event, sufficiently fast to prevent the buildup of a detectable concentration of the Tl(II) intermediate. The essential correctness of this mechanism is confirmed by the observation of Kochi and Bethea(104) of a quantative yield of two moles of carbon dioxide per mole of Tl(III) acetate. A careful search for additional features in the spectrum which might be ascribed to a Tl(II) species revealed only a broad line at g ≅ 4.2. However, the intensity of this line did not change upon irradiation and it must be assigned to an impurity. It was considered possible that Tl(II) might be stabilized relative to Tl(I) by a more electron withdrawing ligand. A number of experiments were therefore tried out irradiating Tl(III) trifluoracetate and mixtures of Tl(III) acetate and trifluoracetic acid. A number of new ESR lines were indeed observed in these experiments which are not readily assignable to $\dot{C}F_3$, FCO· or any of the radicals previously discussed. However, irradiation of a sample of trifluoracetic acid in benzene yielded spectra containing the unassigned lines and it was therefore concluded that the radicals did not contain Tl. Tl(I) acetate is not soluble in 10% sulfuric acid. Irradiation

of an acidified solution in benzene showed only relatively weak signals from $\dot{C}H_3$ and $\dot{C}O_2H$, i.e., the radicals expected from acetic acid.

The possible photoreaction of Pb(IV) and Sn(IV) acetates are formally similar to those of Tl(III). Heusler and Loeliger(35) have reported an ESR study of some eleven Pb(IV) carboxylates including the acetate. They found that $\dot{C}H_3$ was the primary product and that $\dot{C}H_2COO^-$ was formed in a subsequent thermal reaction which they postulated to be abstraction of hydrogen by the methyl radical, i.e.,

$$CH_3COO^- + \dot{C}H_3 \longrightarrow \dot{C}H_2COO^- + CH_4$$

In our case, essentially similar spectra were obtained by irradiating lead tetraacetate in frozen benzene solutions (Fig. VI-5). Also, in agreement with Heusler and Loeliger, no ESR spectrum attributable to Pb(III) species was observed. The reasons for this, probably parallel those discussed above for Tl(III) acetate. The occurrence of $\dot{C}H_2COO^-$ in these experiments is a little puzzling in that in previous cases, notably Tl(III) acetate, there is evidence for an abundance of $\dot{C}H_3$ radicals but no indication of their reaction to give $\dot{C}H_2COO^-$ even when both complexed and free acetic acid was present in large excess. Careful examination of the spectrum in Fig.VI-5 convinced us that the acetyl radical, $CH_3CO^{\cdot}$, is also present. The spectra are rather badly overlapped but closely resemble the

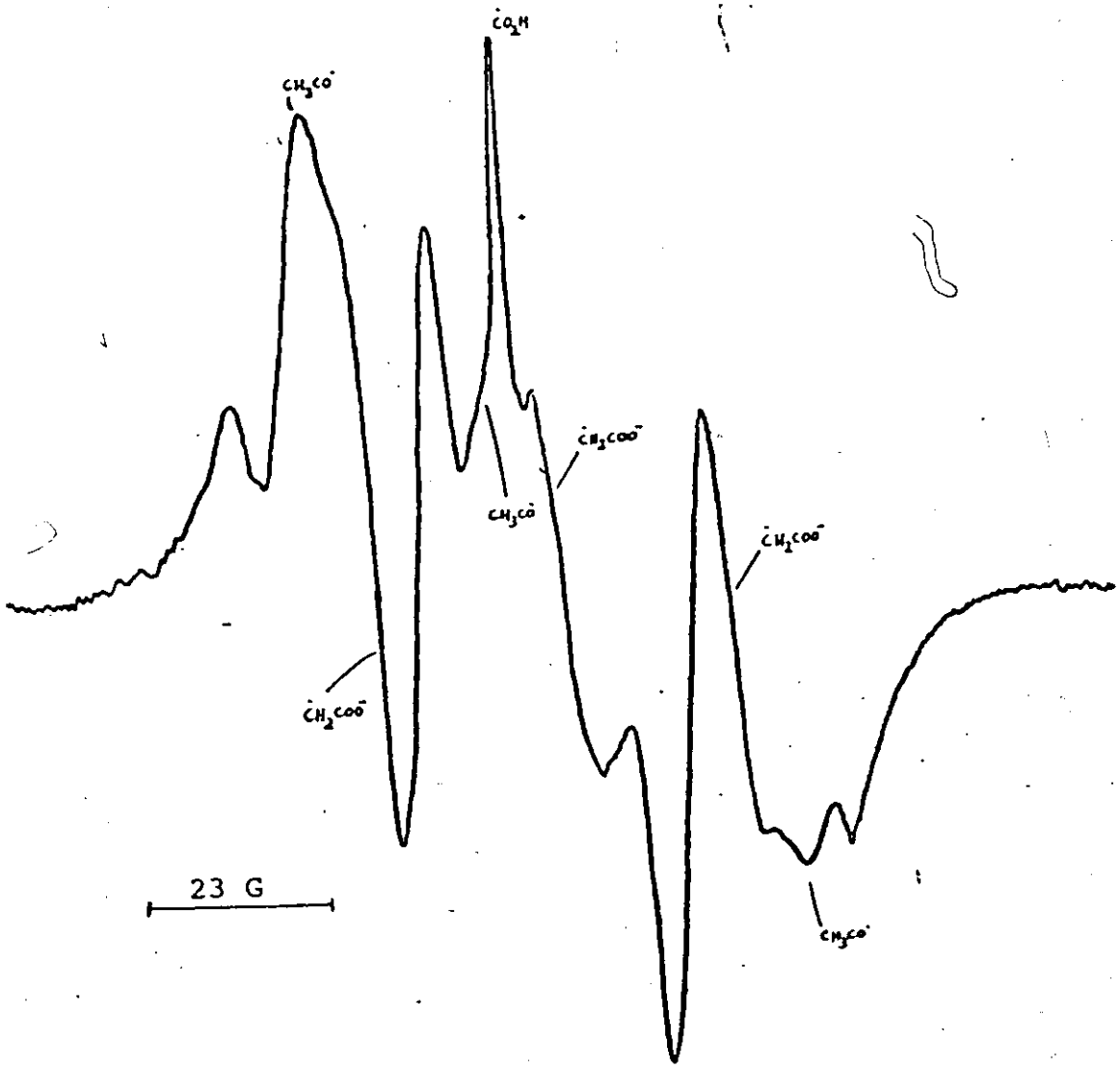

FIGURE VI-5. ESR spectrum obtained after 20 mins irradiation of a solution of 0.1 M Pb(IV) acetate in benzene at 77°K.

published spectra of Morton and Falconer(98) attributed to a mixture of $\dot{C}H_3$ and $CH_3CO^{\cdot}$ radicals obtained by irradiating biacetyl. This observation suggests an alternative reaction for forming $\dot{C}H_2COO^-$ radicals. Acetyl radicals could arise from the reaction

$$CH_3COOH \xrightarrow{h\nu} CH_3CO^{\cdot} + \dot{O}H \quad (1)$$

The hydroxyl radicals are not observed but it is known(115) that such radicals react readily with acetate ions to abstract hydrogen.

$$CH_3COO^- + \dot{O}H \longrightarrow \dot{C}H_2COO^- + H_2O$$

Thus, it is postulated that the observation of $\dot{C}H_2COO^-$ is an indication that the hydroxyl radical is a primary product and that the former radical is not associated with the photolytic reaction giving $\dot{C}H_3$. A number of further experiments were carried out with the objective of detecting a Pb(III) species. Photolyses using the trifluoracetate gave unidentified spectra identical to those described for the analogous Tl(III) compound. A number of organometallic compounds were also photolysed in the hope that a Pb(III) alkyl or aryl derivatives might be more stable. $Pb(CH_3)_3(OCOCH_3)$, photolysed in frozen acidified aqueous solution gave only a very strong $\dot{C}H_3$ signal. $Pb(C_6H_5)_3(OCOCH_3)$, photolysed in benzene gave a spectrum which

probably arises from the phenyl radical with some additional weak lines from the methyl radical. It is therefore deduced that in these organometallic compounds the primary photochemical process is the breaking of the metal-carbon bond. A number of Sn(IV) organometallic compounds were also photolysed with a similar objective in view. $Sn(C_6H_5)_3(OCOCH_3)$ gave phenyl radicals, $Sn(C_4H_9)_3(OCOCH_3)$ and $Sn(C_4H_9)_2(OCOCH_3)_2$ gave butyl radicals and $Sn(C_3H_7)_3(OCOCH_3)$ gave propyl radicals. Fig. VI-6 shows some examples of the spectra obtained with these compounds. In each case $\dot{C}H_3$ and $\dot{C}O_2H$ were also observed indicating that both the hydrocarbon moiety and the acetate are susceptible to photolysis in these tin compounds. However, no spectrum assignable to a tin (III) species was obtained.

Finally, we turn to studies of the photolysis of iron acetates. It has been noted above that on passing along the series of acetates of Zn(II), Ni(II) and Co(II), the ESR spectra become increasingly more intense and signals from $H^{\cdot}$ and $HCO^{\cdot}$ appear in addition to those from $\dot{C}H_3$ and $CO_2^{\cdot-}$. Fe(II) continues this series but with some added complications. Photolyses were carried out in frozen aqueous solutions and the products observed are dependent on the acid concentration. Photochemical oxidation is a likely process so there is a possibility that some of the products could arise from Fe(III) species. However, irradiation of Fe(III) acetate solutions gives only very weak $\dot{C}H_3$ and $H^{\cdot}$ signals at all acid concentrations. The photolysis of Fe(III) compounds is therefore making no con-

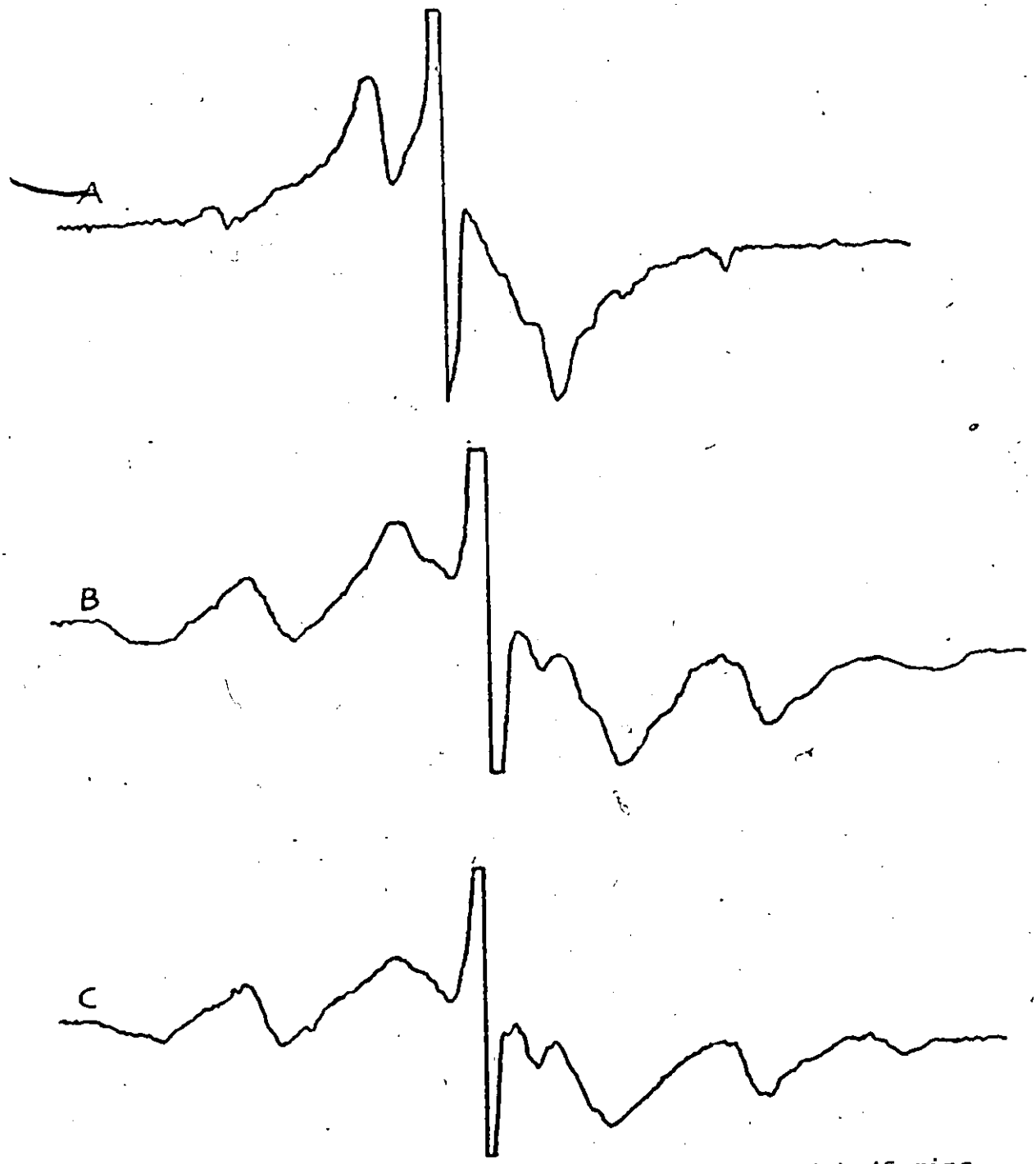

FIGURE VI-6. ESR spectra obtained at 77°K after (A) 45 mins irradiation of 0.1 M Sn(IV) triphenyl acetate in benzene, (B) 1 hour irradiation of Sn(IV) tri-N-butyl acetate, (C) 75 mins irradiation of Sn(IV) tri-N-propyl acetate in benzene.

tribution to the intense ESR spectra displayed by Fe(II) acetate solutions. No signal is observed if a frozen neutral solution of Fe(II) acetate is irradiated. As the concentration of sulfuric acid is increased up to 0.5%, an increasingly more intense spectrum containing the radicals $\dot{C}H_3$, $\dot{C}H_2COO^-$, $CH_3CO^{\cdot}$ and $\dot{C}O_2H$ is observed. The full spectrum obtained in this case is shown in Fig. VI-7A and the central part of the same spectrum is shown in Fig. VI-8A. There are also weak indications of $HCO^{\cdot}$ in this spectrum. Between 0.5% and 0.75% of sulfuric acid the intensity of this spectrum decreases steadily and at 0.75% only weak signals from $\dot{C}H_3$ and $\dot{C}O_2H$ remain. This corresponds closely to the spectrum obtained by photolysing acetic acid.

At higher acid concentrations the intensity of the spectrum increases markedly and $H^{\cdot}$ and $HCO^{\cdot}$ become the principal species present. The full spectrum obtained at high acid concentration is shown in Fig. VI-7B, while the resolved central part of the same spectrum is shown in Fig. VI-8B. Irradiation of ferrous ammonium sulfate gives only weak $H^{\cdot}$ spectra at low acid concentration, but a very strong signal appears in high acid solutions. The following interpretation of these results is therefore suggested. At high acid concentration the predominant species in solution is the hydrated ferrous ion. Nikolskii et al.(116), have carried out electrochemical studies of aqueous solutions of Fe(II) and Fe(III) acetates and concluded that $Fe(CH_3COO)^+$ predominates at low

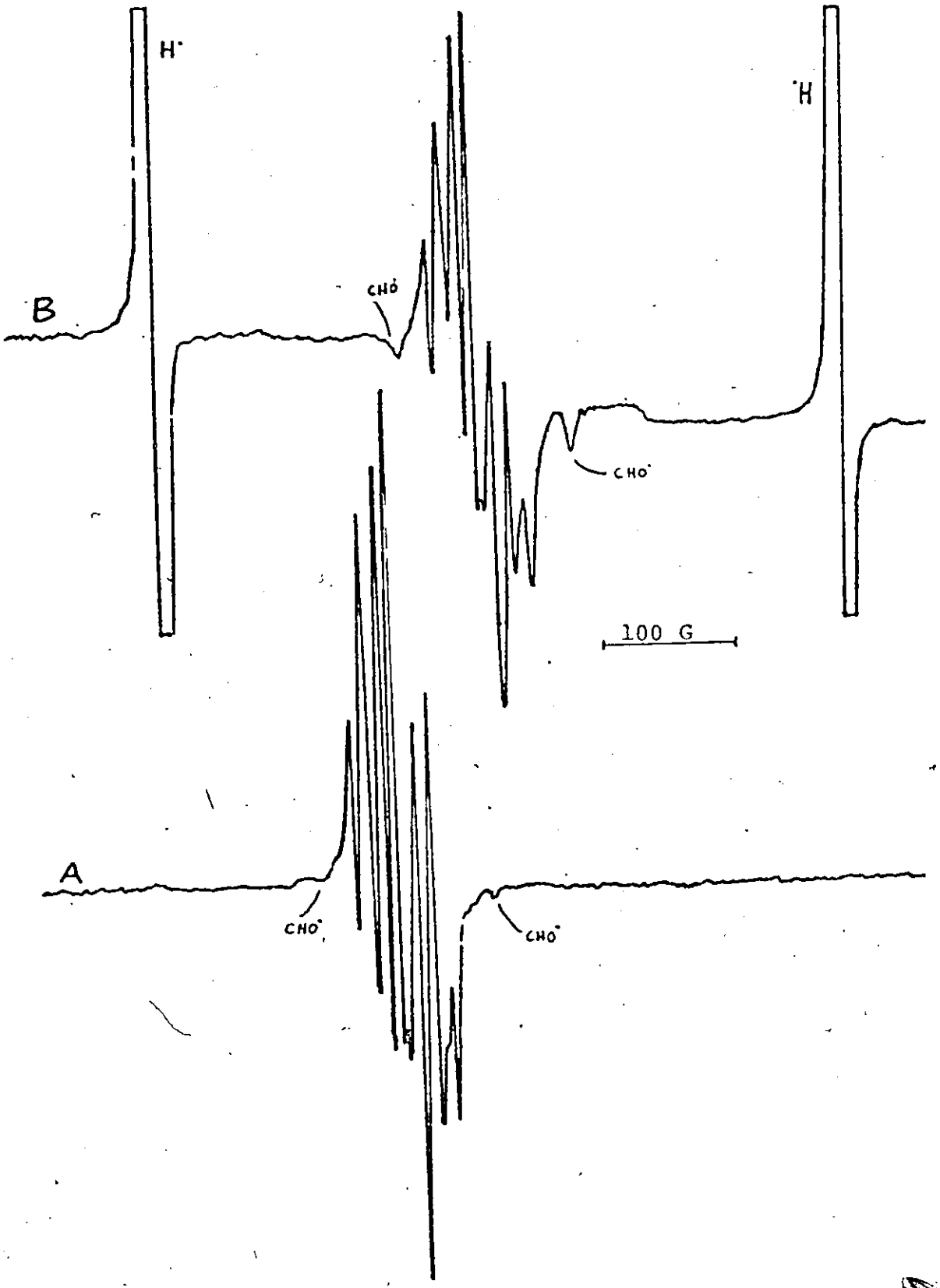

FIGURE VI-7. ESR spectra obtained at 77°K after 30 mins irradiation of 0.1 M Fe(II) acetate, (A) in 0.5% H_2SO_4, (B) in 10% H_2SO_4.

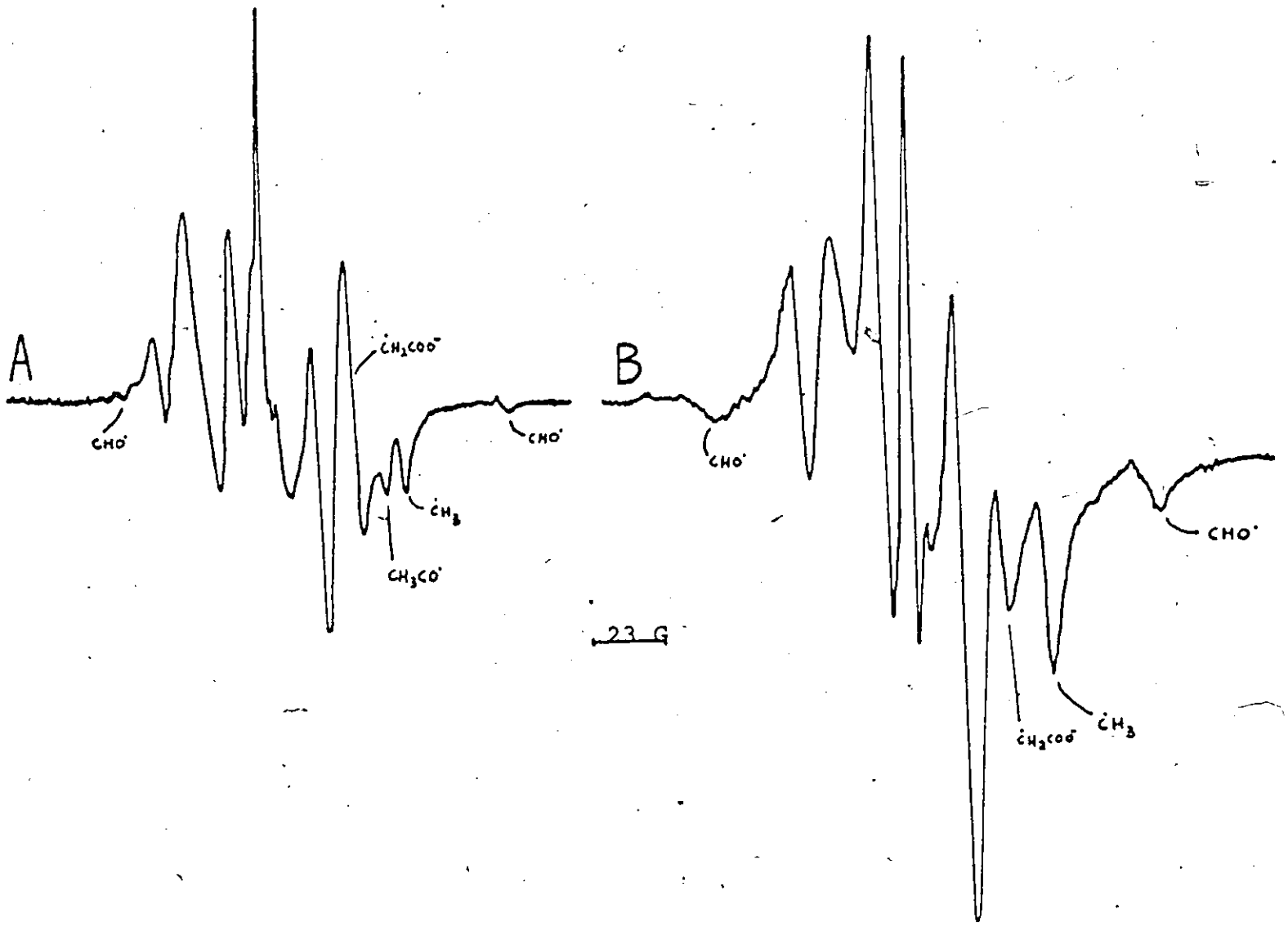

FIGURE VI-8. ESR spectra representing the resolved central part of the spectra of Fig. VI-7, obtained after 30 mins irradiation of a solution of 0.1 M Fe(II) acetate at 77°K, (A) in 0.5% H_2SO_4, (B) in 10% H_2SO_4.

acid concentration and hydrated Fe^{2+} at high acid concentration. The photolysis of hydrated Fe^{2+} has been the subject of numerous investigations and the observation of hydrogen atom ESR spectra has been reported previously(27,28,117). It is noted that hydrogen atoms are not observed at 0.75% sulfuric acid, at which concentration, no hydrated Fe^{2+} is present. This observation apparently supports the mechanism proposed by Jortner and Stein(118) which involves reaction of hydrogen ions with the initial photochemical product, i.e.,

$$Fe^{2+}(H_2O) \xrightarrow{h\nu} [Fe^{3+}\ H_2O^-]$$

$$[Fe^{3+}\ H_2O^-] + H^+ \longrightarrow Fe^{3+}(H_2O) + H^\cdot$$

With the exception of $\dot{C}H_3$, which can arise directly from the photolysis of the acetic acid present, all the other products observed by ESR arise from secondary reactions. This was demonstrated by warming experiments. On warming, the $H^\cdot$ spectrum disappears, the $\dot{C}H_3$ spectrum remains constant and $HCO^\cdot$, $\dot{C}H_2COOH$ and $CH_3CO^\cdot$, all increase in intensity. This is illustrated in Fig. VI-9. Possible secondary reactions are :

$$CH_3COOH + H^\cdot \longrightarrow \dot{C}H_3OH + CHO^\cdot$$

$$CH_3COOH + H^\cdot \longrightarrow \dot{C}H_2COOH + H_2$$

$$CH_3COOH + H^\cdot \longrightarrow CH_3CO^\cdot + H_2O$$

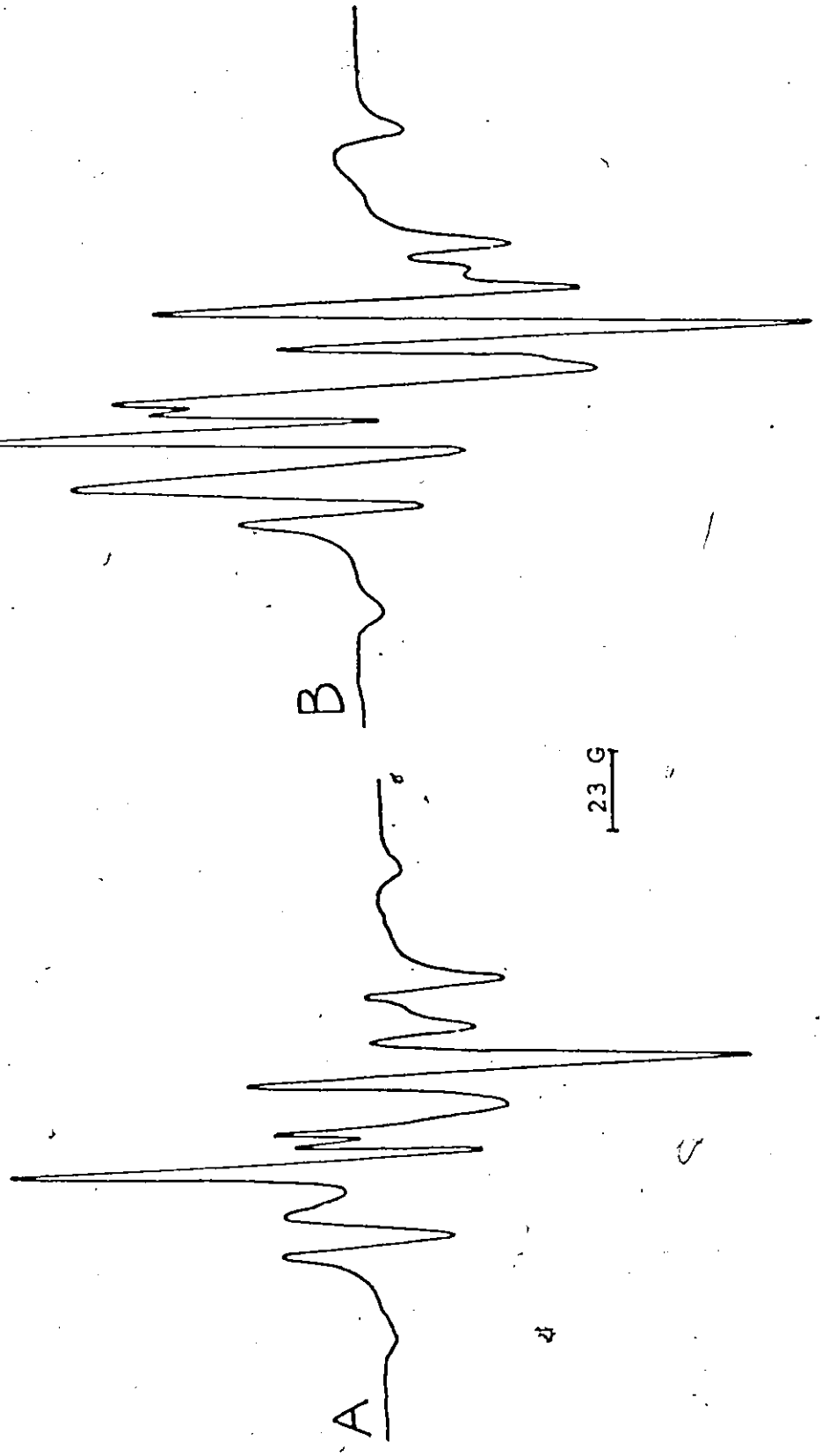

FIGURE VI-9. (A) ESR spectrum obtained after 90 mins irradiation of a solution of 0.1 M Fe(II) acetate in 10% H_2SO_4. (B) same sample after warming. Gains unchanged.

At low acid concentrations we are apparently observing photochemical reactions of coordinated acetate ions. The radicals observed can be accounted for the photochemical reactions discussed previously. Since the Fe^{2+} is capable of oxidation there are however some further possibilities, e.g.,

$$Fe(CH_3COO)^+ \longrightarrow Fe^{3+} + CH_3CO\cdot + OH^-$$

Finally, the results discussed above are summarized in Table VI-1. These results demonstrate that the photochemistry of metal acetates is both quantitatively and qualitatively different from that of acetic acid. Of the four primary reactions postulated by Aushoos and Steacie(99), ESR evidence has been obtained for all three which produce radicals. The direct decomposition to methane and carbon monoxide is not susceptible to study by this method. For the uncomplexed acid, decomposition to methyl radicals and $\dot{C}O_2H$ radicals predominates. For the complexed acid or ion, hydrogen atoms and acetyl radicals have also been observed as primary products together with a variety of secondary radicals. Acetate ions can be coordinated to metals either as monodentate or bidentate ligands(30). An X-ray structural determination (119), for example, has shown that it is bidentate in $Zn(CH_3COO)_2.2H_2O$. In principle, infrared spectroscopy can distinguish these possibilities(30) but in most cases the conclusions from the data in the literature(120) appear to be

TABLE VI-1.

Radical products detected by ESR during the UV-irradiation of metal acetates and related organometallic compounds at 77°K.

COMPOUND	SOLVENT	RADICALS	FIGURE	REMARKS
CH_3COOH	Benzene	$\dot{C}H_3$, $\dot{C}O_2H$, $\dot{C}_6H_5$		The identification of $\dot{C}_6H_5$ is uncertain.
0.2 M CH_3COONa	10% H_2SO_4	$\dot{C}H_3$, $\dot{C}O_2H$	VI-1	
0.1 M Zinc(II) acetate	10% H_2SO_4	$\dot{C}H_3$, $\dot{C}O_2H$, $\dot{H}$, $\dot{C}HO$	VI-2A	In all these cases, $\dot{C}H_3$ and $\dot{C}O_2H$ are the principal species, but on passing from Zn to Co, increasing amount of the new radical species $\dot{H}$ and $\dot{C}HO$ are observed. Also, the ESR spectra are more intense than those obtained with acetic acid alone.
0.1 M Indium(III)Acetate	10% H_2SO_4	$\dot{C}H_3$, $\dot{C}O_2H$, $\dot{H}$, $\dot{C}HO$		
0.1 M Nickel(II)Acetate	10% H_2SO_4	$\dot{C}H_3$, $\dot{C}O_2H$, $\dot{H}$, $\dot{C}HO$		
0.1 M Cobalt(II)Acetate	10% H_2SO_4	$\dot{C}H_3$, $\dot{C}O_2H$, $\dot{H}$, $\dot{C}HO$	VI-2B	
0.1 M Mercury(II)Acetate	10% H_2SO_4	$\dot{C}H_3$, $\dot{C}O_2H$		In these cases also the ESR signal is more intense but $\dot{H}$ or $\dot{C}HO$ radicals are not observed.
0.1 M Lead(II)Acetate	Benzene	$\dot{C}H_3$, $\dot{C}O_2H$	VI-3	

TABLE VI-1 (continued)

COMPOUND	SOLVENT	RADICALS	FIGURE	REMARKS
0.1 M Tl(III)Acetate	10% H_2SO_4	$\dot{C}H_3$, Satellite lines	VI-4	Very strong $\dot{C}H_3$ signal is observed. No ESR spectrum attributable to Tl(II) is observed. The satellites disappear if H_2O is replaced with D_2O. The unidentified lines observed in some cases are also observed in the spectra obtained by irradiating trifluoroacetic acid in C_6H_6.
0.1 M Tl(III)Acetate + 0.2M CF_3COOH	"	$\dot{C}H_3$, Satellite lines, unidentified lines		
0.1 M Tl(III)trifluoroacetate	40% H_2SO_4	Unidentified lines		
0.1 M Tl(III)Acetate	10% H_2SO_4 (D_2O)	$\dot{C}H_3$		
0.1 M Tl(I)Acetate	Benzene/ CH_3COOH	$\dot{C}H_3$, $\dot{C}O_2H$		Weak signals
0.1 M Lead(IV)Acetate	Benzene	$\dot{C}H_3$, $\dot{C}H_2COO^-$, $CH_3CO^{\cdot}$, $\dot{C}O_2H$	VI-5	No ESR spectrum attributable to Pb(III) was observed. The unidentified lines were also obtained by irradiating CF_3COOH in benzene.
0.1 M Lead(IV)Acetate	Benzene/ CF_3COOH	Unidentified lines		

TABLE VI-1 (continued)

COMPOUND	SOLVENT	RADICALS	FIGURE	REMARKS
Pb(IV) Trimethylacetate	10% H_2SO_4	$\dot{C}H_3$		In all these cases the spectra of the different radicals were superimposed. The radicals, $\dot{C}O_2H$; propyl, butyl, and in some cases $\dot{C}H_3$, are clearly identified. The identification of $\dot{C}_6H_5$ however, is uncertain.
Pb(IV) Triphenylacetate	Benzene	$\dot{C}H_3$, $\dot{C}_6H_5$, $\dot{C}O_2H$		
Sn(IV) Triphenylacetate	"	" " "	VI-6A	
Sn(IV) Tri-N-butyl acetate	"	$\dot{C}H_3$, $CH_3\dot{C}H_2CH_2\dot{C}H_2$, $\dot{C}O_2H$	VI-6B	
Sn(IV) Di-N-butylacetate	—	$CH_3CH_2CH_2\dot{C}H_2$, $\dot{C}O_2H$		
Sn(IV) Tri-N-propylacetate	Benzene	$CH_3CH_2\dot{C}H_2$, $\dot{C}O_2H$	VI-6C	
Fe(III) Acetate	0.5% H_2SO_4	$\dot{C}H_3$, $\dot{H}$		In both cases, $\dot{C}H_3$ and $\dot{H}$ spectra are very weak.
Fe(III) Acetate	10% H_2SO_4	$\dot{C}H_3$, $\dot{H}$		

TABLE VI-1 (continued)

COMPOUND	SOLVENT	RADICALS	FIGURE	REMARKS
0.1 M Fe(II) Acetate	H_2O	NO SIGNAL		
"	0.2% H_2SO_4 ⋮ 0.5% H_2SO_4	$\dot{C}H_3$, $\dot{C}H_2COO^-$, $CH_3CO^{\cdot}$, $\dot{C}O_2H$, $CHO^{\cdot}$ (weak)	VI-7A VI-8A	The overall intensity of the signal increases as the acid concentration increases from 0.2% to up 0.5%. From 0.55% to 0.75% H_2SO_4, the intensity gradually decreases and eventually only the $\dot{C}H_3$ and $\dot{C}O_2H$ signals are observed.
"	0.55% H_2SO_4 ⋮ 0.75% H_2SO_4	$\dot{C}H_3$, $\dot{C}O_2H$		
"	0.75% H_2SO_4 ⋮ 10% H_2SO_4	$\dot{C}H_3$, $\dot{C}H_2COOH$, $\dot{C}O_2H$, $\dot{H}$, $CHO^{\cdot}$ (The overall signal increases with increasing acid concentration)	VI-7B VI-8B	At high acid concentration the main products are $\dot{H}$ & $CHO^{\cdot}$. On warming, the $\dot{H}$ spectrum disappears, the $\dot{C}H_3$ spec. remains constant and $HCO^{\cdot}$, $\dot{C}H_2COOH$ and $CH_3CO^{\cdot}$, all increase in intensity (Fig. VI-9).
Fe(II) Sulfate	H_2O	$\dot{H}$		Very weak signal
"	0.5% H_2SO_4	$\dot{H}$		"
"	10% H_2SO_4	$\dot{H}$		Very strong signal

ambiguous. It would be tempting to correlate the very different photochemistry of say the Tl(III) and Fe(II) acetates with different forms of coordination but further structural work on acetates in solution would be necessary to make this meaningful.

CHAPTER VII

SIMULTANEOUS ELECTRON SPIN-NUCLEAR SPIN TRANSITIONS IN SOLID SOLUTIONS OF METHYL RADICALS

A. INTRODUCTION

Second order transitions due to simultaneous changes in the spin state of a single proton and the spin state of the unpaired electron are occasionally observed in ESR spectra. They are induced by a weak dipole-dipole coupling between the electron magnetic moment and the magnetic moment of the neighbouring proton. These transitions were first detected as satellites accompanying the main lines of atomic hydrogen produced in γ-irradiated frozen acids(37,121). A theoretical treatment of these satellites has been given by Trammell, Zeldes, and Livingston(38) who also predicted a second and even third set of satellites corresponding to two and three neighbouring protons simultaneously changing states. This was confirmed experimentally by Kohnlein and Venable(39) who observed additional sets of lines in the ESR spectra of atomic hydrogen at high microwave power levels. There have been only two instances however, in which the satellites appear in ESR spectra of free radicals, i.e., the ESR spectra of γ-irradiated single crystals of thymidine(40) and barbituric acid dihydrate(41). In either case, absolute determination of which protons in the

crystal give rise to these satellite lines was not made, but in the case of barbituric acid dihydrate it was assumed that the protons of the water molecules in the hydrated crystal are responsible for this effect. In the present chapter, experimental evidence of the occurrence of second order transitions in the ESR spectrum of methyl radicals is presented. These transitions are attributed to the flipping of a single proton of the solvent nearby to which the electron spin is weakly coupled through dipole-dipole interaction. In addition, the effective single proton distance from the carbon nucleus of the methyl radical has been estimated as a function of temperature.

B. PRELIMINARY OBSERVATIONS

In the process of examining the photochemistry of Tl(III) acetate, the ESR spectra of methyl radicals (produced during the UV-irradiation of $Tl(OCOCH_3)_3$ in 10% H_2SO_4 at 77°K) clearly showed satellite lines accompanying the main absorption lines, Fig. VII-1A. The separation of the satellites from the main hyperfine lines, in frequency units, is close to the proton resonance frequency for the particular magnetic field strength at which the observation is made. Thus, the observed separation of 4.85 gauss compared favourably with the theoretically predicted value of 4.95 gauss for magnetic field 3,250G. Also, preliminary power-saturation experiments indicated that:

(a) the intensity ratio of the satellite to the main transition increases on increasing the microwave power (this

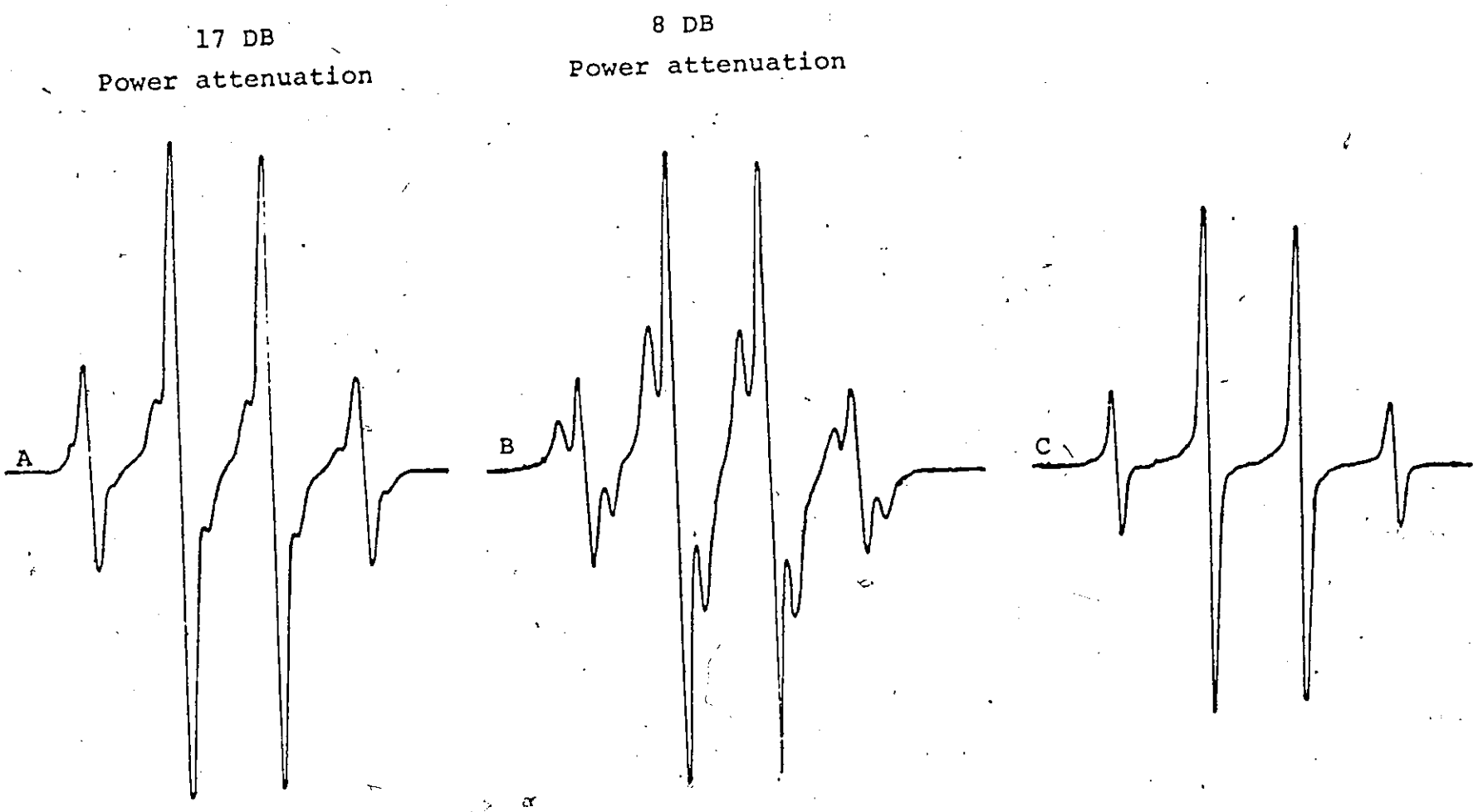

FIGURE VII-1. Methyl radical ESR spectra obtained after 2 hrs irradiation of 0.1 M Tl(III) acetate in 10% H_2SO_4 at 77°K, (A) microwave power attenuation 17 DB, (B) power attenuation 8 DB, (C) obtained in 10% H_2SO_4 disolved in D_2O - power attenuation 8 DB.

is in agreement with previous experimental observations), Fig. VII-1B.

(b) no additional sets of satellites appeared even at high microwave power.

It was therefore confirmed that the observed satellites correspond to a single proton concurrently changing state with the change in spin state of the electron. Furthermore, a solution of $Tl(OCOCH_3)_3$ in 10% H_2SO_4 - where H_2O has now been replaced by D_2O - was irradiated and its ESR spectrum recorded at 77°K, Fig. VII-1C. The fact that satellite lines could not be found in this spectrum is expected if the weak dipole-dipole coupling is to a Deuteron rather than to a proton (in this case the separation of the satellites is reduced by a factor $g_D/g_H = 0.153$ and therefore the satellites cannot be resolved). This observation on the other hand, would mean that the nuclei which give rise to the satellites are protons of the water molecules.

C. EFFECTIVE SINGLE-PROTON DISTANCE AS A FUNCTION OF TEMPERATURE

In their theoretical treatment, Trammell et al.(38) have derived expressions in which the intensity ratio of the satellites to the main absorption line is related to the average distance of the flipping protons from the nucleus on which the spin density is concentrated (see Ch.II, Sec.B-4c). The single-proton distance for randomly oriented systems is given

by equation,

$$T_1/2T_2 \cong (3/20)\left\langle \sum_i \frac{g_e^2 \beta_e^2}{H^2 r_i^6} \right\rangle \qquad (7.1)$$

where T_1, T_2 are the intensities of the satellite and the main line, respectively, H is the applied field and r_i represents the distance of the ith flipping proton from the nucleus on which the spin density is concentrated. In order to obtain the correct experimental ratio $T_1/2T_2$, certain corrections had to be made, namely corrections for saturation effects and also for overlap of the lines. This was achieved as follows: A sample of $Tl(OCOCH_3)_3$ in 10% H_2SO_4 was irradiated for ~1 hr. Using always the same irradiated sample, SEVEN groups of ESR spectra of the low field central line of the methyl radical (H=3,250G) were recorded at seven different temperatures ranging from -182°C to -122°C at 10°C intervals. Each group consisted of seven spectra obtained at different microwave power levels, but otherwise, recorded under the same conditions (instrumental). Each experimental spectrum was analyzed on the basis of a corresponding computer-calculated spectrum. This calculation was made on the following assumptions:

(a) The spectrum is composed of three lines each represented by the derivative of a Gaussian curve with two adjustable parameters, the amplitude and width.

(b) The two satellite lines on each side of the main

line are of equal intensity relative to each other but have different intensity relative to the central line.

(c) The separation of the satellites from the main line is constant and taken to be 4.85G (experimental value).

(d) All three lines have the same linewidth (peak to peak).

By introducing 30 data points from each experimental spectrum, the computer was programmed(122) for optimum spectrum fit by varying the intensity and linewidth parameters. For each spectrum fit the intensities of the satellite lines and the main line were read directly on the calculated spectrum. An example of a spectrum fit is shown in Fig. VII-2A .

The saturation behaviour of the satellites and the main transition is shown in Fig. VII-2B , where the corrected intensities (for overlap) are plotted against the microwave power. Also, the plot of the intensity ratio versus microwave power is shown in Fig. VII-2C . From the plot the corrected value of $T_1/2T_2$ (for saturation) is obtained by extrapolating to zero power. Finally, this value obtained for the different temperatures, is used in equation (7.1) for the calculation of the effective single-proton distance, defined as

$$r_{eff} = \left[\left\langle \sum_i \frac{1}{r_i^6} \right\rangle \right]^{-1/6} \qquad (7.2)$$

The plot of r_{eff} versus temperature is shown in Fig. VII-2D .

D.DISCUSSION

The previous reports of the observation of satellite

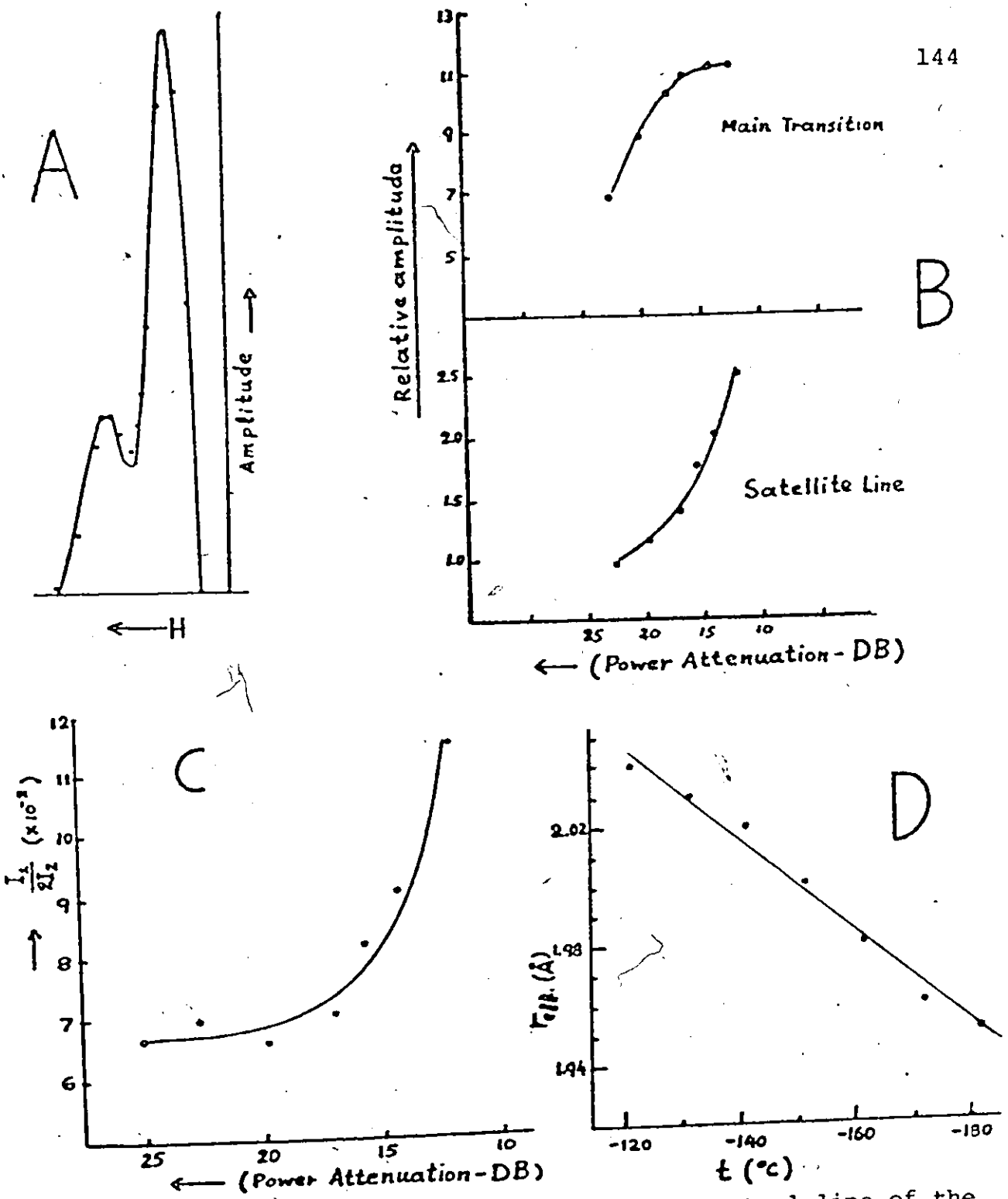

FIGURE VII-2. (A) One half of the low field central line of the methyl radical and its satellite(—) compared with the calculated spectrum (·). (B) Microwave power saturation of the main transition and the satellite of the low field central line of methyl radical. (C) Plot of $I_1/2I_2$ (I_1=satellite intensity, I_2=intensity of main transition) vs power attenuation, corresponding to t= -182°C. (D) Variation of the effective single-proton distance, r_{eff}, with temperature.

lines in ESR spectra have referred to either hydrogen atoms or to complex organic radicals obtained by γ-irradiation of single crystals. The present results are of interest in that they refer to a small radical of known geometry and because it has proved possible to study the effects as a function of temperature. From the method of producing the radicals, the possibility that the interacting proton was located on a neighbouring acetate ion was initially considered, since the reaction,

$$\dot{C}H_3 + CH_3COO^- \longrightarrow CH_4 + \dot{C}H_2COO^-$$

had to be postulated to occur in acetate photochemistry at low temperatures (see Ch. VI). However, the disappearance of the satellites when the irradiation is carried out in D_2O demonstrates that this is not the case and that the interaction is with a solvent proton. The calculated internuclear separation of 1.95 Å between the methyl carbon and the solvent proton at -182°C may be compared with the value of 1.73 Å obtained from atomic hydrogen satellites. This relatively short separation places some clear limitations on the nature of the radical's environment. The interacting proton cannot be in the plane of the methyl radical since the C-H bond length of 1.1 Å plus the hydrogen Van der Waals radius of 1.0 Å clearly will not allow the observed internuclear separation. A much more plausible model is one in which the proton is situated perpendicular to the plane of the methyl radical. Examination of a molecular model of the ice crystal shows that the observed separation

is consistent with that of a proton perpendicular to the plane of the radical for either the case where a $\dot{C}H_3$ radical has been substituted for a H_2O molecule in the lattice or for the case where a $\dot{C}H_3$ radical has been introduced in one of the open "cages" in the ice lattice. We are not able to postulate a specific site. The increase in the separation to 2.04 Å at -122°C on warming can be correlated with the expansion of the ice lattice. At temperatures higher than -100°C methyl radicals are no longer observed. Presumably diffusion and subsequent recombination of the radicals becomes possible at this temperature. Analysis of this temperature dependence has not been attempted, but the observation of these satellites would seem to offer an interesting approach to the study of crystal lattice behaviour.

REFERENCES

1. O.H.Griffith and A.S.Waggoner, Accounts of Chem. Research, 2, 17(1969).
2. E.G.Rozantzev and M.B.Neiman, Tetrahedron, 20, 131(1964).
3. R.Briere, H.Lemaire, and A.Rassat, Bull.Soc. Chim.France, 3273(1965).
4. E.G.Rozantzev and Yu.V.Kokhanov, Izv. Akad. Nauk SSSR, Ser. Khim., 1477(1966).
5. E.G.Rozantzev and L.A.Krinitzkaya, Tetrahedron, 21, 491(1965).
6. A.K.Hoffmann and A.T.Henderson, J.Am. Chem. Soc., 83, 4671(1961).
7. P.Hemmerich, Proc. Roy. Soc. (London), A302, 335(1967).
8. M.T.Jones and W.D.Phillips, Ann. Rev. Phys. Chem., 17, 323(1966)
9. F.A.Walker, R.L.Carlin and P.H.Rieger, J.Chem. Phys., 45, 4181(1966).
10. B.J.Corden and P.H.Rieger, Inor. Chem., 10, 263(1971).
11. J.B.Farmer, F.G.Herring and R.L.Tapping, Can. J. Chem., 50, 2079(1972).
12. S.Herzog and R.Taube, Z.Chem., 2, 208(1962).
13. G.E.Coates and S.I.E.Green, J.Chem. Soc., 3340(1962).
14. S.I.Weissman and I.M.Brown, J.Am. Chem. Soc., 85, 2528(1963).
15. D.R.Eaton, Inorg. Chem., 3, 1268(1964).
16. J.Gendell, J.H.Freed, and G.K.Fraenkel, J. Chem. Phys., 37, 2832(1962).
17. G.Vincow and G.K.Fraenkel, J. Chem. Phys., 34, 1333(1961).
18. W.Beck, K.Schmidtner and H.J.Keller, Chem. Bez., 100, 503(1967).

19. W.Beck and K. Schmidtner, Chem. Ber. 100, 3363(1967).

20. G.A.Abakumov, V.D.Tikhonov, and G.A.Razavaev, Dokl. Chem. 187, 561(1969).

21. T.B.Eames and B.M.Hoffmann, J. Am. Chem. Soc., 93, 3141(1971).

22. R.A.Zelonka and M.C.Baird, J. Am. Chem. Soc., 93, 6066 (1971).

23. V.E.Kholmogorov, Rus. Chem. Rev., 37, 628(1968).

24. V.Balzani and V.Carassiti, "Photochemistry of Coordination Compounds", Acad. Press (1970).

25. N. Uri, Chem. Rev., 50, 375(1952).

26. D.J.Ingram, W.G.Hodgson, C.A.Parker, and W.T.Rees, Nature, 176, 1227(1955).

27. P.N.Moorthy and J.J.Weiss, J. Chem. Phys., 42, 3121(1965).

28. P.N.Moorthy and J.J.Weiss, J. Chem. Phys., 42, 3127(1965).

29. P.L.Airey and F.S.Dainton, Proc. R.Soc. Lond., A291, 340(1966).

30. F.S.Dainton and F.T.Jones, Trans. Faraday Soc., 61, 1681(1965).

31. P.B.Ayscough, R.G.Collins and F.S.Dainton, Nature, 205, 965(1965).

32. P.B.Ayscough, R.G.Collins, J. Phys. Chem., 70, 3128(1966).

33. J.J.Weiss, Ber. Bunsenges. Physic. Chem., 73, 131(1969).

34. D.R.Eaton and S.R.Stuart, J. Phys. Chem., 72, 400(1968).

35. von K. Heusler and H.Loeliger, Helv. Chim. Acta, 52, 1495(1969).

36. H.D.Burrows, D. Greatorex, and T.J.Kemp, J. Am. Chem. Soc., 93, 2539(1971).

37. H.Zeldes and R. Livingston, Phys. Rev. 96, 1702(1954).

38. G.T.Trammel, H.Zerdes, and R.Livingston, Phys. Rev., 110, 630(1958).

39. W.Köhnlein and J.H.Venable, Nature, 215, 618(1967).

40. R.Pruden, W.Snipes, and W.Gordy, Proc. Natl. Acad. Sci., 53, 917(1965).

41. W.Snipes, W.Bernhard, J. Chem. Phys., 43, 2921(1965).

42. A.Carrington and A.D.McLachlan, "Introduction to Magnetic Resonance", Harper and Row, New York, 1967.

43. P.B.Ayscough, "Electron Paramagnetic Resonance in Chemistry", Barnes and Noble, New York, 1967.

44. C.P.Poole,Jr. and H.A.Farach, "The Theory of Magnetic Resonance", Wiley-Interscience, New York, 1972.

45. E.T.Kaiser and L.Kevan, "Radical Ions", Wiley-Interscience, New York, 1968, p.p. 1-33.

46. H.M.McConnell, J. Chem. Phys., 24, 632, 764(1956).

47. S.I.Weissman, J. Chem. Phys., 25, 890(1956).

48. (a) H.M.McConnell and D.B.Chesnut, J. Chem. Phys., 28, 107(1958).
(b) H.M.McConnell, Ibid., 28, 1188(1958).

49. A.D.McLachlan, H.H.Dearman, and R. Lefebvre, J. Chem. Phys., 33, 65(1960).

50. H.S.Jarrett, J. Chem. Phys., 25, 1289(1956).

51. (a) H.S.Gutowsky, H.Kusumoto, T.H. Brown, and D.H. Anderson, J. Chem. Phys., 30, 860(1959); (b) T.H.Brown, D.H.Anderson and H.S.Gutowsky, ibid., 33, 720(1960); (c) M.E.Anderson, G.E.Pake and T.R.Tuttle,Jr., ibid., 33, 1581(1960); (d) M.E.Anderson, P.J.Zandstra and T.R.Tuttle, Jr., ibid., 33, 1591(1960).

52. J.R.Bolton, J. Chem. Phys., 43, 309(1965).

53. J.P.Colpa and J.R.Bolton, Mol. Phys., 6, 273(1963).

54. J.Higuchi, J. Chem. Phys., 39, 3455(1963).

55. G. Giacometti, P.L.Nordio, and M.V.Pavan, Theor. Chim. Acta(Berlin) 1, 404(1963).

56. M.Karplus and G.K.Fraenkel, 35, 1312(1961).

57. J.C.M.Henning, J. Chem. Phys., 44, 2139(1966).

58. R.Bersohn, J. Chem. Phys., 24, 1066(1956).

59. A.D.McLachlan, Mol. Phys., 1, 233(1958).

60. D.B.Chesnut, J. Chem. Phys., 29, 43(1958).

61. C.A.Coulson and V.A.Crawford, J. Chem. Soc., 2052(1953).

62 (a) E.Huckel, Z.Physik, 76, 628(1932); (b) C.A.Coulson and H.C.Longuet-Higgins, Proc. Roy. Soc. (London), A192, 16(1947); (c) C.A.Coulson, Proc. Roy. Soc. (London), A.164, 383(1938).

63. A.D.McLachlan, Mol. Phys., 3, 233(1960).

64. J.A.Pople, and R.K.Nesbet, J. Chem. Phys., 22 571(1954).

65. R.Pariser, and R.G. Parr, J. Chem. Phys., 21, 466, 767 (1953).

66. A.Brickstock, and J.A.Pople, Trans. Faraday Soc., 50, 901(1954).

67. Miyagawa, I., and W.Gordy, J. Chem. Phys., 32, 255(1960).

68. C.P.Poole,Jr., "Electron Spin Resonance (a Comprehensive Treatise on Experimental Techniques)", Wiley-Interscience, New York, 1967.

69. Denshi News edition 35, published May 1, 1964.

70. J.J.Windle and A.K.Wiersema, J. Chem. Phys., 39, 1139 (1963).

71. G.N.Schrauser, Accounts of Chemical Research, 2, 72(1969).

72. E.T.Kaiser and L.Kevan, "Radical Ions", Wiley-Interscience, New York, 1968, p.p 94-104.

73. H.Lemaire, Y.Marechat, R.Ramasseul and A.Rassat, Bull. Soc. Chim., France, 372(1965).

74. L.F.Fieser and M.Fieser, "Reagents for Organic Synthesis", John Wiley and Sons,Inc., New York 1967, p.876.

75. M.S.Kharasch et O.Reinmuth, "Grignard Reactions of Non-Metallic Substances", Prentice Hall Inc., New York, 1954, p.26.

76. B.M.Hoffmann and T.B.Eames, J. Am. Chem. Soc., 91, 5168 (1969).

77. J.Gendall, J. Freed and G.K.Fraenkel, J. Chem. Phys., 37, 2832(1962).

78. N.Hirota, Thesis, Washington University, 1963.

79. R.Ramaseul and A.Rassat, Quantum Aspects of Heterocyclic Compounds in Chemistry and Biochemistry, Ed. E.D.Bergman and B.Pullman, Jerusalem, 1970, p. 270.

80. P.D.Sullivan and J.R.Bolton, "The Alternating Linewidth Effect", Advances in MAGNETIC RESONANCE, 4, 39(1970).

81. A.K.Hoffmann, A.M.Feldman, E.Gallblum and W.G.Hodgson, J. Am. Chem. Soc., 86, 639(1964).

82. R.J.Faber, F.W.Markley and J.A.Weil, J. Chem. Phys., 46, 1652(1967).

83. D.F.Evans, J. Chem. Soc., 2003(1959).

84. B.M.Hoffmann and T.B.Eames, J. Am. Chem. Soc., 91, 2169(1969).

85. Average values from a number of nitroxide spectra contained in "Atlas of Electron Spin Resonance Spectra", B.H.J.Bielski and J.M.Gebicki, Academic Press (1967) p.p. 380-404.

86. J.C.Baird, J. Chem. Phys., 37, 1879(1962).

87. J.D.Roberts, R.E.McMahon and J.S.Hine, J. Am. Chem. Soc., 72, 4237(1950).

88. G.A.Olah and J.A.Olah, Carbonium Ions, Vol. 2, p. 720. Ed. G.A.Olah and R.Schleyer, Interscience(1970).

89. M.Saunders and E.L.Hagen, J. Am. Chem. Soc., 90, 2436(1968).

90. W.L.Waltz and R.G.Sutherland, Chem. Soc. Rev., 1, 241(1972).

91. J.Valentine, Adv. in Photochemistry, 6, 123(1969).

92. E.L.Simmons and W.W.Wendlandt, Coord. Chem. Rev., 7, 11(1971).

93. D.R.Eaton, Spectroscopy in Inorganic Chemistry, 1, 29(1970).

94. F.S.Dainton and D.G.L.James, Trans. Farad. Soc., 54, 649(1958).

95. G.A.Shagisultanova, L.K.Neokladnova and A.L.Pasnyak, Dokl. Akad. Nauk. S.S.S.R., 162, 1333(1965).

96. A.L.Pasnyak and G.A.Shagisultanova, Dokl, Akad. Nauk. S.S.S.R., 173, 612(1967).

97. E.G.Janzen and B.J.Blackbourn, J. Am. Chem. Soc., 91, 4481(1969).

98. J.G.Calvert and J.N.Pitts, Photochemistry, p. 428, John Wiley (1966).

99. P.Aushoos and E.W.R.Steacie, Can. J. Chem., 33, 1530 (1955).

100. L.Farkas and O. Wansborough-Jones, Z.Physik Chem., B.18, 124(1932).

101. K.Cusius and W.Schanzer, Ber., 75B, 1795(1942).

102. M.Burton, J. Am. Chem. Soc., 58, 692, 1645(1936).

103. R.A.Sheldon and J.K.Kochi, J. Am. Chem. Soc., 90, 6688(1968).

104. J.K.Kochi and T.W.Bethea, J. Org. Chem., 33, 75(1968).

105. R.Livingston, H.Zeldes and E.H.Taylor, Disc. Farad. Soc., 19, 166(1955).

106. H.Fischer, Magnetic Properties of Free Radicals,Landolt-Bornstein Group (II), Vol. 1, Springer-Verlag(1965).

107. R.W.Fessenden and R.H.Schuler, J. Chem. Phys., 38, 773 (1963).

108. F.J.Adrian, E.L.Cochran and V.A.Bowers, J. Chem. Phys., 36, 1661(1962).

109. J.R.Morton and W.E.Falconer, Nature, 197, 1103(1963).

110. A.Horsfield, J.R.Morton and D.H.Whiffen, Mol. Phys., 4, 327(1961).

111. R.F.Weiner and W.S.Koski, J. Am. Chem. Soc., 85,873(1963).

112. D.W.Ovenall and D.H. Whiffen, Mol. Phys., 4, 135(1961).

113. G.W.Chantry, A. Horsfield, J.R.Morton and D.H.Whiffen, Mol. Phys., 5, 589(1962).

114. Ultra-violet Spectra of Organic Compounds.

115. U.V. Atlas of Organic Compounds, Plenum Press(1971).

116. W.T.Dixon, R.O.C. Norman and A.L.Buley, J. Chem. Soc., 3625(1964).

117. B.P.Nikol'skii, M.S.Zakharcoskii, I.N.Kuznetsova and A.A.Pendin, Russ. J. Inorg. Chem., 14, 99(1969).

118. V.Balzani and V.Carassiti, Photochemistry of Coordination Compounds, Academic Press(1970), p. 159.

119. J.Jortner and G.Stein, J. Phys. Chem.,66, 1258(1962).

120. K.Nakamoto, "Infrared Spectra of Inorganic and Coordination Compounds", 2nd edition, Wiley-Interscience (1970).

121. R.Livingston, H.Zeldes and E.H.Taylor, Disc. Farad, Soc., 19, 166(1955).

122. R.Fletcher, Computer J., 13, 317(1970).